



HAL
open science

Search for long-lived stopped R-hadrons decaying out-of-time with pp collisions using the ATLAS detector

G. Aad, S. Albrand, J. Brown, Q. Buat, B. Clement, J. Collot, S. Crépé-Renaudin, B. Dechenaux, T. Delemontex, P.A. Delsart, et al.

► To cite this version:

G. Aad, S. Albrand, J. Brown, Q. Buat, B. Clement, et al.. Search for long-lived stopped R-hadrons decaying out-of-time with pp collisions using the ATLAS detector. *Physical Review D*, 2013, 88, pp.112003. 10.1103/PhysRevD.88.112003 . in2p3-00876570

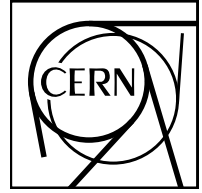
HAL Id: in2p3-00876570

<https://in2p3.hal.science/in2p3-00876570v1>

Submitted on 21 Sep 2023

HAL is a multi-disciplinary open access archive for the deposit and dissemination of scientific research documents, whether they are published or not. The documents may come from teaching and research institutions in France or abroad, or from public or private research centers.

L'archive ouverte pluridisciplinaire **HAL**, est destinée au dépôt et à la diffusion de documents scientifiques de niveau recherche, publiés ou non, émanant des établissements d'enseignement et de recherche français ou étrangers, des laboratoires publics ou privés.



CERN-PH-EP-2013-161

Submitted to: Physical Review D

Search for long-lived stopped R -hadrons decaying out-of-time with pp collisions using the ATLAS detector

The ATLAS Collaboration

Abstract

An updated search is performed for gluino, top squark, or bottom squark R -hadrons that have come to rest within the ATLAS calorimeter, and decay at some later time to hadronic jets and a neutralino, using 5.0 and 22.9 fb⁻¹ of pp collisions at 7 and 8 TeV, respectively. Candidate decay events are triggered in selected empty bunch crossings of the LHC in order to remove pp collision backgrounds. Selections based on jet shape and muon-system activity are applied to discriminate signal events from cosmic ray and beam-halo muon backgrounds. In the absence of an excess of events, improved limits are set on gluino, stop, and sbottom masses for different decays, lifetimes, and neutralino masses. With a neutralino of mass 100 GeV, the analysis excludes gluinos with mass below 832 GeV (with an expected lower limit of 731 GeV), for a gluino lifetime between 10 μ s and 1000 s in the generic R -hadron model with equal branching ratios for decays to $q\bar{q}\tilde{\chi}^0$ and $g\tilde{\chi}^0$. Under the same assumptions for the neutralino mass and squark lifetime, top squarks and bottom squarks in the Regge R -hadron model are excluded with masses below 379 and 344 GeV, respectively.

Search for long-lived stopped R -hadrons decaying out-of-time with pp collisions using the ATLAS detector

The ATLAS Collaboration

An updated search is performed for gluino, top squark, or bottom squark R -hadrons that have come to rest within the ATLAS calorimeter, and decay at some later time to hadronic jets and a neutralino, using 5.0 and 22.9 fb⁻¹ of pp collisions at 7 and 8 TeV, respectively. Candidate decay events are triggered in selected empty bunch crossings of the LHC in order to remove pp collision backgrounds. Selections based on jet shape and muon-system activity are applied to discriminate signal events from cosmic ray and beam-halo muon backgrounds. In the absence of an excess of events, improved limits are set on gluino, stop, and sbottom masses for different decays, lifetimes, and neutralino masses. With a neutralino of mass 100 GeV, the analysis excludes gluinos with mass below 832 GeV (with an expected lower limit of 731 GeV), for a gluino lifetime between 10 μ s and 1000 s in the generic R -hadron model with equal branching ratios for decays to $q\bar{q}\tilde{\chi}^0$ and $g\tilde{\chi}^0$. Under the same assumptions for the neutralino mass and squark lifetime, top squarks and bottom squarks in the Regge R -hadron model are excluded with masses below 379 and 344 GeV, respectively.

I. INTRODUCTION

Long-lived massive particles appear in many theories beyond the Standard Model [1]. They are predicted in R -parity-conserving supersymmetry (SUSY) [2–15] models, such as split SUSY [16, 17] and gauge-mediated SUSY breaking [18–24], as well as other scenarios such as universal extra dimensions [25] and leptoquark extensions [26]. For instance, split SUSY addresses the hierarchy problem via the same fine-tuning mechanism that solves the cosmological constant problem; SUSY can be broken at a very high energy scale, leading to heavy scalars, light fermions, and a light, finely tuned, Higgs boson [16]. Within this phenomenological picture, squarks would thus be much heavier than gluinos, suppressing the gluino decay. If the lifetime of the gluino is long enough, it would hadronize into R -hadrons, color-singlet states of R -mesons ($\tilde{g}q\bar{q}$), R -baryons ($\tilde{g}qqq$), and R -gluinoballs ($\tilde{g}g$). Other models, notably R -parity-violating SUSY, could produce a long-lived squark that would also form an R -hadron, e.g. $t\bar{q}$. The phenomenology of the top squark (stop) or the bottom squark (sbottom) is comparable to the gluino case but with a smaller production cross section [27, 28].

R -hadron interactions in matter are highly uncertain, but some features are well predicted. The gluino, stop, or sbottom can be regarded as a heavy, non-interacting spectator, surrounded by a cloud of interacting quarks. R -hadrons may change their properties through strong interactions with the detector. Most R -mesons would turn into R -baryons [29], and they could also change their electric charge through these interactions. At the Large Hadron Collider (LHC) at CERN [30], the R -hadrons would be produced in pairs and approximately back-to-back in the plane transverse to the beam direction. Some fraction of these R -hadrons would lose all of their momentum, mainly from ionization energy loss, and come to rest within the detector volume, only to decay to a neutralino ($\tilde{\chi}^0$) and hadronic jets at some later time.

A previous search for stopped gluino R -hadrons was

performed by the D0 Collaboration [31], which excluded a signal for gluinos with masses up to 250 GeV. That analysis, however, could use only the filled crossings in the Tevatron bunch scheme and suppressed collision-related backgrounds by demanding that there was no non-diffractive interaction in the events. Search techniques similar to those described herein have also been employed by the CMS Collaboration [32, 33] using 4 fb⁻¹ of 7 TeV data under the assumptions that $m_{\tilde{g}} - m_{\tilde{\chi}^0} > 100$ GeV and $\text{BR}(\tilde{g} \rightarrow g\tilde{\chi}^0) = 100\%$. The resulting limit, at 95% credibility level, is $m_{\tilde{g}} > 640$ GeV for gluino lifetimes from 10 μ s to 1000 s. ATLAS has up to now studied 31 pb⁻¹ of data from 2010 [34], resulting in the limit $m_{\tilde{g}} > 341$ GeV, under similar assumptions.

This analysis complements previous ATLAS searches for long-lived particles [35, 36] that are less sensitive to particles with initial $\beta \ll 1$. By relying primarily on calorimetric measurements, this analysis is also sensitive to events where R -hadron charge flipping may make reconstruction in the inner tracker and the muon system impossible. Detection of stopped R -hadrons could also lead to a measurement of their lifetime and decay properties. Moreover, the search is sensitive to any new physics scenario producing large out-of-time energy deposits in the calorimeter with minimal additional detector activity.

II. THE ATLAS DETECTOR AND EVENT RECONSTRUCTION

The ATLAS detector [37] consists of an inner tracking system (ID) surrounded by a thin superconducting solenoid, electromagnetic and hadronic calorimeters and a muon spectrometer (MS). The ID consists of silicon pixel and microstrip detectors, surrounded by a transition radiation straw-tube tracker. The calorimeter system is based on two active media for the electromagnetic and hadronic calorimeters: liquid argon in the inner barrel and end-cap/forward regions, and scintillator tiles

(TileCal) in the outer barrel region for $|\eta| < 1.7$ [38]. The calorimeters are segmented into cells that have typical size 0.1 by 0.1 in η - ϕ space in the TileCal section. The MS, capable of reconstructing tracks within $|\eta| < 2.7$, uses toroidal bending fields generated by three large superconducting magnet systems. There are inner, middle, and outer muon detector stations, each consisting of several precision tracking layers. Local muon track segments (abbreviated to simply “muon segments” from now on) are first found in each station, before being combined into extended muon tracks.

For this analysis, events are reconstructed using “cosmic” settings for the muon system [39], to find muon segments with high efficiency for muons that are “out-of-time” with respect to the expected time for a muon created from a pp collision and traveling at near the speed of light. Such out-of-time muons are present in the two most important background sources. Cosmic ray muons are present at a random time compared to the bunch-crossing time. Beam-halo muons are in time with proton bunches but may appear early if they hit the muon chamber before particles created from the bunch crossing. Using cosmic settings for the muon reconstruction also loosens requirements on the segment direction and does not require the segment to point towards the interaction point.

Jets are constructed from clusters of calorimeter energy deposits [40] using the anti- k_t jet algorithm [41] with the radius parameter set to $R = 0.4$, which assumes the energetic particles originate from the nominal interaction point. This assumption, while not generally valid for this analysis, has been checked and still accurately quantifies the energy released from the stopped R -hadron decays occurring in the calorimeter, as shown by comparisons of test-beam studies of calorimeter energy response with simulation [42]. Jet energy is quoted without correcting for the typical fraction of energy not deposited as ionization in the jet cone area, and the minimum jet transverse momentum (p_T) is 7 GeV. ATLAS jet reconstruction algorithms are described in more detail elsewhere [43]. The missing transverse momentum (E_T^{miss}) is calculated from the p_T of all reconstructed physics objects in the event, as well as all calorimeter energy clusters not associated with jets.

III. LHC BUNCH STRUCTURE AND TRIGGER STRATEGY

The LHC accelerates two counter-rotating proton beams, each divided into 3564 slots for proton bunches separated by 25 ns. When protons are injected into the LHC, not every bunch slot (BCID) is filled. During 2011 and 2012, alternate BCIDs within a “bunch train” were filled, leading to collisions every 50 ns, but there were also many gaps of various lengths between the bunch trains containing adjacent unfilled BCIDs. Filled BCIDs typically had $> 10^{11}$ protons. Unfilled BCIDs could contain

protons due to diffusion from filled BCIDs, but typically $< 10^8$ protons per BCID [44, 45]. The filled and unfilled BCIDs from the two beams can combine to make three different “bunch crossing” scenarios. A *paired* crossing consists of a filled BCID from each beam colliding in ATLAS and is when R -hadrons would be produced. An *unpaired* crossing has a filled BCID from one beam and an unfilled BCID from the other. Finally, in an *empty* crossing the BCIDs from both beams are unfilled.

Standard ATLAS analyses use data collected from the paired crossings, while this analysis searches for physics signatures of metastable R -hadrons produced in paired crossings and decaying during selected empty crossings. This is accomplished with a set of dedicated low-threshold calorimeter triggers that can fire only in the selected empty or unpaired crossings where the background to this search is much lower. The type of each bunch crossing is defined at the start of each LHC “fill” using the ATLAS beam monitors [46]. Crossings at least six BCIDs after a filled crossing are selected, to reduce background in the muon system.

ATLAS has a three-level trigger system consisting of one hardware and two software levels [47]. Signal candidates are collected using a hardware trigger requiring localized calorimeter activity, a so-called jet trigger, with a 30 GeV transverse energy threshold. This trigger could fire only during an empty crossing at least 125 ns after the most recent paired crossing, such that the detector is mostly free of background from previous interactions. The highest-level software trigger then requires a jet with $p_T > 50$ GeV, $|\eta| < 1.3$, and $E_T^{\text{miss}} > 50$ GeV. The software trigger is more robust against detector noise, keeping the final trigger rate to < 1 Hz. After offline reconstruction, only 5% of events with more than two muon segments are saved, and no events with more than 20 muon segments are saved, to reduce the data storage needs since events with muon segments are vetoed in the analysis. A data sample enriched with beam-halo muons is also accepted with a lower-threshold jet trigger that fires in the unpaired crossings, and a sample is collected using a trigger that accepts random events from the empty crossings to study background conditions.

IV. DATA SAMPLES

The data used are summarized in Table I, where the corresponding *delivered* integrated luminosity and recorded live time in the selected empty BCIDs are provided. The early periods of data taking in 2011 are selected as a “cosmic background region” to estimate the rate of background events (mostly from cosmic ray muons, as discussed below). This is motivated by the low integrated luminosity and small number of paired crossings during these initial periods. For a typical signal model that this analysis excludes, less than 3% of events in the cosmic background region are expected to arise from signal processes. As discussed in detail in

TABLE I. The data analyzed in this work and the corresponding integrated delivered luminosity, center-of-mass energy, and live time of the ATLAS detector in the selected empty BCIDs during those periods.

Data period	Delivered luminosity (fb ⁻¹) @ energy (TeV)	Recorded empty live time (hours)
Cosmic	0.3 @ 7	125.8
Search	5.0 @ 7 + 22.9 @ 8	389.3
Total	5.3 @ 7 + 22.9 @ 8	515.1

Sec. VII B, the cosmic ray muon background rate is constant, but the signal production rate scales with luminosity. The later data of 2011 and all of 2012 are used as the “search region”, where an excess of events from R -hadron decays is sought. ATLAS data are taken in *runs*, which typically span one LHC fill, lasting approximately one day.

V. SIMULATION OF R -HADRONS

Monte Carlo simulations are used primarily to determine the reconstruction efficiency and stopping fraction of the R -hadrons, and to study associated systematic uncertainties on the quantities used in the selections. The simulated samples have gluino or squark masses in the range 300–1000 GeV, to which the present analysis is sensitive. The PYTHIA program [48], version 6.427, with CTEQ6L1 parton distribution functions (PDF) [49], is used to simulate pair production of gluinos, stops, or sbottoms. The string hadronization model [50], incorporating specialized hadronization routines [1] for R -hadrons, is used to produce final states containing two R -hadrons.

To compensate for the fact that R -hadron scattering is not strongly constrained, the simulation of R -hadron interactions with matter is handled by a special detector response simulation [29] using GEANT4 [51, 52] routines based on several scattering and spectrum models with different sets of assumptions: the *Generic* [29, 53], *Regge* [54, 55], and *Intermediate* [56] models. Each model makes different assumptions about the R -hadron nuclear interactions and the spectrum of R -hadron states.

Generic: Limited constraints on allowed stable states permit the occurrence of doubly-charged R -hadrons and a wide variety of charge-exchange scenarios. The nuclear scattering model is purely phase-space driven. This model is chosen as the nominal model for gluino R -hadrons.

Regge: Only one (electrically neutral) baryonic state is allowed. The nuclear scattering model employs a triple-Regge formalism. This model is chosen as the nominal model for stop and sbottom R -hadrons.

Intermediate: The spectrum is more restricted than the generic model, while still featuring charged baryonic states. The scattering model used is that of the generic model.

In the simulation, roughly equal numbers of singly-charged and neutral R -hadrons are generated. They undergo an average of 4–6 nuclear interactions with the detector, depending on the R -hadron model, during which their charge can change. The R -hadrons are created on average with about 200 GeV of kinetic energy. Those created with less than about 20 GeV of kinetic energy tend to lose it all, mostly through ionization, and stop in the detector, as shown in Fig. 1. Those that stop in the detector are all charged when they stop, with roughly equal numbers of positive and negative singly-charged states. If the doubly-charged state is allowed (as in the generic model), about half of the stopped R -hadrons would be doubly positive charged.

If a simulated R -hadron comes to rest in the ATLAS detector volume, its location is recorded. Such an R -hadron would bind to a heavy nucleus of an atom in the detector, once it slows down sufficiently, and remain in place indefinitely [57]. Table II shows the probability for a simulated signal event to have at least one R -hadron stopped within the detector volume, for the models considered. The stopping fraction shows no significant dependence on the gluino, stop, or sbottom mass within the statistical uncertainty of the simulation.

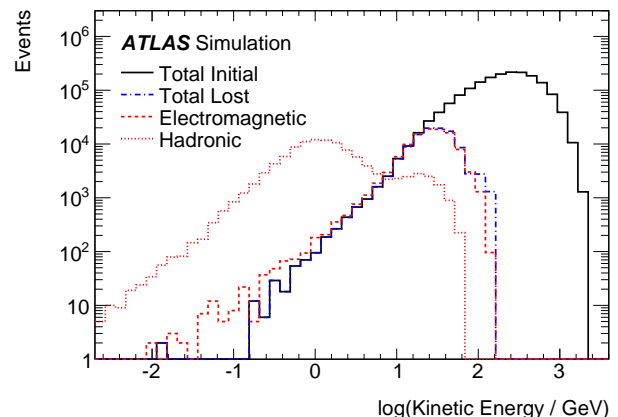


FIG. 1. The kinetic energies of simulated gluino R -hadrons with a mass of 800 GeV in the generic model are shown at initial production (black). The energy lost through hadronic interactions with the detector (red, dotted), electromagnetic ionization (red, dashed), and total (red, dashed-dotted) are also shown, for those R -hadrons that have stopped.

The stopping locations are used as input for a second step of PYTHIA where the decays of the R -hadrons are simulated. A uniform random time translation is applied in a 25 ns time window, from -15 to $+10$ ns, relative to the bunch-crossing time, since the R -hadron would decay at a random time relative to the bunch structure of

TABLE II. The selection efficiency after all selection criteria have been applied, its systematic uncertainty, and the stopping fraction, for all signal samples.

R -hadron model	Gluino/squark decay	Mass (GeV)		Selection efficiency		Relative systematic uncert.		Stopping fraction (%)
		\tilde{g}	$\tilde{\chi}^0$	$E > 100$ GeV	$E > 300$ GeV	$E > 100$ GeV	$E > 300$ GeV	
Generic	$\tilde{g} \rightarrow g/q\bar{q} + \tilde{\chi}^0$	400	100	14.1 %	0.5 %	15.9%	–	12.2 ± 0.1
Generic	$\tilde{g} \rightarrow g/q\bar{q} + \tilde{\chi}^0$	600	100	15.0 %	10.6 %	15.7%	35.3%	
Generic	$\tilde{g} \rightarrow g/q\bar{q} + \tilde{\chi}^0$	800	100	15.5 %	13.9 %	15.8%	16.2%	
Generic	$\tilde{g} \rightarrow g/q\bar{q} + \tilde{\chi}^0$	1000	100	14.8 %	14.1 %	15.1%	15.3%	
Generic	$\tilde{g} \rightarrow g/q\bar{q} + \tilde{\chi}^0$	400	300	3.4 %	< 0.1%	60.1%	–	
Generic	$\tilde{g} \rightarrow g/q\bar{q} + \tilde{\chi}^0$	600	500	4.2 %	< 0.1%	48.7%	–	
Generic	$\tilde{g} \rightarrow g/q\bar{q} + \tilde{\chi}^0$	800	700	4.5 %	< 0.1%	35.6%	–	
Generic	$\tilde{g} \rightarrow g/q\bar{q} + \tilde{\chi}^0$	1000	900	5.7 %	< 0.1%	33.7%	–	
Generic	$\tilde{g} \rightarrow t\bar{t} + \tilde{\chi}^0$	600	100	9.9 %	7.2 %	18.5%	19.8%	
Generic	$\tilde{g} \rightarrow t\bar{t} + \tilde{\chi}^0$	800	100	10.1 %	8.9 %	17.7%	18.4%	
Generic	$\tilde{g} \rightarrow t\bar{t} + \tilde{\chi}^0$	1000	100	9.5 %	8.9 %	16.3%	16.5%	
Generic	$\tilde{g} \rightarrow t\bar{t} + \tilde{\chi}^0$	400	20	8.7 %	4.3 %	18.8%	36.8%	
Generic	$\tilde{g} \rightarrow t\bar{t} + \tilde{\chi}^0$	600	220	9.8 %	5.4 %	17.0%	30.5%	
Generic	$\tilde{g} \rightarrow t\bar{t} + \tilde{\chi}^0$	800	420	8.3 %	4.5 %	17.4%	28.7%	
Generic	$\tilde{g} \rightarrow t\bar{t} + \tilde{\chi}^0$	1000	620	8.7 %	4.7 %	17.4%	33.5%	
Intermediate	$\tilde{g} \rightarrow g/q\bar{q} + \tilde{\chi}^0$	400	100	8.6 %	0.4 %	16.7%	–	
Intermediate	$\tilde{g} \rightarrow g/q\bar{q} + \tilde{\chi}^0$	600	100	8.9 %	6.0 %	15.5%	28.0%	
Intermediate	$\tilde{g} \rightarrow g/q\bar{q} + \tilde{\chi}^0$	800	100	8.4 %	7.4 %	15.5%	16.0%	
Intermediate	$\tilde{g} \rightarrow g/q\bar{q} + \tilde{\chi}^0$	1000	100	7.4 %	6.9 %	16.1%	16.5%	
Regge	$\tilde{g} \rightarrow g/q\bar{q} + \tilde{\chi}^0$	400	100	16.7 %	0.7 %	15.9%	–	5.2 ± 0.1
Regge	$\tilde{g} \rightarrow g/q\bar{q} + \tilde{\chi}^0$	600	100	19.3 %	13.4 %	15.4%	30.6%	
Regge	$\tilde{g} \rightarrow g/q\bar{q} + \tilde{\chi}^0$	800	100	19.4 %	17.2 %	17.8%	15.7%	
Regge	$\tilde{g} \rightarrow g/q\bar{q} + \tilde{\chi}^0$	1000	100	19.6 %	18.4 %	18.8%	17.7%	
Generic	$\tilde{t} \rightarrow t + \tilde{\chi}^0$	300	100	11.0 %	–	15.6%	–	10.1 ± 0.1
Generic	$\tilde{t} \rightarrow t + \tilde{\chi}^0$	400	100	10.1 %	–	16.2%	–	
Generic	$\tilde{t} \rightarrow t + \tilde{\chi}^0$	600	100	9.6 %	4.6 %	16.7%	44.4%	
Generic	$\tilde{t} \rightarrow t + \tilde{\chi}^0$	800	100	10.2 %	7.7 %	16.5%	17.0%	
Generic	$\tilde{t} \rightarrow t + \tilde{\chi}^0$	400	200	10.9 %	–	15.5%	–	
Generic	$\tilde{t} \rightarrow t + \tilde{\chi}^0$	600	400	10.9 %	–	15.9%	–	
Generic	$\tilde{t} \rightarrow t + \tilde{\chi}^0$	800	600	10.7 %	–	16.1%	–	
Regge	$\tilde{b} \rightarrow b + \tilde{\chi}^0$	300	100	7.6 %	–	17.8%	–	5.3 ± 0.1
Regge	$\tilde{b} \rightarrow b + \tilde{\chi}^0$	400	100	10.8 %	–	17.3%	–	
Regge	$\tilde{b} \rightarrow b + \tilde{\chi}^0$	600	100	11.9 %	5.8 %	16.6%	59.6%	
Regge	$\tilde{b} \rightarrow b + \tilde{\chi}^0$	800	100	12.5 %	10.5 %	15.8%	17.0%	
Regge	$\tilde{b} \rightarrow b + \tilde{\chi}^0$	400	300	3.0 %	–	59.1%	–	
Regge	$\tilde{b} \rightarrow b + \tilde{\chi}^0$	600	500	3.9 %	–	50.0%	–	
Regge	$\tilde{b} \rightarrow b + \tilde{\chi}^0$	800	700	3.4 %	–	35.2%	–	
Regge	$\tilde{b} \rightarrow b + \tilde{\chi}^0$	300	200	1.9 %	–	74.0%	–	
Regge	$\tilde{t} \rightarrow t + \tilde{\chi}^0$	300	100	10.5 %	–	16.0%	–	8.1 ± 0.1
Regge	$\tilde{t} \rightarrow t + \tilde{\chi}^0$	400	100	10.2 %	–	16.2%	–	
Regge	$\tilde{t} \rightarrow t + \tilde{\chi}^0$	600	100	10.1 %	4.5 %	17.2%	39.8%	
Regge	$\tilde{t} \rightarrow t + \tilde{\chi}^0$	800	100	10.6 %	8.0 %	16.5%	19.5%	

the LHC, but would be triggered by the ATLAS detector during the corresponding empty BCID. These simulated events then proceed through the standard ATLAS digitization simulation [52] and event reconstruction (but with cosmic ray muon settings). The effects of cavern background, a long-lived background component made up of low-energy γ -rays and x-rays from low-energy neutrons in the cavern, are not included in the simulation directly, but they are accounted for by measuring the muon activity in the randomly-triggered empty data (see Sec. IX). Using the randomly-triggered data, the calorimeter activity due to preceding interactions is found to be negligible compared to the jet energy uncertainty and is ignored.

Different models allow the gluinos to decay via the radiative process, $\tilde{g} \rightarrow g\tilde{\chi}^0$, or via $\tilde{g} \rightarrow q\bar{q}\tilde{\chi}^0$. The results are interpreted assuming either a 50% branching ratio to $g\tilde{\chi}^0$ and 50% to $q\bar{q}\tilde{\chi}^0$, or 100% to $t\bar{t}\tilde{\chi}^0$ as would be the case if the top squark was significantly lighter than the other squarks. Reconstruction efficiencies are typically $\approx 20\%$ higher for $q\bar{q}\tilde{\chi}^0$ compared to $g\tilde{\chi}^0$ decays. The stop (sbottom) is assumed to always decay to a top (bottom) quark and a neutralino. The neutralino mass, $m_{\tilde{\chi}^0}$, is fixed either to 100 GeV, or such that there is only 100 GeV of free energy left in the decay (a compressed scenario).

VI. CANDIDATE SELECTION

First, events are required to pass tight data quality constraints that verify that all parts of the detector were operating normally. Events with calorimeter noise bursts are rejected; this has negligible impact on signal efficiency. The basic selection criteria, imposed to isolate signal-like events from background events, demand at least one high energy jet and no muon segments reconstructed in the muon system passing selections. Since most of the R -hadrons are produced centrally in η , the analysis uses only the central barrel of the calorimeter and requires that the leading jet satisfies $|\eta| < 1.2$. In order to reduce the background, the analysis demands the leading jet energy > 50 GeV. Up to five additional jets are allowed, more than expected for the signal models considered.

The fractional missing E_T is the E_T^{miss} divided by the leading jet p_T and is required to be > 0.5 . This eliminates background from beam-gas and residual pp events, and has minimal impact on the signal efficiencies. To remove events with a single, narrow energy spike in the calorimeter, due to noise in the electronics or data corruption, events are vetoed where the smallest number of cells containing 90% of the energy deposit of the leading jet (n_{90}) is fewer than four. This $n_{90} > 3$ requirement also reduces other background significantly since most large energy deposits from muons in the calorimeter result from hard bremsstrahlung photons, which create short, narrow electromagnetic showers. Large, broad, hadronic showers from deep-inelastic scattering of the muons off nuclei

are far rarer. To further exploit the difference between calorimeter energy deposits from muons and the expected signal, the jet width is required to be > 0.04 , where jet width is the p_T -weighted ΔR average of each constituent from the jet axis and $\Delta R = \sqrt{(\Delta\eta)^2 + (\Delta\phi)^2}$. The fraction of the leading jet energy deposited in the TileCal must be > 0.5 , to reduce background from beam-halo where the incoming muon cannot be detected due to lack of MS coverage at low radius in the forward region.

The analysis then requires that no muon segment with more than four associated hits in a muon station be reconstructed in the event. Muon segments with a small number of measurements are often present from cavern background, noise, and pile-up, as studied in the randomly-triggered data. The events before the muon segment veto, only requiring the leading jet energy > 50 GeV, are studied as a control sample, since the expected signal-to-background ratio is small. Comparisons of the distributions of several jet variables between backgrounds and data can be seen in Fig. 2 for events in this control sample. The backgrounds shown in these figures are estimated using the techniques described in Sec. VII. To remove overlap between the cosmic ray and beam-halo backgrounds in these plots, an event is not considered ‘‘cosmic’’ if it has a muon segment with more than four hits and an angle within 0.2 radians from parallel to the beamline. The same distributions are shown for events after the muon segment veto in Fig. 3. Finally, a leading jet energy requirement of > 100 or > 300 GeV defines two signal regions, sensitive to either a small or large mass difference between the R -hadron and the neutralino in the signal model, respectively. Table II shows the efficiencies of these selections on the signal simulations, and Table III presents the number of data events surviving each of the imposed selection criteria.

VII. BACKGROUND ESTIMATION

A. Beam-Halo Background

Protons in either beam can interact with residual gas in the beampipe, or with the beampipe itself if they stray off orbit, leading to a hadronic shower. If the interaction takes place several hundred meters from ATLAS, most of the shower is absorbed in shielding or surrounding material before reaching ATLAS. The muons from the shower can survive and enter the detector, traveling parallel to the beamline and in time with the (filled) proton BCIDs [58, 59]. The unpaired-crossing data with a jet passing the selection criteria are dominantly beam-halo background. Figure 4 (left) shows an event display of an example beam-halo background candidate event.

To estimate the number of beam-halo events in the empty crossings of the search region, an orthogonal sample of events from the unpaired crossings is used. The ratio of the number of beam-halo events that pass the jet criteria but fail to have a muon segment identified

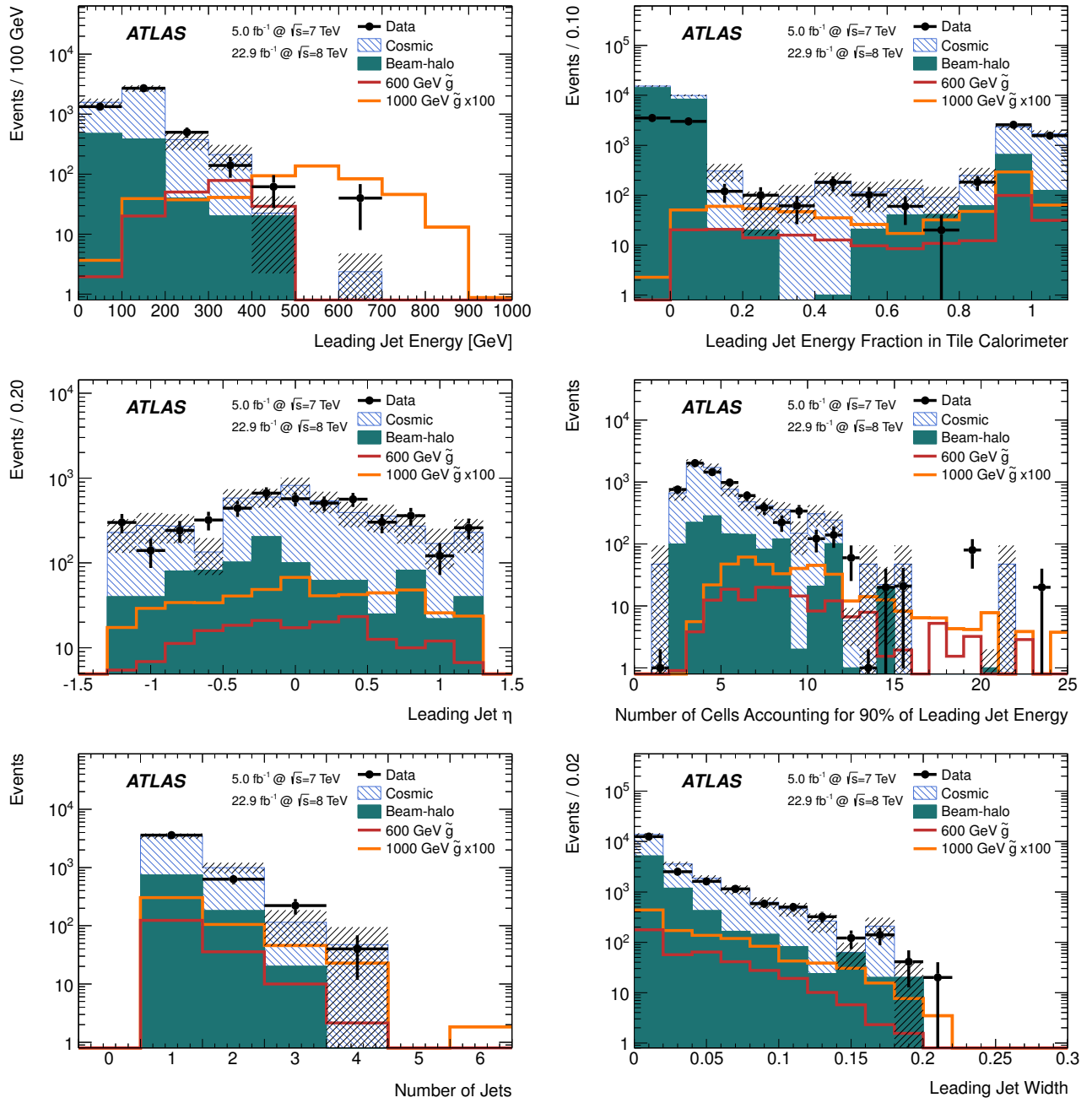


FIG. 2. Jet variables for the empty crossing signal triggers. The requirements in Table III are applied except for leading jet energy > 100 GeV and the muon segment veto. For the quantity being plotted, the corresponding selection criterion is not applied. Histograms are normalized to the expected number of events in the search region. Note that only 5% of data events with more than two muon track segments were kept; they are scaled on these figures by a factor of 20. The top hashed band shows the total statistical uncertainty on the background estimate. The background estimate does not correctly describe beam-halo with low TileCal energy fraction; this region is not used in the analysis. The TileCal energy fraction can be negative or greater than one due to pileup-subtraction corrections.

to those that do have a muon segment identified is measured. This ratio is then multiplied by the number of beam-halo events observed in the signal region that do have an identified muon segment to give the estimate of the number that do not have a muon segment and thus

contribute to background in the signal region. Beam-halo events in the unpaired-crossing data are identified by applying a modified version of the search selection criteria. The muon segment veto is removed, events with leading jet energy > 50 GeV are used, and the $n_{90}>3$

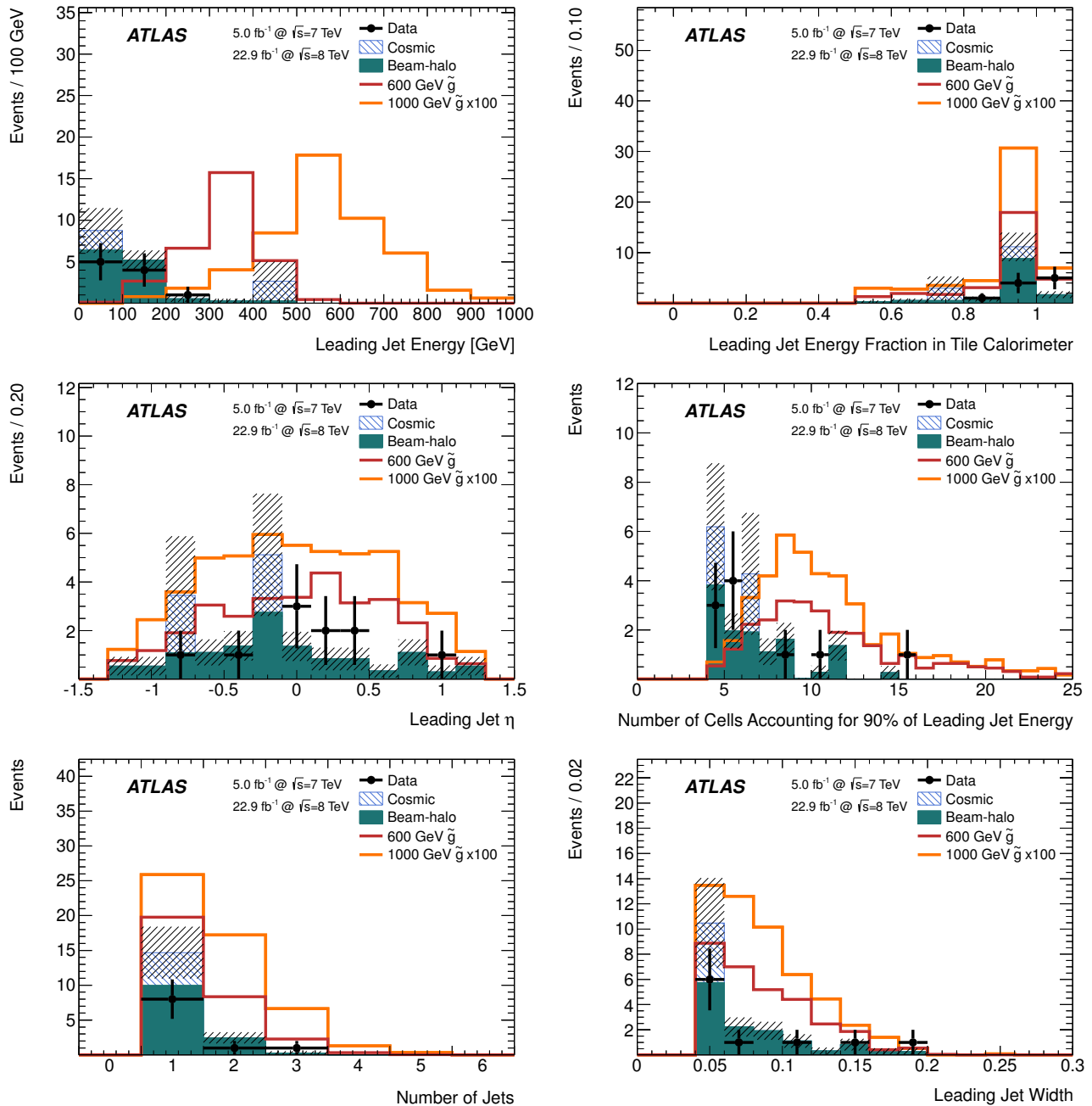


FIG. 3. The event yields in the signal region for candidates with all selection criteria applied (in Table III) including the muon segment veto, but omitting the jet energy > 100 GeV requirement. All samples are scaled to represent their anticipated yields in the search region. The top hashed band shows the total statistical uncertainty on the background estimate.

requirement is not applied. Studies show that the muon efficiency is not significantly correlated with the energy or shape of the jet in the calorimeter for beam-halo events. A muon segment is required to be nearly parallel to the beam pipe, $\theta < 0.2$ or $\theta > (\pi - 0.2)$, and have more than four muon station measurements. Next, beam-halo events that failed to leave a muon segment are counted, allowing the ratio of beam-halo events with no muon seg-

ment identified to be calculated. Then the number of beam-halo muons in the search region (the empty crossings) that did leave a muon segment is counted. The same selection criteria as listed in Table III are used, omitting the 100 GeV requirement. However, instead of a muon segment veto, a parallel muon segment is required. If no events are present, the uncertainty is taken as ± 1 event. Findings are summarized in Table IV.

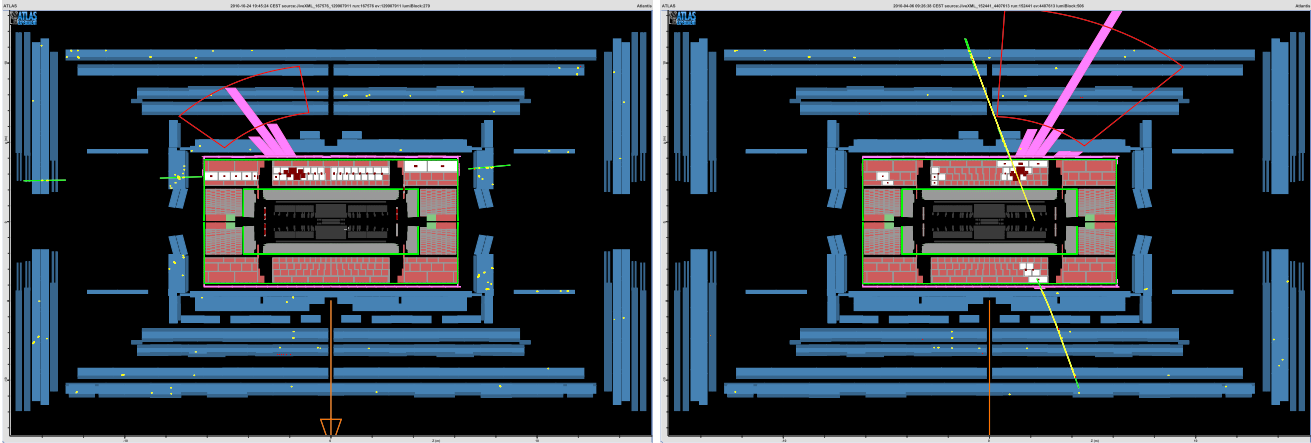


FIG. 4. Left: A beam-halo candidate event during an unpaired crossing in data. This event passed all the selection criteria except for the muon segment veto. Right: A cosmic ray muon candidate event during an empty crossing in data. This event passed all the selection criteria except for the muon segment veto. In both plots, white squares filled with red squares show reconstructed energy deposits in TileCal cells above noise threshold (the fraction of red area indicates the amount of energy in the cell), purple bars show a histogram of total energy in projective TileCal towers, jets are shown by open red trapezoids, muon segments by green line segments in each muon station, and muon tracks by continuous thin yellow lines. E_T^{miss} is shown as an orange arrow.

TABLE III. Number of events after selections for data in the cosmic background and search regions, defined in Table I. The cosmic background region data are shown before and after scaling to the search region, which accounts for the different detector live time and accidental muon segment veto efficiency (if applicable) between the background and search regions. The cumulative efficiency after each cut for a simulated signal of $\tilde{g} \rightarrow g/qq\tilde{\chi}^0$ decays with a gluino mass of 800 GeV and fixed neutralino mass of 100 GeV is also shown. The uncertainties are statistical only.

Selection criteria	Cosmic region	Scaled cosmic region	Search region	$\tilde{g} \rightarrow g/qq\tilde{\chi}^0$ $m_{\tilde{g}} = 800 \text{ GeV}, m_{\tilde{\chi}^0} = 100 \text{ GeV}$
Trigger	49390 ± 920	152800 ± 2800	218076	$71.1 \pm 0.7 \%$
Leading jet $ \eta < 1.2$	44760 ± 870	138500 ± 2700	202015	$60.5 \pm 0.7 \%$
Number of jets < 6	44690 ± 870	138300 ± 2700	201628	$60.4 \pm 0.7 \%$
Fractional $E_T^{\text{miss}} > 0.5$	44680 ± 870	138200 ± 2700	201618	$60.2 \pm 0.7 \%$
Leading jet $n_{90} > 3$	12680 ± 470	39200 ± 1500	85866	$54.2 \pm 0.7 \%$
Leading jet width > 0.04	4130 ± 260	12770 ± 810	34445	$29.9 \pm 0.7 \%$
Leading jet tile E frac. > 0.5	1640 ± 180	5070 ± 560	5396	$22.3 \pm 0.6 \%$
Leading jet energy $> 50 \text{ GeV}$	1640 ± 180	5070 ± 560	5396	$22.3 \pm 0.6 \%$
Muon segment veto	2.0 ± 1.4	4.7 ± 3.4	10	$15.5 \pm 0.6 \%$
Leading jet energy $> 100 \text{ GeV}$	1.0 ± 1.0	2.4 ± 2.4	5	$15.5 \pm 0.6 \%$
Leading jet energy $> 300 \text{ GeV}$	1.0 ± 1.0	2.4 ± 2.4	0	$13.9 \pm 0.5 \%$

B. Cosmic Ray Muon Background

The background from cosmic ray muons is estimated using the cosmic background region (described in Sec. IV). The beam-halo background is estimated for this data sample as described above, and this estimate is subtracted from the observed events passing all selections. Finally, this number of cosmic ray events in the cosmic region is scaled by the ratio of the signal-region to cosmic-region live times to estimate the cosmic ray background in the signal region. Additionally, the cosmic

background estimate is multiplied by the muon-veto efficiency (see Sec. IX) to account for the rejection of background caused by the muon veto. An example cosmic-ray muon background event candidate is shown in Figure 4 (right).

VIII. EVENT YIELDS

Some candidate event displays are shown in Fig. 5. Distributions of jet variables are plotted for events in

TABLE IV. Estimate of beam-halo events entering the search region, as described in Sec. VII A. The ratio of the number of beam-halo muons that do not leave a segment to the number that do leave a segment is calculated from the unpaired data. This ratio is then applied to the number of events in the search region where a segment was reconstructed to yield the beam-halo estimate. The quoted uncertainties are statistical only.

Data region	Leading jet energy (GeV)	Unpaired (all data combined)		Empty	
		Parallel μ	No μ	Parallel μ	Predicted No μ
Cosmic	50	1634	22	82 ± 40	1.1 ± 0.6
Search	50	1634	22	900 ± 130	12 ± 3
Cosmic	100	1634	22	61 ± 35	0.8 ± 0.5
Search	100	1634	22	445 ± 94	6 ± 2
Cosmic	300	1634	22	$0.0_{-0}^{+1.0}$	$0.000_{-0}^{+0.01}$
Search	300	1634	22	40 ± 28	0.5 ± 0.4

the jet energy > 100 GeV signal region after applying all selection criteria and are compared to the estimated backgrounds in Fig. 6. The shapes of these distributions and event yields are consistent. Table V shows the signal region event yields and background estimates. There is no evidence of an excess of events over the background estimate.

IX. CONTRIBUTIONS TO SIGNAL EFFICIENCY

Quantifying the signal efficiency for the stopped R -hadron search presents several unique challenges due to the non-prompt nature of their decays. Specifically there are four sources of inefficiency: stopping fraction (Sec. V), reconstruction efficiency (Table II), accidental muon veto, and probability to have the decay occur in an empty crossing (timing acceptance). Since the first two have been discussed above, only the accidental muon veto and timing acceptance are described here.

A. Accidental Muon Veto

Operating in the empty crossings has the significant advantage of eliminating collision backgrounds. However because such a stringent muon activity veto is employed, a significant number of events are rejected in the offline analysis due to spurious track segments in the muon system, which are not modeled in the signal simulation. Both β -decays from activated nuclei and δ -electrons could produce segments with more than four muon station measurements. This effect is separate from a signal decay producing a muon segment that then vetoes the event. To study the rate of muon segments, events from the empty random trigger data in 2011 and 2012 are examined as a function of run number, since the effect can depend strongly on beam conditions. The rate of these events that have a muon segment from noise or other background is calculated. The efficiency per run

to pass the muon segment veto is applied on a live-time weighted basis to the cosmic background estimate and varies from 98% at the start of 2011 to 70% at the end of 2012. It is still applied to the cosmic background estimate after the muon veto, since the probability to have the cosmic background event pass the analysis selections and contribute to the signal region events depends on it passing the muon veto. The beam-halo background estimate already implicitly accounts for this effect across run periods. For the signal, this effect is accounted for inside the timing acceptance calculation, on a per-run basis.

B. Timing Acceptance

The expected signal decay rate does not scale with instantaneous luminosity. Rather, at any moment in time, the decay rate is a function of the hypothetical R -hadron lifetime and the entire history of delivered luminosity. For example, for longer R -hadron lifetimes the decay rate anticipated in today's run is boosted by luminosity delivered yesterday. To address the complicated time behavior of the R -hadron decays, a timing acceptance is defined for each R -hadron lifetime hypothesis, $\epsilon_T(\tau)$, as the number of R -hadrons decaying in an empty crossing divided by the total number that stopped. The $\epsilon_T(\tau)$ factor thus accounts for the full history of the delivered luminosity and live time recorded in empty crossings. This means the number of R -hadrons expected to be reconstructed is $L \times \sigma \times \epsilon_{\text{stopping}} \times \epsilon_{\text{recon}} \times \epsilon_T(\tau)$, where L is the integrated luminosity, σ is the R -hadron production cross section weighted by integrated luminosity at 7 and 8 TeV, $\epsilon_{\text{stopping}}$ is the stopping fraction, and ϵ_{recon} is the reconstruction efficiency.

To calculate the timing acceptance for the actual 2011 and 2012 LHC and ATLAS run schedule, measurements are combined of the delivered luminosity in each BCID, the bunch structure of each LHC fill, and the live time recorded in empty crossings during each fill, all kept in the ATLAS online conditions database. The efficiency calculation is split into short and long R -hadron life-

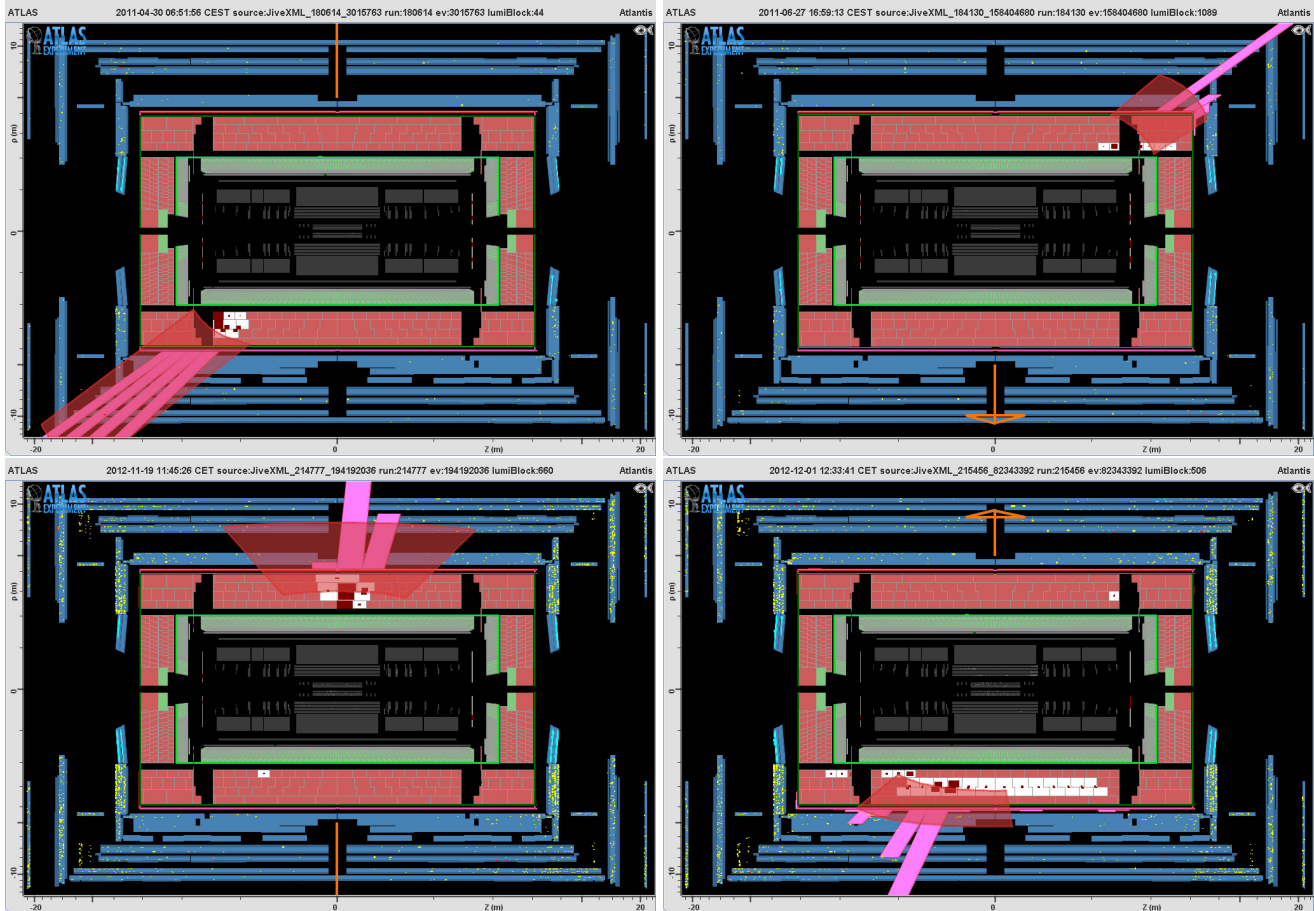


FIG. 5. Some candidate event displays from 2011 (top) and 2012 (bottom) data passing all selections. White squares filled with red squares show reconstructed energy deposits in TileCal cells above noise threshold (the fraction of red area indicates the amount of energy in the cell), purple bars show a histogram of total energy in projective TileCal towers, and jets are shown by red semi-transparent trapezoids. Muons segments are drawn but none are reconstructed in these events. E_T^{miss} is shown as an orange arrow.

times, to simplify the calculation. For R -hadron lifetimes less than 10 seconds, the bunch structure is taken into account, but not the possibility that an R -hadron produced in one run could decay in a later one. For longer R -hadron lifetimes, the bunch structure is averaged over, but the chance that stopped R -hadrons from one run decay in a later one is considered. The resulting timing acceptance is presented in Fig. 7.

X. SYSTEMATIC UNCERTAINTIES

Three sources of systematic uncertainty on the signal efficiency are studied: the R -hadron interaction with matter, the out-of-time decays in the calorimeters, and the effect of the selection criteria. The total uncertainties, added in quadrature, are shown in Table II. In addition to these, a 2.6% uncertainty is assigned to the luminosity measurement [60], fully correlated between the 2011 and 2012 data. To account for occasional dead-time

due to high trigger rates, a 5% uncertainty is assigned to the timing acceptance; this accounts for any mismodeling of the accidental muon veto as well. The gluino, stop, or sbottom pair-production cross-section uncertainty is not included as a systematic uncertainty but is used when extracting limits on their mass by finding the intersection with the cross section -1σ of its uncertainty.

A. R -hadron–Matter Interactions

The various simulated signal samples are used to estimate the systematic uncertainty on the stopping fraction due to the scattering model. There are two sources of theoretical uncertainty: the spectrum of R -hadrons and nuclear interactions. To estimate the effect from different allowed R -hadron states, three different scattering models are employed: generic, Regge, and intermediate (see Sec. V). Each allows a different set of charged states that affect the R -hadron’s electromagnetic interac-

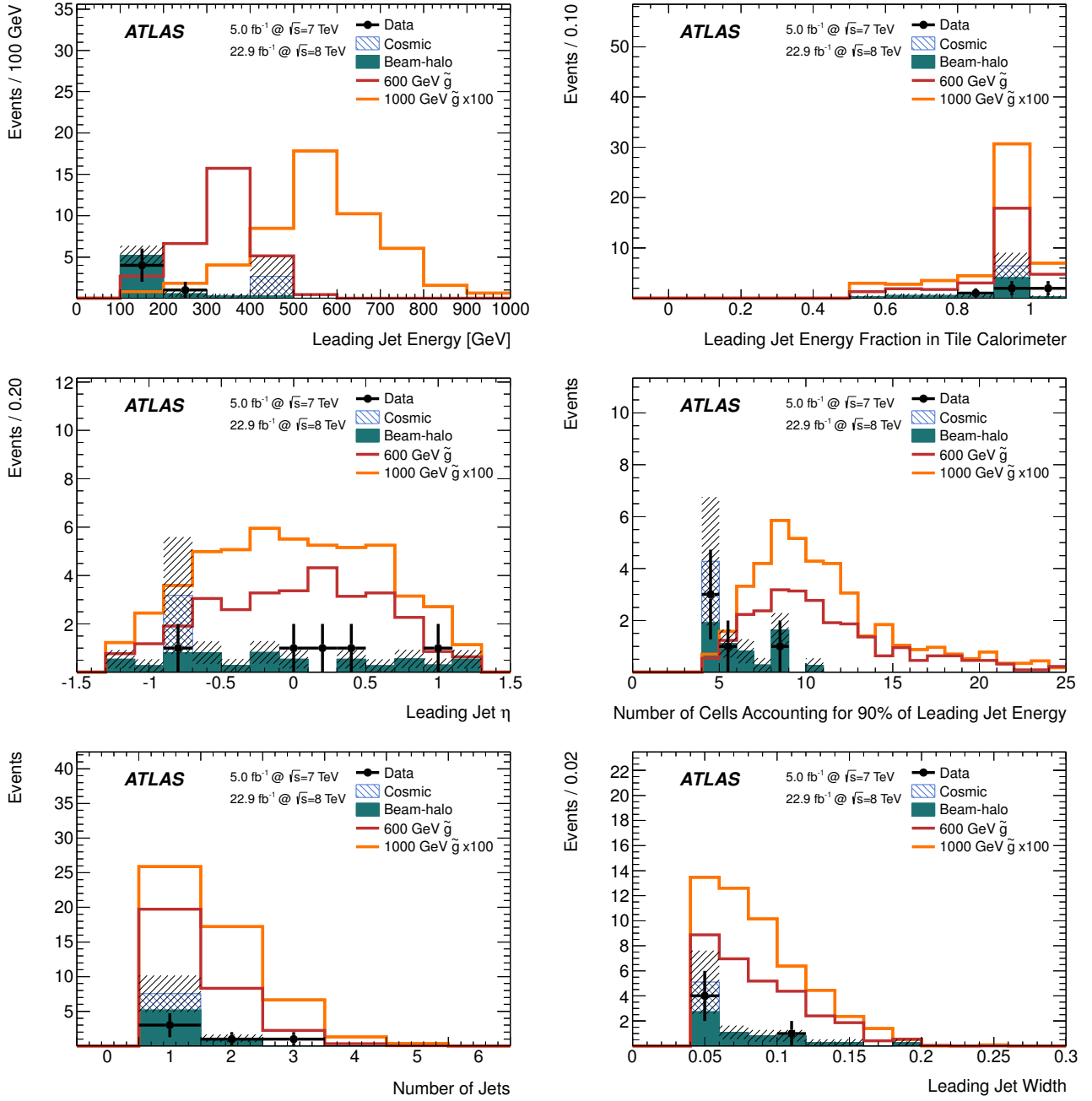


FIG. 6. The event yields in the signal region for candidates with all selections (in Table III) except jet energy > 300 GeV. All samples are scaled to represent their anticipated yields in the search region. The top hashed band shows the total statistical uncertainty on the background estimate.

tion with the calorimeters. Since these models have large differences for the R -hadron stopping fraction, limits are quoted separately for each model, rather than including the differences as a systematic uncertainty on the signal efficiency. There is also uncertainty from the modeling of nuclear interactions of the R -hadron with the calorimeter since these can affect the stopping fraction. The effect is estimated by recalculating the stopping fraction after

doubling and halving the nuclear cross section. The difference gives a relative uncertainty of 11%, which is used as the systematic uncertainty in limit setting.

TABLE V. The number of expected and observed events (with statistical uncertainties) corresponding to each of the selection criteria. The number of expected cosmic events in the search region is calculated by subtracting the expected number of beam-halo background events in the cosmic region (see Table IV) from the number of events observed in the cosmic region (see Table III) and then scaling to the search region. The scaling is simply the ratio of recorded empty live times for the two regions (see Table I) before the muon segment veto is applied. After the muon segment veto is applied, the scaling also accounts for the difference in the muon segment veto efficiency between the cosmic and search regions.

Leading jet energy (GeV)	Muon veto	Cosmic region			Number of events in search region			
		Events	Beam-halo bkgd.	Scaling	Cosmic	Beam-halo	Total background	Observed
50	No	1640	82±40	3.1	4820 ± 570	900 ± 130	5720 ± 590	5396
50	Yes	2	1.1±0.6	2.4	2.1 ± 3.6	12 ± 3	14.2 ± 4.0	10
100	Yes	1	0.8±0.5	2.4	0.4 ± 2.7	6 ± 2	6.4 ± 2.9	5
300	Yes	1	0.000 ^{+0.01} ₋₀	2.4	2.4 ± 2.4	0.5 ± 0.4	2.9 ± 2.4	0

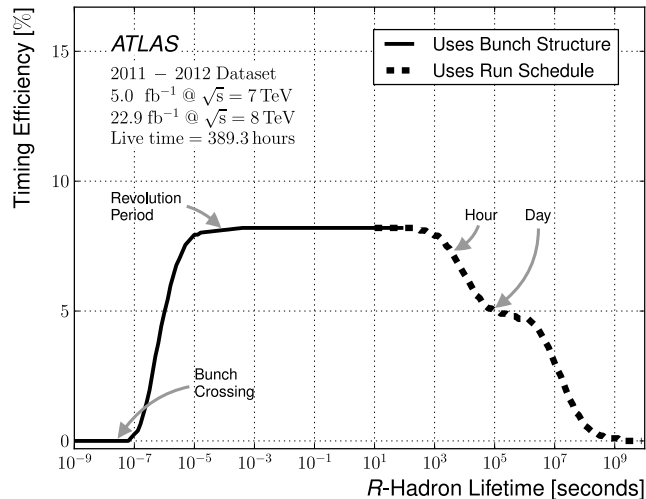


FIG. 7. The timing acceptance for signal as a function of R -hadron lifetime (in seconds). This corresponds to the $\epsilon_T(\tau)$ function described in the text.

B. Timing in the Calorimeters

Since the R -hadron decay is not synchronized with a BCID it is possible that the calorimeters respond differently to the energy deposits in the simulated signals than in data. The simulation considers only a single BCID for each event; it does not simulate the trigger in multiple BCIDs and the firing of the trigger for the first BCID that passes the trigger. In reality, a decay at -15 ns relative to a given BCID might fire the trigger for that BCID, or it may fire the trigger for the following BCID. The reconstructed energy response of the calorimeter can vary between these two cases by up to 10% since the reconstruction is optimized for in-time energy deposits. To estimate the systematic uncertainty, the total number of simulated signal events passing the offline selections is studied when varying the timing offset by 5 ns in each direction (keeping the 25 ns range). This variation conservatively covers the timing difference observed between

simulated signal jets and cosmic ray muon showers. The minimum and maximum efficiency for each mass point is calculated, and the difference is used as the uncertainty, which is always less than 3% across all mass points.

C. Selection Criteria

The systematic uncertainty on the signal efficiency due to selection criteria is evaluated by varying each criterion up and down by its known uncertainty. The uncertainties from each criterion are combined in quadrature and the results are shown in Table II. Varying only the jet energy scale produces most of the total uncertainty from the selection criteria. The jet energy scale uncertainty is taken to be $\pm 10\%$ to allow for non-pointing R -hadron decays and is significantly larger than is used in standard ATLAS analyses. Although test-beam studies showed the energy response agrees between data and simulation for hadronic showers to within a few percent [42], even for non-projective showers, a larger uncertainty is conservatively assigned to cover possible differences between single pions and full jets, and between the test-beam detectors studied and the final ATLAS calorimeter.

D. Systematic Uncertainties on Background Yield

The systematic uncertainty on the estimated cosmic background arises from the small number of events in the cosmic background region. This statistical uncertainty is scaled by the same factor used to propagate the cosmic background region data yield into expectations of background events in the search regions. Similarly, for the beam-halo background, a systematic uncertainty is assigned based on the statistical uncertainty of the estimates in the search regions.

XI. RESULTS

The predicted number of background events agrees well with the observed number of events in the search region, as shown in Table V. Using these yields, upper limits on the number of pair-produced gluino, stop, or sbottom signal events are calculated with a simple event-counting method and then interpreted as a function of their masses for a given range of lifetimes.

A. Limit Setting

A Bayesian method is used to set 95% credibility-level upper limits on the number of signal events that could have been produced. For each limit extraction, pseudo-experiments are run. The number of events is sampled from a Poisson distribution, with mean equal to the signal plus background expectation. The systematic uncertainties are taken into account by varying the Poisson mean according to the effect of variations of the sources of the systematic uncertainties [61]. The latter variations are assumed to follow a Gaussian distribution, which is convolved with the Poisson function. A flat prior is used for the signal strength, to be consistent with previous analyses. A Poisson prior gives less conservative limits that are within 10% of those obtained with the flat prior. Since little background is expected and no pseudo-experiment may produce fewer than zero observed events, the distribution of upper limits is bounded from below at -1.15σ . The input data for the limit-setting algorithm can be seen in Table V. The leading jet energy > 300 GeV region is used to set the limits, except for the compressed models with a small difference between the gluino or squark mass and $m_{\tilde{\chi}^0}$, where the leading jet energy > 100 GeV signal region is used.

Signal cross sections are calculated to next-to-leading order in the strong coupling constant, adding the resummation of soft gluon emission at next-to-leading-logarithmic accuracy (NLO+LL) [62–66]. The nominal cross section and the uncertainty are taken from an envelope of cross-section predictions using different PDF sets and factorization and renormalization scales, as described in Ref. [67]. The number of expected signal events is given by the signal cross sections at 7 and 8 TeV, weighted by the integrated luminosities in the 2011 and 2012 data. Figures 8 and 9 show the limits on the number of produced signal events for the various signal models considered, for R -hadron lifetimes in the plateau acceptance region between 10^{-5} and 10^3 seconds.

To provide limits in terms of the gluino, stop, or sbottom masses, the mass is found where the theoretically predicted number of signal events, using the signal cross sections at -1σ of their uncertainties, intersects the experimental limit on the number of signal events produced. The gluino, stop, and sbottom mass limits for each of the signal models, for lifetimes in the plateau acceptance region between 10^{-5} and 10^3 seconds, can be seen in Ta-

ble VI. Figure 10 shows the mass limits for various signal models as a function of lifetime. Limits are also studied as a function of the mass splitting between the gluino or squark and the neutralino. Figure 11 shows the total reconstruction efficiency for a gluino mass of 600 GeV and mass limits for gluino R -hadrons, in the generic R -hadron model with lifetimes in the plateau acceptance region between 10^{-5} and 10^3 seconds, as a function of this mass splitting between the gluino and the neutralino. A similar dependence exists for stop and sbottom efficiencies and mass limits.

XII. SUMMARY

An updated search is presented for stopped long-lived gluino, stop, and sbottom R -hadrons decaying in the calorimeter, using a jet trigger operating in empty crossings of the LHC. Data from the ATLAS experiment recorded in 2011 and 2012 are used, from 5.0 and 22.9 fb^{-1} of pp collisions at 7 and 8 TeV, respectively. The remaining events after all selections are compatible with the expected rate from backgrounds, predominantly cosmic ray and beam-halo muons where no muon track segment is identified. Limits are set on the gluino, stop, and sbottom masses, for different decays, lifetimes, and neutralino masses. With a neutralino of mass 100 GeV, the analysis excludes $m_{\tilde{g}} < 832$ GeV (with an expected lower limit of 731 GeV), for a gluino lifetime between 10 μs and 1000 s in the generic R -hadron model with equal branching ratios for decays to $q\bar{q}\tilde{\chi}^0$ and $g\tilde{\chi}^0$. For the same $m_{\tilde{\chi}^0}$ and squark lifetime assumptions, stop and sbottom are excluded with masses below 379 and 344 GeV, respectively, in the Regge R -hadron model.

ACKNOWLEDGMENTS

We thank CERN for the very successful operation of the LHC, as well as the support staff from our institutions without whom ATLAS could not be operated efficiently.

We acknowledge the support of ANPCyT, Argentina; YerPhI, Armenia; ARC, Australia; BMWF and FWF, Austria; ANAS, Azerbaijan; SSTC, Belarus; CNPq and FAPESP, Brazil; NSERC, NRC and CFI, Canada; CERN; CONICYT, Chile; CAS, MOST and NSFC, China; COLCIENCIAS, Colombia; MSMT CR, MPO CR and VSC CR, Czech Republic; DNRF, DNSRC and Lundbeck Foundation, Denmark; EPLANET, ERC and NSRF, European Union; IN2P3-CNRS, CEA-DSM/IRFU, France; GNSF, Georgia; BMBF, DFG, HGF, MPG and AvH Foundation, Germany; GSRT and NSRF, Greece; ISF, MINERVA, GIF, DIP and Benoziyo Center, Israel; INFN, Italy; MEXT and JSPS, Japan; CNRST, Morocco; FOM and NWO, Netherlands; BRF and RCN, Norway; MNiSW, Poland; GRICES and FCT, Portugal; MNE/IFA, Romania; MES of Russia and ROSATOM, Russian Federation; JINR; MSTD, Serbia;

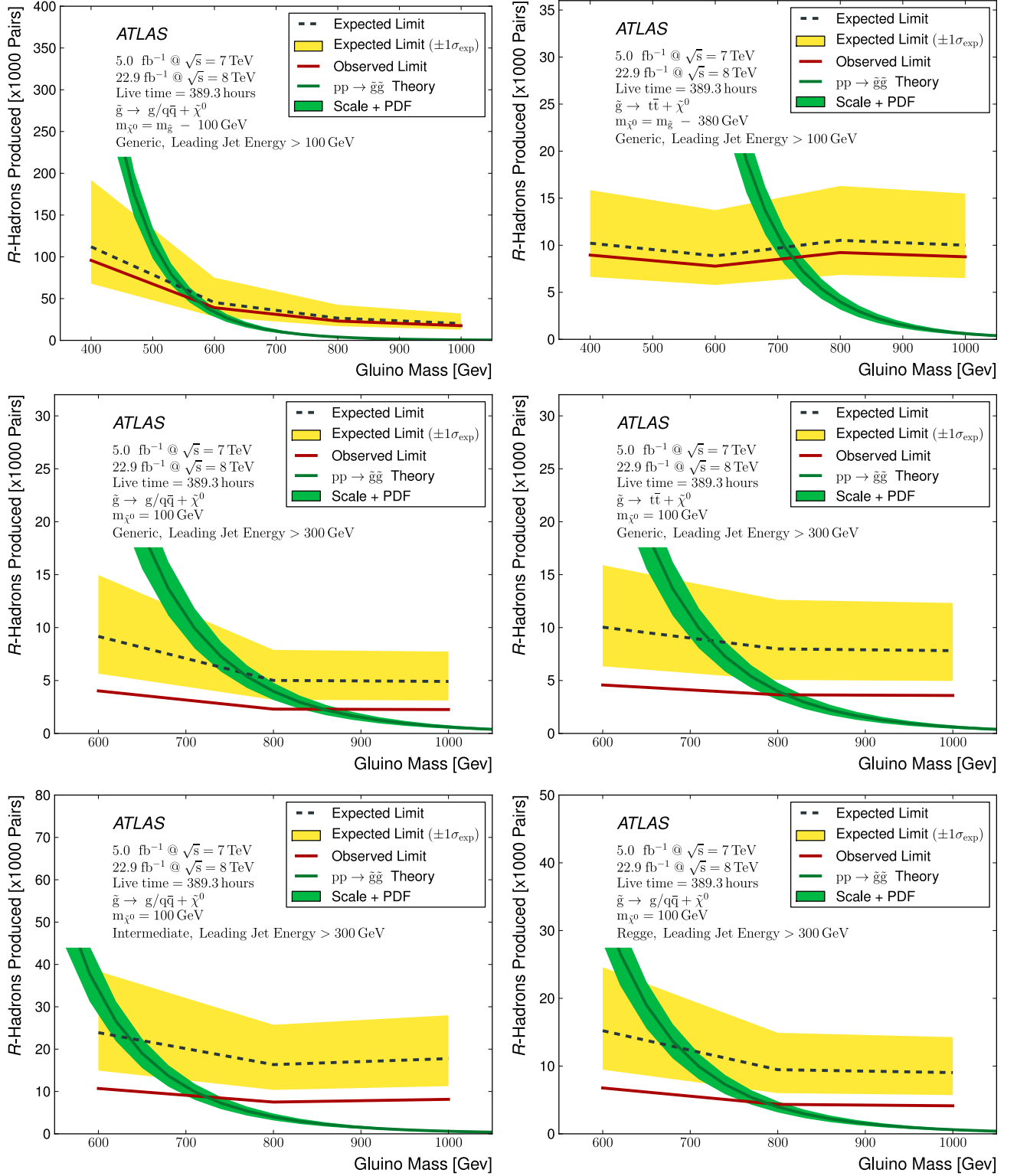


FIG. 8. Bayesian upper limits on gluino events produced versus gluino mass for the various signal models considered, with gluino lifetimes in the plateau acceptance region between 10^{-5} and 10^3 seconds, compared to the theoretical expectations.

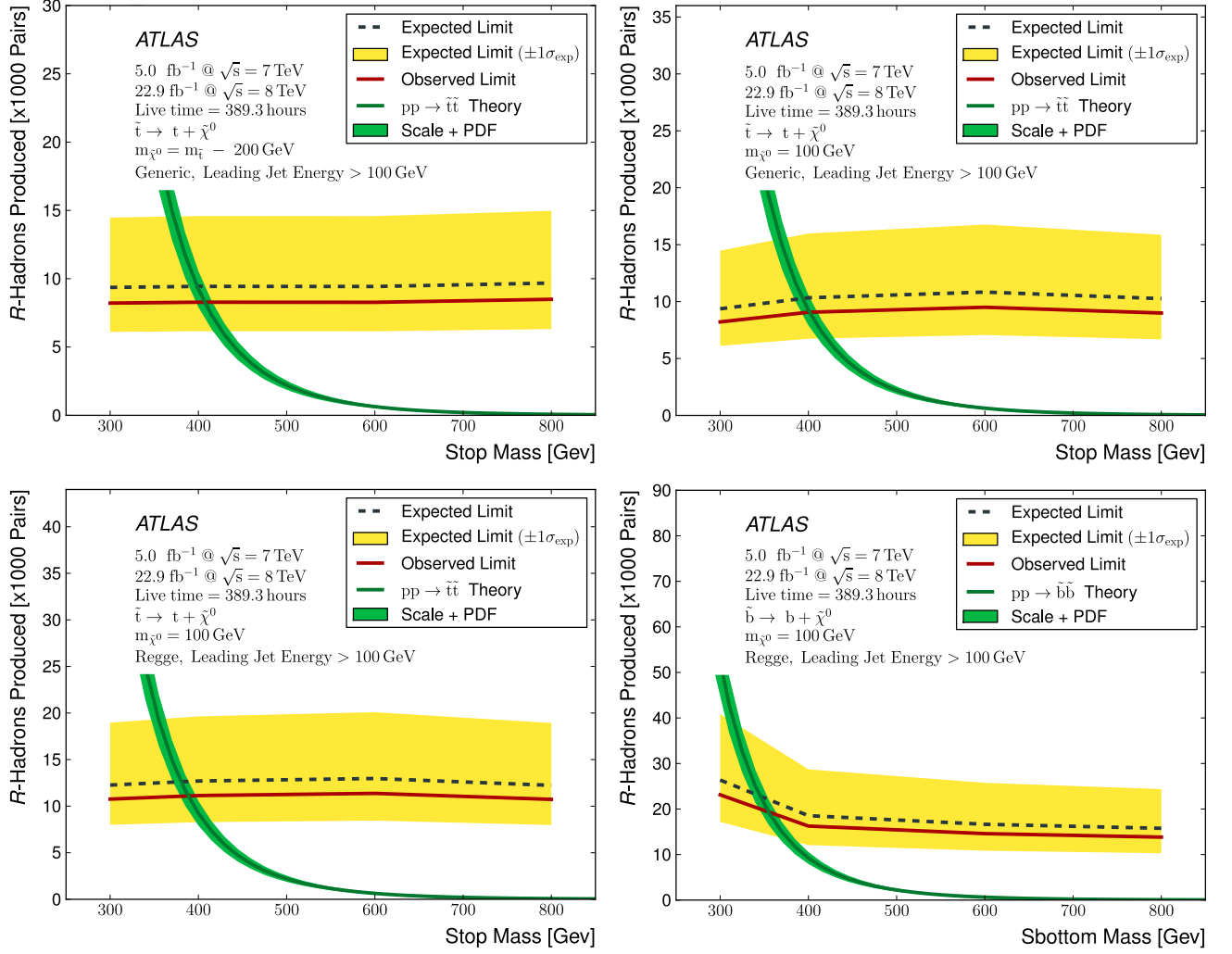


FIG. 9. Bayesian upper limits on stop or sbottom events produced versus stop/sbottom mass for the various signal models considered, with stop/sbottom lifetimes in the plateau acceptance region between 10^{-5} and 10^3 seconds, compared to the theoretical expectations.

TABLE VI. Bayesian lower limits on gluino, stop, and sbottom masses for the various signal models considered, with lifetimes in the plateau acceptance region between 10^{-5} and 10^3 seconds.

Leading jet energy (GeV)	R -hadron model	Gluino/squark decay	Neutralino mass (GeV)	Gluino/squark mass limit (GeV)	
				Expected	Observed
100	Generic	$\tilde{g} \rightarrow g/q\bar{q} + \tilde{\chi}^0$	$m_{\tilde{g}} - 100$	526	545
100	Generic	$\tilde{g} \rightarrow t\bar{t} + \tilde{\chi}^0$	$m_{\tilde{g}} - 380$	694	705
300	Generic	$\tilde{g} \rightarrow g/q\bar{q} + \tilde{\chi}^0$	100	731	832
300	Generic	$\tilde{g} \rightarrow t\bar{t} + \tilde{\chi}^0$	100	700	784
300	Intermediate	$\tilde{g} \rightarrow g/q\bar{q} + \tilde{\chi}^0$	100	615	699
300	Regge	$\tilde{g} \rightarrow g/q\bar{q} + \tilde{\chi}^0$	100	664	758
100	Generic	$\tilde{t} \rightarrow t + \tilde{\chi}^0$	$m_{\tilde{t}} - 200$	389	397
100	Generic	$\tilde{t} \rightarrow t + \tilde{\chi}^0$	100	384	392
100	Regge	$\tilde{t} \rightarrow t + \tilde{\chi}^0$	100	371	379
100	Regge	$\tilde{b} \rightarrow b + \tilde{\chi}^0$	100	334	344

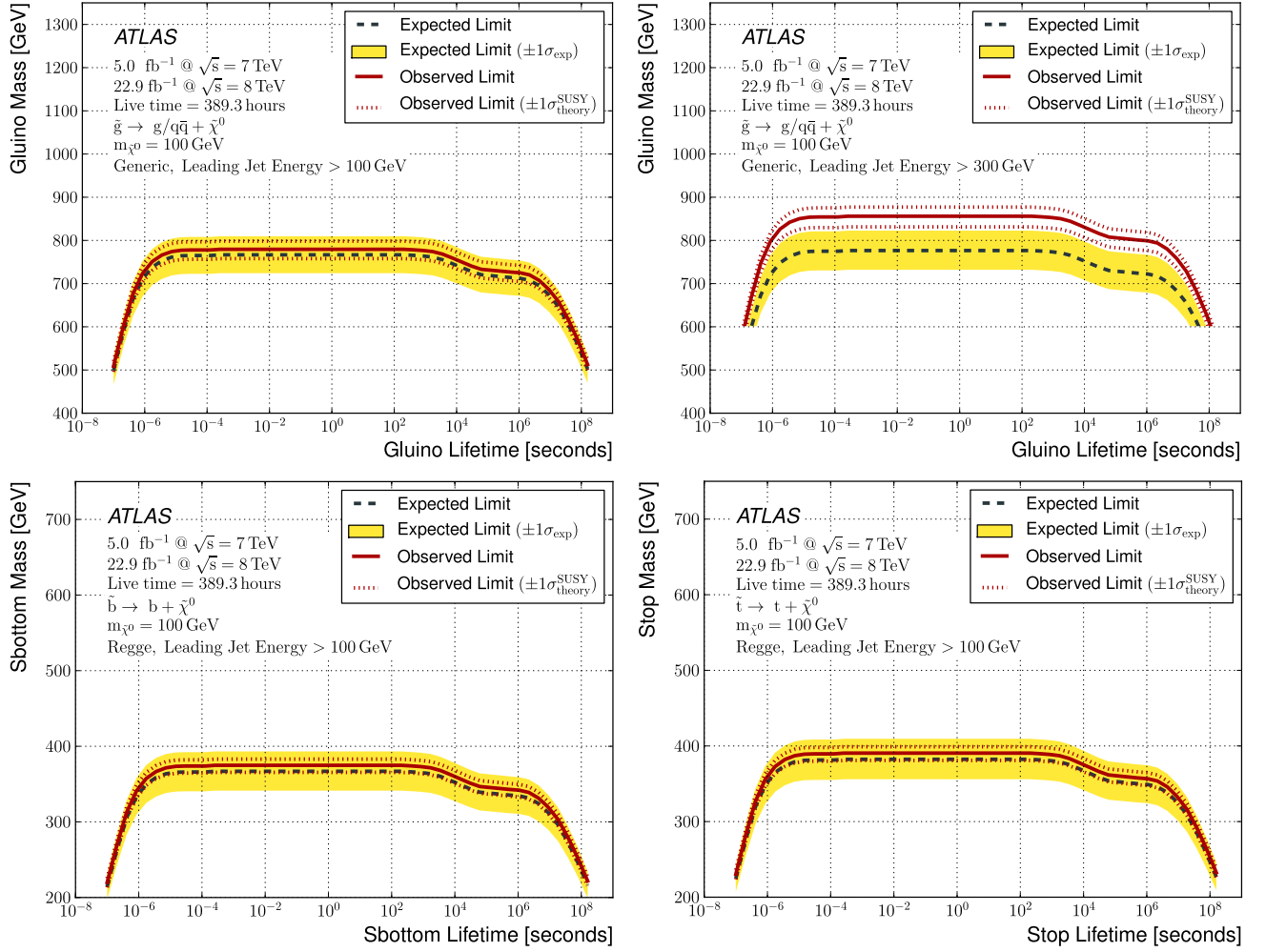


FIG. 10. Bayesian lower limits on gluino, stop, or sbottom mass versus its lifetime, for the two signal regions, with R -hadron lifetimes in the plateau acceptance region between 10^{-5} and 10^3 seconds. An 800 GeV gluino (stop or sbottom), in the generic (Regge) R -hadron model is used as a reference for the stopping fraction and reconstruction efficiency.

MSSR, Slovakia; ARRS and MIZŠ, Slovenia; DST/NRF, South Africa; MINECO, Spain; SRC and Wallenberg Foundation, Sweden; SER, SNSF and Cantons of Bern and Geneva, Switzerland; NSC, Taiwan; TAEK, Turkey; STFC, the Royal Society and Leverhulme Trust, United Kingdom; DOE and NSF, United States of America.

The crucial computing support from all WLCG partners is acknowledged gratefully, in particular from CERN and the ATLAS Tier-1 facilities at TRIUMF (Canada), NDGF (Denmark, Norway, Sweden), CC-IN2P3 (France), KIT/GridKA (Germany), INFN-CNAF (Italy), NL-T1 (Netherlands), PIC (Spain), ASGC (Taiwan), RAL (UK) and BNL (USA) and in the Tier-2 facilities worldwide.

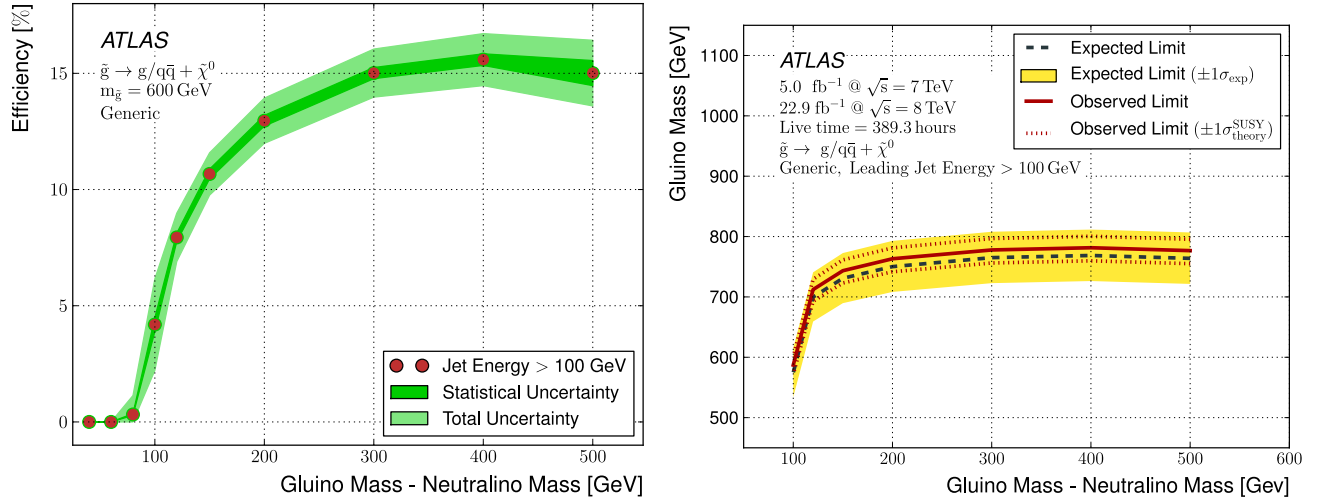


FIG. 11. Total reconstruction efficiency and Bayesian lower limits on gluino mass, as a function of the mass splitting between the gluino and the neutralino, in the generic R -hadron model with gluino lifetimes in the plateau acceptance region between 10^{-5} and 10^3 seconds. A 600 GeV gluino is used as a reference for the reconstruction efficiencies.

- [1] M. Fairbairn et al., *Stable massive particles at colliders*, Phys. Rept. **438** (2007) 1–63, [arXiv:hep-ph/0611040](#).
- [2] H. Miyazawa, *Baryon Number Changing Currents*, Prog. Theor. Phys. **36** (6) (1966) 1266–1276.
- [3] P. Ramond, *Dual Theory for Free Fermions*, Phys. Rev. **D3** (1971) 2415–2418.
- [4] Y. A. Gol’fand and E. P. Likhtman, *Extension of the Algebra of Poincare Group Generators and Violation of p Invariance*, JETP Lett. **13** (1971) 323–326. [Pisma Zh.Eksp.Teor.Fiz.13:452-455,1971].
- [5] A. Neveu and J. H. Schwarz, *Factorizable dual model of pions*, Nucl. Phys. **B31** (1971) 86–112.
- [6] A. Neveu and J. H. Schwarz, *Quark Model of Dual Pions*, Phys. Rev. **D4** (1971) 1109–1111.
- [7] J. Gervais and B. Sakita, *Field theory interpretation of supergauges in dual models*, Nucl. Phys. **B34** (1971) 632–639.
- [8] D. V. Volkov and V. P. Akulov, *Is the Neutrino a Goldstone Particle?*, Phys. Lett. **B46** (1973) 109–110.
- [9] J. Wess and B. Zumino, *A Lagrangian Model Invariant Under Supergauge Transformations*, Phys. Lett. **B49** (1974) 52.
- [10] J. Wess and B. Zumino, *Supergauge Transformations in Four-Dimensions*, Nucl. Phys. **B70** (1974) 39–50.
- [11] P. Fayet, *Supersymmetry and Weak, Electromagnetic and Strong Interactions*, Phys. Lett. **B64** (1976) 159.
- [12] P. Fayet, *Spontaneously Broken Supersymmetric Theories of Weak, Electromagnetic and Strong Interactions*, Phys. Lett. **B69** (1977) 489.
- [13] G. R. Farrar and P. Fayet, *Phenomenology of the Production, Decay, and Detection of New Hadronic States Associated with Supersymmetry*, Phys. Lett. **B76** (1978) 575–579.
- [14] P. Fayet, *Relations Between the Masses of the Superpartners of Leptons and Quarks, the Goldstino Couplings and the Neutral Currents*, Phys. Lett. **B84** (1979) 416.
- [15] S. Dimopoulos and H. Georgi, *Softly Broken Supersymmetry and $SU(5)$* , Nucl. Phys. **B193** (1981) 150.
- [16] N. Arkani-Hamed and S. Dimopoulos, *Supersymmetric unification without low energy supersymmetry and signatures for fine-tuning at the LHC*, JHEP **06** (2005) 073.
- [17] N. Arkani-Hamed, S. Dimopoulos, G. F. Giudice, and A. Romanino, *Aspects of split supersymmetry*, Nucl. Phys. B **709** (2005) 3–46.
- [18] M. Dine and W. Fischler, *A Phenomenological Model of Particle Physics Based on Supersymmetry*, Phys. Lett. **B110** (1982) 227.
- [19] L. Alvarez-Gaume, M. Claudson, and M. B. Wise, *Low-Energy Supersymmetry*, Nucl. Phys. **B207** (1982) 96.
- [20] C. R. Nappi and B. A. Ovrut, *Supersymmetric Extension of the $SU(3) \times SU(2) \times U(1)$ Model*, Phys. Lett. **B113** (1982) 175.
- [21] M. Dine and A. E. Nelson, *Dynamical supersymmetry breaking at low-energies*, Phys. Rev. **D48** (1993) 1277–1287, [arXiv:hep-ph/9303230](#).
- [22] M. Dine, A. E. Nelson, and Y. Shirman, *Low-energy dynamical supersymmetry breaking simplified*, Phys. Rev. **D51** (1995) 1362–1370, [arXiv:hep-ph/9408384](#).
- [23] M. Dine, A. E. Nelson, Y. Nir, and Y. Shirman, *New tools for low-energy dynamical supersymmetry breaking*, Phys. Rev. **D53** (1996) 2658–2669, [arXiv:hep-ph/9507378](#).
- [24] S. Raby, *Gauge-mediated SUSY breaking at an intermediate scale*, Phys. Rev. D **56** (1997) 2852.
- [25] T. Appelquist, H. Cheng, and B. A. Dobrescu, *Bounds on universal extra dimensions*, Phys. Rev. D **64** (2001) .
- [26] C. Friberg, E. Norrbin, and T. Sjostrand, *QCD aspects of leptoquark production at HERA*, Phys. Lett. B. **403** (1997) 329.
- [27] M. Johansen, J. Edsjo, S. Hellman, and D. Milstead, *Long-lived stops in MSSM scenarios with a neutralino LSP*, JHEP **1008** (2010) 005, [arXiv:1003.4540 \[hep-ph\]](#).
- [28] J. A. Evans and Y. Kats, *LHC Coverage of RPV MSSM with Light Stops*, JHEP **1304** (2013) 028, [arXiv:1209.0764 \[hep-ph\]](#).
- [29] A. C. Kraan, *Interactions of heavy stable hadronizing particles*, Eur. Phys. J. **C37** (2004) 91–104, [arXiv:hep-ex/0404001](#).
- [30] L. Evans and P. Bryant, *LHC Machine*, JINST **3** (2008) S08001.
- [31] D0 Collaboration, *Search for stopped gluinos from $p\bar{p}$ collisions at $\sqrt{s} = 1.96$ TeV*, Phys. Rev. Lett. **99** (2007) 131801.
- [32] CMS Collaboration, *Search for stopped gluinos in pp collisions at $\sqrt{s} = 7$ TeV*, Phys. Rev. Lett. **106** (2011) 011801, [arXiv:hep-ex/1011.5861](#).
- [33] CMS Collaboration, *Search for stopped long-lived particles produced in pp collisions at $\sqrt{s} = 7$ TeV*, JHEP **1208** (2012) 026, [arXiv:1207.0106 \[hep-ex\]](#).
- [34] ATLAS Collaboration, *Search for decays of stopped, long-lived particles from 7 TeV pp collisions with the ATLAS detector*, Eur.Phys.J. **C72** (2012) 1965, [arXiv:1201.5595 \[hep-ex\]](#).
- [35] ATLAS Collaboration, *Search for stable hadronising squarks and gluinos with the ATLAS experiment at the LHC*, Phys. Lett. **B701** (2011) 1–19, [arXiv:hep-ex/1103.1984](#).
- [36] ATLAS Collaboration, *Search for heavy long-lived charged particles with the ATLAS detector in pp Collisions at $\sqrt{s} = 7$ TeV*, Phys. Lett. **B703** (2011) 428–446, [arXiv:hep-ex/1106.4495](#).
- [37] ATLAS Collaboration, *The ATLAS Experiment at the CERN Large Hadron Collider*, JINST **3** (2008) S08003.
- [38] ATLAS uses a right-handed coordinate system with its origin at the nominal interaction point (IP) in the center of the detector and the z -axis along the beam pipe. The x -axis points from the IP to the center of the LHC ring, and the y -axis points upward. Cylindrical coordinates (r, ϕ) are used, ϕ being the azimuthal angle around the beam pipe. The pseudorapidity is defined in terms of the polar angle θ as $\eta = -\ln \tan(\theta/2)$.
- [39] ATLAS Collaboration, *Commissioning of the ATLAS Muon Spectrometer with cosmic rays*, The European Physical Journal C **70** (2010) no. 3, 875–916. <http://dx.doi.org/10.1140/epjc/s10052-010-1415-2>.
- [40] W. Lampl, et al., *Calorimeter Clustering Algorithms: Description and Performance*, Tech. Rep.

- ATL-LARG-PUB-2008-002.
 ATL-COM-LARG-2008-003, CERN, Geneva, Apr, 2008.
- [41] M. Cacciari, G. P. Salam, and G. Soyez, *The anti- k_t jet clustering algorithm*, JHEP **04** (2008) 063.
- [42] A. Dotti, A. Lupi, and C. Roda, *Results from ATLAS Tile Calorimeter: a comparison between data and Geant4 simulation*, Nuclear Physics B - Proceedings Supplements **150** (2006) no. 0, 106 – 109.
- [43] ATLAS Collaboration, *Measurement of inclusive jet and dijet cross sections in proton-proton collisions at 7 TeV centre-of-mass energy with the ATLAS detector*, Eur. Phys. J. **C71** (2011) 1521–1571.
- [44] E. Gianfelice-Wendt, W. Bartmann, A. Boccardi, C. Bracco, E. Bravin, et al., *LHC Abort Gap Cleaning Studies During Luminosity Operation*, FERMILAB-CONF-12-142-APC, Fermilab, 2012.
- [45] ATLAS Collaboration, *Measurement of the Rate of Collisions from Satellite Bunches for the April-May 2010 LHC Luminosity Calibration*, ATLAS-CONF-2010-102, CERN, Geneva, Dec, 2010.
- [46] C. Ohm and T. Pauly, *The ATLAS beam pick-up based timing system*, Nucl.Instrum.Meth. **A623** (2010) 558–560, arXiv:0905.3648 [physics.ins-det].
- [47] ATLAS Collaboration, *Performance of the ATLAS Trigger System in 2010*, arXiv:hep-ex/1110.1530v1.
- [48] T. Sjostrand, S. Mrenna, and P. Skands, *PYTHIA 6.4 Physics and Manual*, JHEP **05** (2006) 026, arXiv:hep-ph/0603175.
- [49] J. Pumplin, D. Stump, J. Huston, H. Lai, P. M. Nadolsky, et al., *New generation of parton distributions with uncertainties from global QCD analysis*, JHEP **0207** (2002) 012, arXiv:hep-ph/0201195 [hep-ph].
- [50] B. Andersson, G. Gustafson, G. Ingelman, and T. Sjostrand, *Parton Fragmentation and String Dynamics*, Phys. Rept. **97** (1983) 31–145.
- [51] GEANT4 Collaboration, *GEANT4: A simulation toolkit*, Nucl. Instrum. Meth. **A506** (2003) 250–303.
- [52] ATLAS Collaboration, *The ATLAS simulation infrastructure*, Eur. Phys. J. **C70** (2010) 823–874, arXiv:hep-ex/1005.4568v1.
- [53] R. Mackeprang and A. Rizzi, *Interactions of coloured heavy stable particles in matter*, Eur. Phys. J. **C50** (2007) 353–362, arXiv:hep-ph/0612161.
- [54] Y. R. de Boer, A. B. Kaidalov, D. A. Milstead, and O. I. Piskounova, *Interactions of Heavy Hadrons using Regge Phenomenology and the Quark Gluon String Model*, J. Phys. **G35** (2008) 075009, arXiv:hep-ex/0710.3930.
- [55] R. Mackeprang and D. Milstead, *An Updated Description of Heavy-Hadron Interactions*, Eur. Phys. J. **C66** (2010) 493–501, arXiv:hep-ph/0908.1868.
- [56] G. Farrar, R. Mackeprang, D. Milstead, and J. Roberts, *Limit on the mass of a long-lived or stable gluino*, arXiv:1011.2964.
- [57] A. Arvanitaki, S. Dimopoulos, A. Pierce, S. Rajendran, and J. G. Wacker, *Stopping gluinos*, Phys. Rev. **D76** (2007) 055007, arXiv:hep-ph/0506242.
- [58] L. S. Azhgirey, I. S. Baishiev, K. M. Potter, and V. Talanov, *Machine Induced Background in the High Luminosity Experimental Insertion of the LHC Project*, CERN-LHC-Project-Report-722.
- [59] ATLAS Collaboration, *Characterisation and mitigation of beam-induced backgrounds observed in the ATLAS detector during the 2011 proton-proton run*, JINST **8** (2013) P07004, arXiv:1303.0223 [hep-ex].
- [60] ATLAS Collaboration, *Luminosity Determination in pp Collisions at $\sqrt{s} = 7$ TeV Using the ATLAS Detector at the LHC*, Eur.Phys.J. **C71** (2011) 1630, arXiv:1101.2185 [hep-ex].
- [61] J. Heinrich, C. Blocker, J. Conway, L. Demortier, L. Lyons, G. Punzi, and P. K. Sinervo, *Interval estimation in the presence of nuisance parameters. 1. Bayesian approach*, arXiv:physics/0409129.
- [62] W. Beenakker, R. Hopker, M. Spira, and P. Zerwas, *Squark and gluino production at hadron colliders*, Nucl.Phys. **B492** (1997) 51–103, arXiv:hep-ph/9610490 [hep-ph].
- [63] A. Kulesza and L. Motyka, *Threshold resummation for squark-antisquark and gluino-pair production at the LHC*, Phys.Rev.Lett. **102** (2009) 111802, arXiv:0807.2405 [hep-ph].
- [64] A. Kulesza and L. Motyka, *Soft gluon resummation for the production of gluino-gluino and squark-antisquark pairs at the LHC*, Phys.Rev. **D80** (2009) 095004, arXiv:0905.4749 [hep-ph].
- [65] W. Beenakker, S. Brensing, M. Kramer, A. Kulesza, E. Laenen, et al., *Soft-gluon resummation for squark and gluino hadroproduction*, JHEP **0912** (2009) 041, arXiv:0909.4418 [hep-ph].
- [66] W. Beenakker, S. Brensing, M. Kramer, A. Kulesza, E. Laenen, et al., *Squark and gluino hadroproduction*, Int.J.Mod.Phys. **A26** (2011) 2637–2664, arXiv:1105.1110 [hep-ph].
- [67] M. Kramer, A. Kulesza, R. van der Leeuw, M. Mangano, S. Padhi, et al., *Supersymmetry production cross sections in pp collisions at $\sqrt{s} = 7$ TeV*, arXiv:1206.2892 [hep-ph].

The ATLAS Collaboration

G. Aad⁴⁸, T. Abajyan²¹, B. Abbott¹¹², J. Abdallah¹², S. Abdel Khalek¹¹⁶, O. Abdinov¹¹, R. Aben¹⁰⁶, B. Abi¹¹³, M. Abolins⁸⁹, O.S. AbouZeid¹⁵⁹, H. Abramowicz¹⁵⁴, H. Abreu¹³⁷, Y. Abulaiti^{147a,147b}, B.S. Acharya^{165a,165b,a}, L. Adamczyk^{38a}, D.L. Adams²⁵, T.N. Addy⁵⁶, J. Adelman¹⁷⁷, S. Adomeit⁹⁹, T. Adye¹³⁰, S. Aefsky²³, T. Agatonovic-Jovin^{13b}, J.A. Aguilar-Saavedra^{125b,b}, M. Agustoni¹⁷, S.P. Ahlen²², A. Ahmad¹⁴⁹, F. Ahmadov^{64,c}, M. Ahsan⁴¹, G. Aielli^{134a,134b}, T.P.A. Åkesson⁸⁰, G. Akimoto¹⁵⁶, A.V. Akimov⁹⁵, M.A. Alam⁷⁶, J. Albert¹⁷⁰, S. Albrand⁵⁵, M.J. Alconada Verzini⁷⁰, M. Aleksa³⁰, I.N. Aleksandrov⁶⁴, F. Alessandria^{90a}, C. Alexa^{26a}, G. Alexander¹⁵⁴, G. Alexandre⁴⁹, T. Alexopoulos¹⁰, M. Alhroob^{165a,165c}, M. Aliev¹⁶, G. Alimonti^{90a}, L. Alio⁸⁴, J. Alison³¹, B.M.M. Allbrooke¹⁸, L.J. Allison⁷¹, P.P. Allport⁷³, S.E. Allwood-Spiers⁵³, J. Almond⁸³, A. Aloisio^{103a,103b}, R. Alon¹⁷³, A. Alonso³⁶, F. Alonso⁷⁰, A. Altheimer³⁵, B. Alvarez Gonzalez⁸⁹, M.G. Alvigi^{103a,103b}, K. Amako⁶⁵, Y. Amaral Coutinho^{24a}, C. Amelung²³, V.V. Ammosov^{129,*}, S.P. Amor Dos Santos^{125a}, A. Amorim^{125a,d}, S. Amoroso⁴⁸, N. Amram¹⁵⁴, C. Anastopoulos³⁰, L.S. Ancu¹⁷, N. Andari³⁰, T. Andeen³⁵, C.F. Anders^{58b}, G. Anders^{58a}, K.J. Anderson³¹, A. Andreazza^{90a,90b}, V. Andrei^{58a}, X.S. Anduaga⁷⁰, S. Angelidakis⁹, P. Anger⁴⁴, A. Angerami³⁵, F. Anghinolfi³⁰, A.V. Anisenkov¹⁰⁸, N. Anjos^{125a}, A. Annovi⁴⁷, A. Antonaki⁹, M. Antonelli⁴⁷, A. Antonov⁹⁷, J. Antos^{145b}, F. Anulli^{133a}, M. Aoki¹⁰², L. Aperio Bella¹⁸, R. Apolle^{119,e}, G. Arabidze⁸⁹, I. Aracena¹⁴⁴, Y. Arai⁶⁵, A.T.H. Arce⁴⁵, S. Arfaoui¹⁴⁹, J-F. Arguin⁹⁴, S. Argyropoulos⁴², E. Arik^{19a,*}, M. Arik^{19a}, A.J. Armbruster⁸⁸, O. Arnaez⁸², V. Arnal⁸¹, O. Arslan²¹, A. Artamonov⁹⁶, G. Artoni²³, S. Asai¹⁵⁶, N. Asbah⁹⁴, S. Ask²⁸, B. Åsman^{147a,147b}, L. Asquith⁶, K. Assamagan²⁵, R. Astalos^{145a}, A. Astbury¹⁷⁰, M. Atkinson¹⁶⁶, N.B. Atlay¹⁴², B. Auerbach⁶, E. Auge¹¹⁶, K. Augsten¹²⁷, M. Auresseau^{146b}, G. Avolio³⁰, D. Axen¹⁶⁹, G. Azuelos^{94,f}, Y. Azuma¹⁵⁶, M.A. Baak³⁰, C. Bacci^{135a,135b}, A.M. Bach¹⁵, H. Bachacou¹³⁷, K. Bachas¹⁵⁵, M. Backes³⁰, M. Backhaus²¹, J. Backus Mayes¹⁴⁴, E. Badescu^{26a}, P. Bagiacchi^{133a,133b}, P. Bagnaia^{133a,133b}, Y. Bai^{33a}, D.C. Bailey¹⁵⁹, T. Bain³⁵, J.T. Baines¹³⁰, O.K. Baker¹⁷⁷, S. Baker⁷⁷, P. Balek¹²⁸, F. Balli¹³⁷, E. Banas³⁹, Sw. Banerjee¹⁷⁴, D. Banfi³⁰, A. Bangert¹⁵¹, V. Bansal¹⁷⁰, H.S. Bansil¹⁸, L. Barak¹⁷³, S.P. Baranov⁹⁵, T. Barber⁴⁸, E.L. Barberio⁸⁷, D. Barberis^{50a,50b}, M. Barbero⁸⁴, D.Y. Bardin⁶⁴, T. Barillari¹⁰⁰, M. Barisonzi¹⁷⁶, T. Barklow¹⁴⁴, N. Barlow²⁸, B.M. Barnett¹³⁰, R.M. Barnett¹⁵, A. Baroncelli^{135a}, G. Barone⁴⁹, A.J. Barr¹¹⁹, F. Barreiro⁸¹, J. Barreiro Guimarães da Costa⁵⁷, R. Bartoldus¹⁴⁴, A.E. Barton⁷¹, V. Bartsch¹⁵⁰, A. Bassalat¹¹⁶, A. Basye¹⁶⁶, R.L. Bates⁵³, L. Batkova^{145a}, J.R. Batley²⁸, M. Battistin³⁰, F. Bauer¹³⁷, H.S. Bawa^{144,g}, S. Beale⁹⁹, T. Beau⁷⁹, P.H. Beauchemin¹⁶², R. Beccherle^{50a}, P. Bechtel²¹, H.P. Beck¹⁷, K. Becker¹⁷⁶, S. Becker⁹⁹, M. Beckingham¹³⁹, A.J. Beddall^{19c}, A. Beddall^{19c}, S. Bedikian¹⁷⁷, V.A. Bednyakov⁶⁴, C.P. Bee⁸⁴, L.J. Beemster¹⁰⁶, T.A. Beermann¹⁷⁶, M. Begel²⁵, C. Belanger-Champagne⁸⁶, P.J. Bell⁴⁹, W.H. Bell⁴⁹, G. Bella¹⁵⁴, L. Bellagamba^{20a}, A. Bellerive²⁹, M. Bellomo³⁰, A. Belloni⁵⁷, O.L. Beloborodova^{108,h}, K. Belotskiy⁹⁷, O. Beltramello³⁰, O. Benary¹⁵⁴, D. Bencheikroun^{136a}, K. Bendtz^{147a,147b}, N. Benekos¹⁶⁶, Y. Benhammou¹⁵⁴, E. Benhar Nocchioli⁴⁹, J.A. Benitez Garcia^{160b}, D.P. Benjamin⁴⁵, J.R. Bensinger²³, K. Benslama¹³¹, S. Bentvelsen¹⁰⁶, D. Berge³⁰, E. Bergeaas Kuutmann¹⁶, N. Berger⁵, F. Berghaus¹⁷⁰, E. Berglund¹⁰⁶, J. Beringer¹⁵, C. Bernard²², P. Bernat⁷⁷, R. Bernhard⁴⁸, C. Bernius⁷⁸, F.U. Bernlochner¹⁷⁰, T. Berry⁷⁶, P. Berta¹²⁸, C. Bertella⁸⁴, F. Bertolucci^{123a,123b}, M.I. Besana^{90a}, G.J. Besjes¹⁰⁵, O. Bessidskaia^{147a,147b}, N. Besson¹³⁷, S. Bethke¹⁰⁰, W. Bhimji⁴⁶, R.M. Bianchi¹²⁴, L. Bianchini²³, M. Bianco³⁰, O. Biebel⁹⁹, S.P. Bieniek⁷⁷, K. Bierwagen⁵⁴, J. Biesiada¹⁵, M. Biglietti^{135a}, J. Bilbao De Mendizabal⁴⁹, H. Bilokon⁴⁷, M. Bindi^{20a,20b}, S. Binet¹¹⁶, A. Bingul^{19c}, C. Bini^{133a,133b}, B. Bittner¹⁰⁰, C.W. Black¹⁵¹, J.E. Black¹⁴⁴, K.M. Black²², D. Blackburn¹³⁹, R.E. Blair⁶, J.-B. Blanchard¹³⁷, T. Blazek^{145a}, I. Bloch⁴², C. Blocker²³, J. Blocki³⁹, W. Blum^{82,*}, U. Blumenschein⁵⁴, G.-J. Bobbink¹⁰⁶, V.S. Bobrovnikov¹⁰⁸, S.S. Bocchetta⁸⁰, A. Bocci⁴⁵, C.R. Boddy¹¹⁹, M. Boehler⁴⁸, J. Boek¹⁷⁶, T.T. Boek¹⁷⁶, N. Boelaert³⁶, J.A. Bogaerts³⁰, A.G. Bogdanchikov¹⁰⁸, A. Bogouch^{91,*}, C. Bohm^{147a}, J. Bohm¹²⁶, V. Boisvert⁷⁶, T. Bold^{38a}, V. Boldea^{26a}, A.S. Boldyrev⁹⁸, N.M. Bolnet¹³⁷, M. Bomben⁷⁹, M. Bona⁷⁵, M. Boonekamp¹³⁷, S. Bordini⁷⁹, C. Borer¹⁷, A. Borisov¹²⁹, G. Borissov⁷¹, M. Borri⁸³, S. Borroni⁴², J. Bortfeldt⁹⁹, V. Bortolotto^{135a,135b}, K. Bos¹⁰⁶, D. Boscherini^{20a}, M. Bosman¹², H. Boterenbrood¹⁰⁶, J. Bouchami⁹⁴, J. Boudreau¹²⁴, E.V. Bouhova-Thacker⁷¹, D. Boumediene³⁴, C. Bourdarios¹¹⁶, N. Bousson⁸⁴, S. Boutouil^{136d}, A. Boveia³¹, J. Boyd³⁰, I.R. Boyko⁶⁴, I. Bozovic-Jelisavcic^{13b}, J. Bracinik¹⁸, P. Branchini^{135a}, A. Brandt⁸, G. Brandt¹⁵, O. Brandt⁵⁴, U. Bratzler¹⁵⁷, B. Brau⁸⁵, J.E. Brau¹¹⁵, H.M. Braun^{176,*}, S.F. Brazzale^{165a,165c}, B. Brelier¹⁵⁹, K. Brendlinger¹²¹, R. Brenner¹⁶⁷, S. Bressler¹⁷³, T.M. Bristow⁴⁶, D. Britton⁵³, F.M. Brochu²⁸, I. Brock²¹, R. Brock⁸⁹, F. Broggi^{90a}, C. Bromberg⁸⁹, J. Bronner¹⁰⁰, G. Brooijmans³⁵, T. Brooks⁷⁶, W.K. Brooks^{32b}, E. Brost¹¹⁵, G. Brown⁸³, J. Brown⁵⁵, P.A. Bruckman de Renstrom³⁹, D. Bruncko^{145b}, R. Bruneliere⁴⁸, S. Brunet⁶⁰, A. Bruni^{20a}, G. Bruni^{20a}, M. Bruschi^{20a}, L. Bryngemark⁸⁰, T. Buanes¹⁴, Q. Buat⁵⁵, F. Bucci⁴⁹, J. Buchanan¹¹⁹, P. Buchholz¹⁴², R.M. Buckingham¹¹⁹, A.G. Buckley⁴⁶, S.I. Buda^{26a}, I.A. Budagov⁶⁴, B. Budick¹⁰⁹, F. Buehrer⁴⁸, L. Bugge¹¹⁸, O. Bulekov⁹⁷, A.C. Bundock⁷³, M. Bunse⁴³, H. Burckhart³⁰, S. Burdin⁷³, T. Burgess¹⁴, S. Burke¹³⁰, I. Burnmeister⁴³, E. Busato³⁴, V. Büscher⁸², P. Bussey⁵³, C.P. Buszello¹⁶⁷, B. Butler⁵⁷, J.M. Butler²², A.I. Butt³, C.M. Buttar⁵³, J.M. Butterworth⁷⁷, W. Buttinger²⁸, A. Buzatu⁵³, M. Byszewski¹⁰, S. Cabrera Urbán¹⁶⁸, D. Caforio^{20a,20b},

O. Cakir^{4a}, P. Calafiura¹⁵, G. Calderini⁷⁹, P. Calfayan⁹⁹, R. Calkins¹⁰⁷, L.P. Caloba^{24a}, R. Caloi^{133a,133b}, D. Calvet³⁴, S. Calvet³⁴, R. Camacho Toro⁴⁹, P. Camarri^{134a,134b}, D. Cameron¹¹⁸, L.M. Caminada¹⁵, R. Caminal Armadans¹², S. Campana³⁰, M. Campanelli⁷⁷, V. Canale^{103a,103b}, F. Canelli³¹, A. Canepa^{160a}, J. Cantero⁸¹, R. Cantrill⁷⁶, T. Cao⁴⁰, M.D.M. Capeans Garrido³⁰, I. Caprini^{26a}, M. Caprini^{26a}, M. Capua^{37a,37b}, R. Caputo⁸², R. Cardarelli^{134a}, T. Carli³⁰, G. Carlino^{103a}, L. Carminati^{90a,90b}, S. Caron¹⁰⁵, E. Carquin^{32a}, G.D. Carrillo-Montoya^{146c}, A.A. Carter⁷⁵, J.R. Carter²⁸, J. Carvalho^{125a,i}, D. Casadei⁷⁷, M.P. Casado¹², C. Caso^{50a,50b,*}, E. Castaneda-Miranda^{146b}, A. Castelli¹⁰⁶, V. Castillo Gimenez¹⁶⁸, N.F. Castro^{125a}, G. Cataldi^{72a}, P. Catastini⁵⁷, A. Catinaccio³⁰, J.R. Catmore³⁰, A. Cattai³⁰, G. Cattani^{134a,134b}, S. Caughron⁸⁹, V. Cavaliere¹⁶⁶, D. Cavalli^{90a}, M. Cavalli-Sforza¹², V. Cavasinni^{123a,123b}, F. Ceradini^{135a,135b}, B. Cerio⁴⁵, A.S. Cerqueira^{24b}, A. Cerri¹⁵, L. Cerrito⁷⁵, F. Cerutti¹⁵, A. Cervelli¹⁷, S.A. Cetin^{19b}, A. Chafaq^{136a}, D. Chakraborty¹⁰⁷, I. Chalupkova¹²⁸, K. Chan³, P. Chang¹⁶⁶, B. Chapleau⁸⁶, J.D. Chapman²⁸, J.W. Chapman⁸⁸, D.G. Charlton¹⁸, V. Chavda⁸³, C.A. Chavez Barajas³⁰, S. Cheatham⁸⁶, S. Chekanov⁶, S.V. Chekulaev^{160a}, G.A. Chelkov⁶⁴, M.A. Chelstowska⁸⁸, C. Chen⁶³, H. Chen²⁵, S. Chen^{33c}, X. Chen¹⁷⁴, Y. Chen³⁵, Y. Cheng³¹, A. Cheplakov⁶⁴, R. Cherkaoui El Moursli^{136e}, V. Chernyatin^{25,*}, E. Cheu⁷, L. Chevalier¹³⁷, V. Chiarella⁴⁷, G. Chiefari^{103a,103b}, J.T. Childers³⁰, A. Chilingarov⁷¹, G. Chiodini^{72a}, A.S. Chisholm¹⁸, R.T. Chislett⁷⁷, A. Chitan^{26a}, M.V. Chizhov⁶⁴, G. Choudalakis³¹, S. Chouridou⁹, B.K.B. Chow⁹⁹, I.A. Christidi⁷⁷, A. Christov⁴⁸, D. Chromek-Burckhart³⁰, M.L. Chu¹⁵², J. Chudoba¹²⁶, G. Ciapetti^{133a,133b}, A.K. Ciftci^{4a}, R. Ciftci^{4a}, D. Cinca⁶², V. Cindro⁷⁴, A. Cicio¹⁵, M. Cirilli⁸⁸, P. Cirkovic^{13b}, Z.H. Citron¹⁷³, M. Citterio^{90a}, M. Ciubancan^{26a}, A. Clark⁴⁹, P.J. Clark⁴⁶, R.N. Clarke¹⁵, J.C. Clemens⁸⁴, B. Clement⁵⁵, C. Clement^{147a,147b}, Y. Coadou⁸⁴, M. Cobal^{165a,165c}, A. Coccaro¹³⁹, J. Cochran⁶³, S. Coelli^{90a}, L. Coffey²³, J.G. Cogan¹⁴⁴, J. Coggeshall¹⁶⁶, J. Colas⁵, B. Cole³⁵, S. Cole¹⁰⁷, A.P. Colijn¹⁰⁶, C. Collins-Tooth⁵³, J. Collot⁵⁵, T. Colombo^{58c}, G. Colon⁸⁵, G. Compostella¹⁰⁰, P. Conde Muiño^{125a}, E. Coniavitis¹⁶⁷, M.C. Conidi¹², S.M. Consonni^{90a,90b}, V. Consorti⁴⁸, S. Constantinescu^{26a}, C. Conta^{120a,120b}, G. Conti⁵⁷, F. Conventi^{103a,j}, M. Cooke¹⁵, B.D. Cooper⁷⁷, A.M. Cooper-Sarkar¹¹⁹, N.J. Cooper-Smith⁷⁶, K. Copic¹⁵, T. Cornelissen¹⁷⁶, M. Corradi^{20a}, F. Corriveau^{86,k}, A. Corso-Radu¹⁶⁴, A. Cortes-Gonzalez¹², G. Cortiana¹⁰⁰, G. Costa^{90a}, M.J. Costa¹⁶⁸, D. Costanzo¹⁴⁰, D. Côté⁸, G. Cottin^{32a}, L. Courneyea¹⁷⁰, G. Cowan⁷⁶, B.E. Cox⁸³, K. Cranmer¹⁰⁹, G. Cree²⁹, S. Crépe-Renaudin⁵⁵, F. Crescioli⁷⁹, M. Cristinziani²¹, G. Crosetti^{37a,37b}, C.-M. Cuciu^{26a}, C. Cuenca Almenar¹⁷⁷, T. Cuhadar Donszelmann¹⁴⁰, J. Cummings¹⁷⁷, M. Curatolo⁴⁷, C. Cuthbert¹⁵¹, H. Czirr¹⁴², P. Czodrowski⁴⁴, Z. Czyczula¹⁷⁷, S. D'Auria⁵³, M. D'Onofrio⁷³, A. D'Orazio^{133a,133b}, M.J. Da Cunha Sargedas De Sousa^{125a}, C. Da Via⁸³, W. Dabrowski^{38a}, A. Dafinca¹¹⁹, T. Dai⁸⁸, F. Dallaire⁹⁴, C. Dallapiccola⁸⁵, M. Dam³⁶, D.S. Damiani¹³⁸, A.C. Daniells¹⁸, V. Dao¹⁰⁵, G. Darbo^{50a}, G.L. Darlea^{26c}, S. Darmora⁸, J.A. Dassoulas⁴², W. Davey²¹, C. David¹⁷⁰, T. Davidek¹²⁸, E. Davies^{119,e}, M. Davies⁹⁴, O. Davignon⁷⁹, A.R. Davison⁷⁷, Y. Davygora^{58a}, E. Dawe¹⁴³, I. Dawson¹⁴⁰, R.K. Daya-Ishmukhametova²³, K. De⁸, R. de Asmundis^{103a}, S. De Castro^{20a,20b}, S. De Cecco⁷⁹, J. de Graat⁹⁹, N. De Groot¹⁰⁵, P. de Jong¹⁰⁶, C. De La Taille¹¹⁶, H. De la Torre⁸¹, F. De Lorenzi⁶³, L. De Nooij¹⁰⁶, D. De Pedis^{133a}, A. De Salvo^{133a}, U. De Sanctis^{165a,165c}, A. De Santo¹⁵⁰, J.B. De Vivie De Regie¹¹⁶, G. De Zorzi^{133a,133b}, W.J. Dearnaley⁷¹, R. Debbe²⁵, C. Debenedetti⁴⁶, B. Dechenaux⁵⁵, D.V. Dedovich⁶⁴, J. Degenhardt¹²¹, J. Del Peso⁸¹, T. Del Prete^{123a,123b}, T. Delemontex⁵⁵, F. Deliot¹³⁷, M. Deliyergiyev⁷⁴, A. Dell'Acqua³⁰, L. Dell'Asta²², M. Della Pietra^{103a,j}, D. della Volpe^{103a,103b}, M. Delmastro⁵, P.A. Delsart⁵⁵, C. Deluca¹⁰⁶, S. Demers¹⁷⁷, M. Demichev⁶⁴, A. Demilly⁷⁹, B. Demirkoz^{12,l}, S.P. Denisov¹²⁹, D. Derendarz³⁹, J.E. Derkaoui^{136d}, F. Derue⁷⁹, P. Dervan⁷³, K. Desch²¹, P.O. Deviveiros¹⁰⁶, A. Dewhurst¹³⁰, B. DeWilde¹⁴⁹, S. Dhaliwal¹⁰⁶, R. Dhullipudi^{78,m}, A. Di Ciaccio^{134a,134b}, L. Di Ciaccio⁵, C. Di Donato^{103a,103b}, A. Di Girolamo³⁰, B. Di Girolamo³⁰, A. Di Mattia¹⁵³, B. Di Micco^{135a,135b}, R. Di Nardo⁴⁷, A. Di Simone⁴⁸, R. Di Sipio^{20a,20b}, D. Di Valentino²⁹, M.A. Diaz^{32a}, E.B. Diehl⁸⁸, J. Dietrich⁴², T.A. Dietzsch^{58a}, S. Diglio⁸⁷, K. Dindar Yagci⁴⁰, J. Dingfelder²¹, C. Dionisi^{133a,133b}, P. Dita^{26a}, S. Dita^{26a}, F. Dittus³⁰, F. Djama⁸⁴, T. Djobava^{51b}, M.A.B. do Vale^{24c}, A. Do Valle Wemans^{125a,n}, T.K.O. Doan⁵, D. Dobos³⁰, E. Dobson⁷⁷, J. Dodd³⁵, C. Doglioni⁴⁹, T. Doherty⁵³, T. Dohmae¹⁵⁶, Y. Doi^{65,*}, J. Dolejsi¹²⁸, Z. Dolezal¹²⁸, B.A. Dolgoshein^{97,*}, M. Donadelli^{24d}, S. Donati^{123a,123b}, J. Donini³⁴, J. Dopke³⁰, A. Doria^{103a}, A. Dos Anjos¹⁷⁴, A. Dotti^{123a,123b}, M.T. Dova⁷⁰, A.T. Doyle⁵³, M. Dris¹⁰, J. Dubbert⁸⁸, S. Dube¹⁵, E. Dubreuil³⁴, E. Duchovni¹⁷³, G. Duckeck⁹⁹, D. Duda¹⁷⁶, A. Dudarev³⁰, F. Dudziak⁶³, L. Duflot¹¹⁶, L. Duguid⁷⁶, M. Dührssen³⁰, M. Dunford^{58a}, H. Duran Yildiz^{4a}, M. Düren⁵², M. Dwuznik^{38a}, J. Ebke⁹⁹, W. Edson², C.A. Edwards⁷⁶, N.C. Edwards⁴⁶, W. Ehrenfeld²¹, T. Eifert¹⁴⁴, G. Eigen¹⁴, K. Einsweiler¹⁵, E. Eisenhandler⁷⁵, T. Ekelof¹⁶⁷, M. El Kacimi^{136c}, M. Ellert¹⁶⁷, S. Elles⁵, F. Ellinghaus⁸², K. Ellis⁷⁵, N. Ellis³⁰, J. Elmsheuser⁹⁹, M. Eling³⁰, D. Emelianov¹³⁰, Y. Enari¹⁵⁶, O.C. Endner⁸², R. Engelmann¹⁴⁹, A. Engl⁹⁹, J. Erdmann¹⁷⁷, A. Ereditato¹⁷, D. Eriksson^{147a}, G. Ernis¹⁷⁶, J. Ernst², M. Ernst²⁵, J. Ernwein¹³⁷, D. Errede¹⁶⁶, S. Errede¹⁶⁶, E. Ertel⁸², M. Escalier¹¹⁶, H. Esch⁴³, C. Escobar¹²⁴, X. Espinal Curull¹², B. Esposito⁴⁷, F. Etienne⁸⁴, A.I. Etievre¹³⁷, E. Etzion¹⁵⁴, D. Evangelakou⁵⁴, H. Evans⁶⁰, L. Fabbri^{20a,20b}, G. Facini³⁰, R.M. Fakhruddinov¹²⁹, S. Falciano^{133a}, Y. Fang^{33a}, M. Fanti^{90a,90b}, A. Farbin⁸, A. Farilla^{135a}, T. Farooque¹⁵⁹, S. Farrell¹⁶⁴, S.M. Farrington¹⁷¹, P. Farthouat³⁰, F. Fassi¹⁶⁸, P. Fassnacht³⁰, D. Fassouliotis⁹, B. Fathollahzadeh¹⁵⁹, A. Favareto^{50a,50b}, L. Fayard¹¹⁶, P. Federic^{145a}, O.L. Fedin¹²², W. Fedorko¹⁶⁹, M. Fehling-Kaschek⁴⁸, L. Felgioni⁸⁴,

C. Feng^{33d}, E.J. Feng⁶, H. Feng⁸⁸, A.B. Fenyuk¹²⁹, J. Ferencei^{145b}, W. Fernando⁶, S. Ferrag⁵³, J. Ferrando⁵³, V. Ferrara⁴², A. Ferrari¹⁶⁷, P. Ferrari¹⁰⁶, R. Ferrari^{120a}, D.E. Ferreira de Lima⁵³, A. Ferrer¹⁶⁸, D. Ferrere⁴⁹, C. Ferretti⁸⁸, A. Ferretto Parodi^{50a,50b}, M. Fiascaris³¹, F. Fiedler⁸², A. Filipčić⁷⁴, M. Filipuzzi⁴², F. Filthaut¹⁰⁵, M. Fincke-Keeler¹⁷⁰, K.D. Finelli⁴⁵, M.C.N. Fiolhais^{125a,i}, L. Fiorini¹⁶⁸, A. Firan⁴⁰, J. Fischer¹⁷⁶, M.J. Fisher¹¹⁰, E.A. Fitzgerald²³, M. Flechl⁴⁸, I. Fleck¹⁴², P. Fleischmann¹⁷⁵, S. Fleischmann¹⁷⁶, G.T. Fletcher¹⁴⁰, G. Fletcher⁷⁵, T. Flick¹⁷⁶, A. Floderus⁸⁰, L.R. Flores Castillo¹⁷⁴, A.C. Florez Bustos^{160b}, M.J. Flowerdew¹⁰⁰, T. Fonseca Martin¹⁷, A. Formica¹³⁷, A. Forti⁸³, D. Fortin^{160a}, D. Fournier¹¹⁶, H. Fox⁷¹, P. Francavilla¹², M. Franchini^{20a,20b}, S. Franchino³⁰, D. Francis³⁰, M. Franklin⁵⁷, S. Franz⁶¹, M. Fraternali^{120a,120b}, S. Fratina¹²¹, S.T. French²⁸, C. Friedrich⁴², F. Friedrich⁴⁴, D. Froidevaux³⁰, J.A. Frost²⁸, C. Fukunaga¹⁵⁷, E. Fullana Torregrosa¹²⁸, B.G. Fulsom¹⁴⁴, J. Fuster¹⁶⁸, C. Gabaldon⁵⁵, O. Gabizon¹⁷³, A. Gabrielli^{20a,20b}, A. Gabrielli^{133a,133b}, S. Gadatsch¹⁰⁶, T. Gadfort²⁵, S. Gadowski⁴⁹, G. Gagliardi^{50a,50b}, P. Gagnon⁶⁰, C. Galea⁹⁹, B. Galhardo^{125a}, E.J. Gallas¹¹⁹, V. Gallo¹⁷, B.J. Gallop¹³⁰, P. Gallus¹²⁷, G. Galster³⁶, K.K. Gan¹¹⁰, R.P. Gandrajula⁶², J. Gao^{33b,o}, Y.S. Gao^{144,g}, F.M. Garay Walls⁴⁶, F. Garberson¹⁷⁷, C. García¹⁶⁸, J.E. García Navarro¹⁶⁸, M. Garcia-Sciveres¹⁵, R.W. Gardner³¹, N. Garelli¹⁴⁴, V. Garonne³⁰, C. Gatti⁴⁷, G. Gaudio^{120a}, B. Gaur¹⁴², L. Gauthier⁹⁴, P. Gauzzi^{133a,133b}, I.L. Gavrilenko⁹⁵, C. Gay¹⁶⁹, G. Gaycken²¹, E.N. Gazis¹⁰, P. Ge^{33d,p}, Z. Gece¹⁶⁹, C.N.P. Gee¹³⁰, D.A.A. Geerts¹⁰⁶, Ch. Geich-Gimbel²¹, K. Gellerstedt^{147a,147b}, C. Gemme^{50a}, A. Gemmel⁵³, M.H. Genest⁵⁵, S. Gentile^{133a,133b}, M. George⁵⁴, S. George⁷⁶, D. Gerbaudo¹⁶⁴, A. Gershon¹⁵⁴, H. Ghazlane^{136b}, N. Ghodbane³⁴, B. Giacobbe^{20a}, S. Giagu^{133a,133b}, V. Giangiobbe¹², P. Giannetti^{123a,123b}, F. Gianotti³⁰, B. Gibbard²⁵, S.M. Gibson⁷⁶, M. Gilchriese¹⁵, T.P.S. Gillam²⁸, D. Gillberg³⁰, A.R. Gillman¹³⁰, D.M. Gingrich^{3,f}, N. Giokaris⁹, M.P. Giordani^{165c}, R. Giordano^{103a,103b}, F.M. Giorgi¹⁶, P. Giovannini¹⁰⁰, P.F. Giraud¹³⁷, D. Giugni^{90a}, C. Giuliani⁴⁸, M. Giunta⁹⁴, B.K. Gjelsten¹¹⁸, I. Gkialas^{155,q}, L.K. Gladilin⁹⁸, C. Glasman⁸¹, J. Glatzer²¹, A. Glazov⁴², G.L. Glonti⁶⁴, M. Goblirsch-Kolb¹⁰⁰, J.R. Goddard⁷⁵, J. Godfrey¹⁴³, J. Godlewski³⁰, C. Goeringer⁸², S. Goldfarb⁸⁸, T. Golling¹⁷⁷, D. Golubkov¹²⁹, A. Gomes^{125a,d}, L.S. Gomez Fajardo⁴², R. Gonçalo⁷⁶, J. Goncalves Pinto Firmino Da Costa⁴², L. Gonella²¹, S. González de la Hoz¹⁶⁸, G. Gonzalez Parra¹², M.L. Gonzalez Silva²⁷, S. Gonzalez-Sevilla⁴⁹, J.J. Goodson¹⁴⁹, L. Goossens³⁰, P.A. Gorbounov⁹⁶, H.A. Gordon²⁵, I. Gorelov¹⁰⁴, G. Gorfine¹⁷⁶, B. Gorini³⁰, E. Gorini^{72a,72b}, A. Gorišek⁷⁴, E. Gornicki³⁹, A.T. Goshaw⁶, C. Gössling⁴³, M.I. Gostkin⁶⁴, I. Gough Eschrich¹⁶⁴, M. Gouighri^{136a}, D. Goujdami^{136c}, M.P. Goulette⁴⁹, A.G. Goussiou¹³⁹, C. Goy⁵, S. Gozpinar²³, H.M.X. Grabas¹³⁷, L. Graber⁵⁴, I. Grabowska-Bold^{38a}, P. Grafström^{20a,20b}, K.-J. Grahn⁴², J. Gramling⁴⁹, E. Gramstad¹¹⁸, F. Grancagnolo^{72a}, S. Grancagnolo¹⁶, V. Grassi¹⁴⁹, V. Gratchev¹²², H.M. Gray³⁰, J.A. Gray¹⁴⁹, E. Graziani^{135a}, O.G. Grebenyuk¹²², Z.D. Greenwood^{78,m}, K. Gregersen³⁶, I.M. Gregor⁴², P. Grenier¹⁴⁴, J. Griffiths⁸, N. Grigalashvili⁶⁴, A.A. Grillo¹³⁸, K. Grimm⁷¹, S. Grinstein^{12,r}, Ph. Gris³⁴, Y.V. Grishkevich⁹⁸, J.-F. Grivaz¹¹⁶, J.P. Grohs⁴⁴, A. Grohsjean⁴², E. Gross¹⁷³, J. Grosse-Knetter⁵⁴, J. Groth-Jensen¹⁷³, Z.J. Grout¹⁵⁰, K. Grybel¹⁴², F. Guescini⁴⁹, D. Guest¹⁷⁷, O. Gueta¹⁵⁴, C. Guicheney³⁴, E. Guido^{50a,50b}, T. Guillemin¹¹⁶, S. Guindon², U. Gul⁵³, C. Gumpert⁴⁴, J. Gunther¹²⁷, J. Guo³⁵, S. Gupta¹¹⁹, P. Gutierrez¹¹², N.G. Gutierrez Ortiz⁵³, C. Gutsche⁷⁷, N. Guttman¹⁵⁴, O. Gutzwiller¹⁷⁴, C. Guyot¹³⁷, C. Gwenlan¹¹⁹, C.B. Gwilliam⁷³, A. Haas¹⁰⁹, C. Haber¹⁵, H.K. Hadavand⁸, P. Haefner²¹, S. Hageboeck²¹, Z. Hajduk³⁹, H. Hakobyan¹⁷⁸, D. Hall¹¹⁹, G. Halladjian⁶², K. Hamacher¹⁷⁶, P. Hamal¹¹⁴, K. Hamano⁸⁷, M. Hamer⁵⁴, A. Hamilton^{146a,s}, S. Hamilton¹⁶², L. Han^{33b}, K. Hanagaki¹¹⁷, K. Hanawa¹⁵⁶, M. Hance¹⁵, C. Handel⁸², P. Hanke^{58a}, J.R. Hansen³⁶, J.B. Hansen³⁶, J.D. Hansen³⁶, P.H. Hansen³⁶, P. Hansson¹⁴⁴, K. Hara¹⁶¹, A.S. Hard¹⁷⁴, T. Harenberg¹⁷⁶, S. Harkusha⁹¹, D. Harper⁸⁸, R.D. Harrington⁴⁶, O.M. Harris¹³⁹, P.F. Harrison¹⁷¹, F. Hartjes¹⁰⁶, A. Harvey⁵⁶, S. Hasegawa¹⁰², Y. Hasegawa¹⁴¹, S. Hassani¹³⁷, S. Haug¹⁷, M. Hauschild³⁰, R. Hauser⁸⁹, M. Havranek²¹, C.M. Hawkes¹⁸, R.J. Hawkins³⁰, A.D. Hawkins⁸⁰, T. Hayashi¹⁶¹, D. Hayden⁸⁹, C.P. Hays¹¹⁹, H.S. Hayward⁷³, S.J. Haywood¹³⁰, S.J. Head¹⁸, T. Heck⁸², V. Hedberg⁸⁰, L. Heelan⁸, S. Heim¹²¹, B. Heinemann¹⁵, S. Heisterkamp³⁶, J. Hejbal¹²⁶, L. Helary²², C. Heller⁹⁹, M. Heller³⁰, S. Hellman^{147a,147b}, D. Hellmich²¹, C. Helsen³⁰, J. Henderson¹¹⁹, R.C.W. Henderson⁷¹, A. Henrichs¹⁷⁷, A.M. Henriques Correia³⁰, S. Henrot-Versille¹¹⁶, C. Hensel⁵⁴, G.H. Herbert¹⁶, C.M. Hernandez⁸, Y. Hernández Jiménez¹⁶⁸, R. Herrberg-Schubert¹⁶, G. Herten⁴⁸, R. Hertenberger⁹⁹, L. Hervas³⁰, G.G. Hesketh⁷⁷, N.P. Hesse¹⁰⁶, R. Hickling⁷⁵, E. Higón-Rodriguez¹⁶⁸, J.C. Hill²⁸, K.H. Hiller⁴², S. Hillert²¹, S.J. Hillier¹⁸, I. Hinchliffe¹⁵, E. Hines¹²¹, M. Hirose¹¹⁷, D. Hirschbuehl¹⁷⁶, J. Hobbs¹⁴⁹, N. Hod¹⁰⁶, M.C. Hodgkinson¹⁴⁰, P. Hodgson¹⁴⁰, A. Hoecker³⁰, M.R. Hoferkamp¹⁰⁴, J. Hoffman⁴⁰, D. Hoffmann⁸⁴, J.I. Hofmann^{58a}, M. Hohlfield⁸², S.O. Holmgren^{147a}, T.M. Hong¹²¹, L. Hooft van Huysduynen¹⁰⁹, J.-Y. Hostachy⁵⁵, S. Hou¹⁵², A. Houtmadat^{136a}, J. Howard¹¹⁹, J. Howarth⁸³, M. Hrabovsky¹¹⁴, I. Hristova¹⁶, J. Hrivnac¹¹⁶, T. Hryn'ova⁵, P.J. Hsu⁸², S.-C. Hsu¹³⁹, D. Hu³⁵, X. Hu²⁵, Y. Huang^{146c}, Z. Hubacek³⁰, F. Hubaut⁸⁴, F. Huegging²¹, A. Huettmann⁴², T.B. Huffman¹¹⁹, E.W. Hughes³⁵, G. Hughes⁷¹, M. Huhtinen³⁰, T.A. Hülsing⁸², M. Hurwitz¹⁵, N. Huseynov^{64,c}, J. Huston⁸⁹, J. Huth⁵⁷, G. Iacobucci⁴⁹, G. Iakovidis¹⁰, I. Ibragimov¹⁴², L. Iconomidou-Fayard¹¹⁶, J. Idarraga¹¹⁶, P. Iengo^{103a}, O. Igonkina¹⁰⁶, T. Iizawa¹⁷², Y. Ikegami⁶⁵, K. Ikematsu¹⁴², M. Ikeno⁶⁵, D. Iliadis¹⁵⁵, N. Ilic¹⁵⁹, Y. Inamaru⁶⁶, T. Ince¹⁰⁰, P. Ioannou⁹, M. Iodice^{135a}, K. Iordanidou⁹, V. Ippolito^{133a,133b}, A. Irles Quiles¹⁶⁸, C. Isaksson¹⁶⁷, M. Ishino⁶⁷, M. Ishitsuka¹⁵⁸, R. Ishmukhametov¹¹⁰, C. Issever¹¹⁹, S. Istin^{19a}, A.V. Ivashin¹²⁹, W. Iwanski³⁹,

H. Iwasaki⁶⁵, J.M. Izen⁴¹, V. Izzo^{103a}, B. Jackson¹²¹, J.N. Jackson⁷³, M. Jackson⁷³, P. Jackson¹, M.R. Jaekel³⁰, V. Jain², K. Jakobs⁴⁸, S. Jakobsen³⁶, T. Jakoubek¹²⁶, J. Jakubek¹²⁷, D.O. Jamin¹⁵², D.K. Jana¹¹², E. Jansen⁷⁷, H. Jansen³⁰, J. Janssen²¹, M. Janus¹⁷¹, R.C. Jared¹⁷⁴, G. Jarlskog⁸⁰, L. Jeanty⁵⁷, G.-Y. Jeng¹⁵¹, I. Jen-La Plante³¹, D. Jennens⁸⁷, P. Jenni^{48,t}, J. Jentzsch⁴³, C. Jeske¹⁷¹, S. Jézéquel⁵, M.K. Jha^{20a}, H. Ji¹⁷⁴, W. Ji⁸², J. Jia¹⁴⁹, Y. Jiang^{33b}, M. Jimenez Belenguer⁴², S. Jin^{33a}, O. Jinnouchi¹⁵⁸, M.D. Joergensen³⁶, D. Joffe⁴⁰, K.E. Johansson^{147a}, P. Johansson¹⁴⁰, K.A. Johns⁷, K. Jon-And^{147a,147b}, G. Jones¹⁷¹, R.W.L. Jones⁷¹, T.J. Jones⁷³, P.M. Jorge^{125a}, K.D. Joshi⁸³, J. Jovicevic¹⁴⁸, X. Ju¹⁷⁴, C.A. Jung⁴³, R.M. Jungst³⁰, P. Jussel⁶¹, A. Juste Rozas^{12,r}, M. Kaci¹⁶⁸, A. Kaczmarek³⁹, P. Kadlecik³⁶, M. Kado¹¹⁶, H. Kagan¹¹⁰, M. Kagan¹⁴⁴, E. Kajomovitz⁴⁵, S. Kalinin¹⁷⁶, S. Kama⁴⁰, N. Kanaya¹⁵⁶, M. Kaneda³⁰, S. Kaneti²⁸, T. Kanno¹⁵⁸, V.A. Kantserov⁹⁷, J. Kanzaki⁶⁵, B. Kaplan¹⁰⁹, A. Kapliy³¹, D. Kar⁵³, K. Karakostas¹⁰, N. Karastathis¹⁰, M. Karneviskiy⁸², S.N. Karpov⁶⁴, K. Karthik¹⁰⁹, V. Kartvelishvili⁷¹, A.N. Karyukhin¹²⁹, L. Kashif¹⁷⁴, G. Kasieczka^{58b}, R.D. Kass¹¹⁰, A. Kastanas¹⁴, Y. Kataoka¹⁵⁶, A. Katre⁴⁹, J. Katzy⁴², V. Kaushik⁷, K. Kawagoe⁶⁹, T. Kawamoto¹⁵⁶, G. Kawamura⁵⁴, S. Kazama¹⁵⁶, V.F. Kazanin¹⁰⁸, M.Y. Kazarinov⁶⁴, R. Keeler¹⁷⁰, P.T. Keener¹²¹, R. Kehoe⁴⁰, M. Keil⁵⁴, J.S. Keller¹³⁹, H. Keoshkerian⁵, O. Kepka¹²⁶, B.P. Kerševan⁷⁴, S. Kersten¹⁷⁶, K. Kessoku¹⁵⁶, J. Keung¹⁵⁹, F. Khalil-zada¹¹, H. Khandanyan^{147a,147b}, A. Khanov¹¹³, D. Kharchenko⁶⁴, A. Khodinov⁹⁷, A. Khomich^{58a}, T.J. Khoo²⁸, G. Khorauli²¹, A. Khoroshilov¹⁷⁶, V. Khovanskiy⁹⁶, E. Khramov⁶⁴, J. Khubua^{51b}, H. Kim^{147a,147b}, S.H. Kim¹⁶¹, N. Kimura¹⁷², O. Kind¹⁶, B.T. King⁷³, M. King⁶⁶, R.S.B. King¹¹⁹, S.B. King¹⁶⁹, J. Kirk¹³⁰, A.E. Kiryunin¹⁰⁰, T. Kishimoto⁶⁶, D. Kisielewska^{38a}, T. Kitamura⁶⁶, T. Kittelmann¹²⁴, K. Kiuchi¹⁶¹, E. Kladiva^{145b}, M. Klein⁷³, U. Klein⁷³, K. Kleinknecht⁸², P. Klimek^{147a,147b}, A. Klimentov²⁵, R. Klingenberg⁴³, J.A. Klinger⁸³, E.B. Klinkby³⁶, T. Klioutchnikova³⁰, P.F. Klok¹⁰⁵, E.-E. Kluge^{58a}, P. Kluit¹⁰⁶, S. Kluth¹⁰⁰, E. Kneringer⁶¹, E.B.F.G. Knoops⁸⁴, A. Knue⁵⁴, B.R. Ko⁴⁵, T. Kobayashi¹⁵⁶, M. Kobel⁴⁴, M. Kocian¹⁴⁴, P. Kodys¹²⁸, S. Koenig⁸², P. Koevesarki²¹, T. Koffas²⁹, E. Koffeman¹⁰⁶, L.A. Kogan¹¹⁹, S. Kohlmann¹⁷⁶, F. Kohn⁵⁴, Z. Kohout¹²⁷, T. Kohriki⁶⁵, T. Koi¹⁴⁴, H. Kolanoski¹⁶, I. Koletsou^{90a}, J. Koll⁸⁹, A.A. Komar^{95,*}, Y. Komori¹⁵⁶, T. Kondo⁶⁵, K. Köneke⁴⁸, A.C. König¹⁰⁵, T. Kono^{65,u}, R. Konoplich^{109,v}, N. Konstantinidis⁷⁷, R. Kopeliansky¹⁵³, S. Koperny^{38a}, L. Köpke⁸², A.K. Kopp⁴⁸, K. Korcyl³⁹, K. Kordas¹⁵⁵, A. Korn⁴⁶, A.A. Korol¹⁰⁸, I. Korolkov¹², E.V. Korolkova¹⁴⁰, V.A. Korotkov¹²⁹, O. Kortner¹⁰⁰, S. Kortner¹⁰⁰, V.V. Kostyukhin²¹, S. Kotov¹⁰⁰, V.M. Kotov⁶⁴, A. Kotwal⁴⁵, C. Kourkoumelis⁹, V. Kouskoura¹⁵⁵, A. Koutsman^{160a}, R. Kowalewski¹⁷⁰, T.Z. Kowalski^{38a}, W. Kozanecki¹³⁷, A.S. Kozhin¹²⁹, V. Kral¹²⁷, V.A. Kramarenko⁹⁸, G. Kramberger⁷⁴, M.W. Krasny⁷⁹, A. Krasznahorkay¹⁰⁹, J.K. Kraus²¹, A. Kravchenko²⁵, S. Kreiss¹⁰⁹, J. Kretzschmar⁷³, K. Kreutzfeldt⁵², N. Krieger⁵⁴, P. Krieger¹⁵⁹, K. Kroeninger⁵⁴, H. Kroha¹⁰⁰, J. Kroll¹²¹, J. Kroseberg²¹, J. Krstic^{13a}, U. Kruchonak⁶⁴, H. Krüger²¹, T. Kruker¹⁷, N. Krumnack⁶³, Z.V. Krumshteyn⁶⁴, A. Kruse¹⁷⁴, M.C. Kruse⁴⁵, M. Kruskal²², T. Kubota⁸⁷, S. Kuday^{4a}, S. Kuehn⁴⁸, A. Kugel^{58c}, T. Kuhl⁴², V. Kukhtin⁶⁴, Y. Kulchitsky⁹¹, S. Kuleshov^{32b}, M. Kuna^{133a,133b}, J. Kunkle¹²¹, A. Kupco¹²⁶, H. Kurashige⁶⁶, M. Kurata¹⁶¹, Y.A. Kurochkin⁹¹, R. Kurumida⁶⁶, V. Kus¹²⁶, E.S. Kuwertz¹⁴⁸, M. Kuze¹⁵⁸, J. Kvita¹⁴³, R. Kwee¹⁶, A. La Rosa⁴⁹, L. La Rotonda^{37a,37b}, L. Labarga⁸¹, S. Lablak^{136a}, C. Lacasta¹⁶⁸, F. Lacava^{133a,133b}, J. Lacey²⁹, H. Lacker¹⁶, D. Lacour⁷⁹, V.R. Lacuesta¹⁶⁸, E. Ladygin⁶⁴, R. Lafaye⁵, B. Laforge⁷⁹, T. Lagouri¹⁷⁷, S. Lai⁴⁸, H. Laier^{58a}, E. Laisne⁵⁵, L. Lambourne⁷⁷, C.L. Lampen⁷, W. Lampl⁷, E. Lançon¹³⁷, U. Landgraf⁴⁸, M.P.J. Landon⁷⁵, V.S. Lang^{58a}, C. Lange⁴², A.J. Lankford¹⁶⁴, F. Lanni²⁵, K. Lantzsck³⁰, A. Lanza^{120a}, S. Laplace⁷⁹, C. Lapoire²¹, J.F. Laporte¹³⁷, T. Lari^{90a}, A. Larner¹¹⁹, M. Lassnig³⁰, P. Laurelli⁴⁷, V. Lavorini^{37a,37b}, W. Lavrijsen¹⁵, P. Laycock⁷³, B.T. Le⁵⁵, O. Le Dortz⁷⁹, E. Le Guirriec⁸⁴, E. Le Menedeu¹², T. LeCompte⁶, F. Ledroit-Guillon⁵⁵, C.A. Lee¹⁵², H. Lee¹⁰⁶, J.S.H. Lee¹¹⁷, S.C. Lee¹⁵², L. Lee¹⁷⁷, G. Lefebvre⁷⁹, M. Lefebvre¹⁷⁰, M. Legendre¹³⁷, F. Legger⁹⁹, C. Leggett¹⁵, A. Lehan⁷³, M. Lehmacher²¹, G. Lehmann Miotto³⁰, A.G. Leister¹⁷⁷, M.A.L. Leite^{24d}, R. Leitner¹²⁸, D. Lellouch¹⁷³, B. Lemmer⁵⁴, V. Lendermann^{58a}, K.J.C. Leney^{146c}, T. Lenz¹⁰⁶, G. Lenzen¹⁷⁶, B. Lenzi³⁰, R. Leone⁷, K. Leonhardt⁴⁴, S. Leontsinis¹⁰, C. Leroy⁹⁴, J.-R. Lessard¹⁷⁰, C.G. Lester²⁸, C.M. Lester¹²¹, J. Levêque⁵, D. Levin⁸⁸, L.J. Levinson¹⁷³, A. Lewis¹¹⁹, G.H. Lewis¹⁰⁹, A.M. Leyko²¹, M. Leyton¹⁶, B. Li^{33b,w}, B. Li⁸⁴, H. Li¹⁴⁹, H.L. Li³¹, S. Li⁴⁵, X. Li⁸⁸, Z. Liang^{119,x}, H. Liao³⁴, B. Liberti^{134a}, P. Lichard³⁰, K. Lie¹⁶⁶, J. Liebal²¹, W. Liebig¹⁴, C. Limbach²¹, A. Limosani⁸⁷, M. Limper⁶², S.C. Lin^{152,y}, F. Linde¹⁰⁶, B.E. Lindquist¹⁴⁹, J.T. Linnemann⁸⁹, E. Lipeles¹²¹, A. Lipniacka¹⁴, M. Lisovyi⁴², T.M. Liss¹⁶⁶, D. Lissauer²⁵, A. Lister¹⁶⁹, A.M. Litke¹³⁸, B. Liu¹⁵², D. Liu¹⁵², J.B. Liu^{33b}, K. Liu^{33b,z}, L. Liu⁸⁸, M. Liu⁴⁵, M. Liu^{33b}, Y. Liu^{33b}, M. Livan^{120a,120b}, S.S.A. Livermore¹¹⁹, A. Lleres⁵⁵, J. Llorente Merino⁸¹, S.L. Lloyd⁷⁵, F. Lo Sterzo^{133a,133b}, E. Lobodzinska⁴², P. Loch⁷, W.S. Lockman¹³⁸, T. Loddenkoetter²¹, F.K. Loebinger⁸³, A.E. Loevschall-Jensen³⁶, A. Loginov¹⁷⁷, C.W. Loh¹⁶⁹, T. Lohse¹⁶, K. Lohwasser⁴⁸, M. Lokajicek¹²⁶, V.P. Lombardo⁵, R.E. Long⁷¹, L. Lopes^{125a}, D. Lopez Mateos⁵⁷, B. Lopez Paredes¹⁴⁰, J. Lorenz⁹⁹, N. Lorenzo Martinez¹¹⁶, M. Losada¹⁶³, P. Loscutoff¹⁵, M.J. Losty^{160a,*}, X. Lou⁴¹, A. Lounis¹¹⁶, J. Love⁶, P.A. Love⁷¹, A.J. Lowe^{144,g}, F. Lu^{33a}, H.J. Lubatti¹³⁹, C. Luci^{133a,133b}, A. Lucotte⁵⁵, D. Ludwig⁴², I. Ludwig⁴⁸, J. Ludwig⁴⁸, F. Luehring⁶⁰, W. Lukas⁶¹, L. Luminari^{133a}, E. Lund¹¹⁸, J. Lundberg^{147a,147b}, O. Lundberg^{147a,147b}, B. Lund-Jensen¹⁴⁸, M. Lungwitz⁸², D. Lynn²⁵, R. Lysak¹²⁶, E. Lytken⁸⁰, H. Ma²⁵, L.L. Ma^{33d}, G. Maccarrone⁴⁷, A. Macchiolo¹⁰⁰, B. Maček⁷⁴, J. Machado Miguens^{125a}, D. Macina³⁰, R. Mackeprang³⁶, R. Madar⁴⁸, R.J. Madaras¹⁵, H.J. Maddocks⁷¹, W.F. Mader⁴⁴, A. Madsen¹⁶⁷, M. Maeno⁸, T. Maeno²⁵, L. Magnoni¹⁶⁴, E. Magradze⁵⁴,

K. Mahboubi⁴⁸, J. Mahlstedt¹⁰⁶, S. Mahmoud⁷³, G. Mahout¹⁸, C. Maiani¹³⁷, C. Maidantchik^{24a}, A. Maio^{125a,d},
 S. Majewski¹¹⁵, Y. Makida⁶⁵, N. Makovec¹¹⁶, P. Mal^{137,aa}, B. Malaescu⁷⁹, Pa. Malecki³⁹, V.P. Maleev¹²²,
 F. Malek⁵⁵, U. Mallik⁶², D. Malon⁶, C. Malone¹⁴⁴, S. Maltezos¹⁰, V.M. Malyshev¹⁰⁸, S. Malyukov³⁰, J. Mamuzic^{13b},
 L. Mandelli^{90a}, I. Mandic⁷⁴, R. Mandrysch⁶², J. Maneira^{125a}, A. Manfredini¹⁰⁰, L. Manhaes de Andrade Filho^{24b},
 J.A. Manjarres Ramos¹³⁷, A. Mann⁹⁹, P.M. Manning¹³⁸, A. Manousakis-Katsikakis⁹, B. Mansoulie¹³⁷,
 R. Mantifel⁸⁶, L. Mapelli³⁰, L. March¹⁶⁸, J.F. Marchand²⁹, F. Marchese^{134a,134b}, G. Marchiori⁷⁹, M. Marcisovsky¹²⁶,
 C.P. Marino¹⁷⁰, C.N. Marques^{125a}, F. Marroquin^{24a}, Z. Marshall¹⁵, L.F. Marti¹⁷, S. Marti-Garcia¹⁶⁸, B. Martin³⁰,
 B. Martin⁸⁹, J.P. Martin⁹⁴, T.A. Martin¹⁷¹, V.J. Martin⁴⁶, B. Martin dit Latour⁴⁹, H. Martinez¹³⁷, M. Martinez^{12,r},
 S. Martin-Haugh¹⁵⁰, A.C. Martyniuk¹⁷⁰, M. Marx¹³⁹, F. Marzano^{133a}, A. Marzin¹¹², L. Masetti⁸², T. Mashimo¹⁵⁶,
 R. Mashinistov⁹⁵, J. Masik⁸³, A.L. Maslennikov¹⁰⁸, I. Massa^{20a,20b}, N. Massol⁵, P. Mastrandrea¹⁴⁹,
 A. Mastroberardino^{37a,37b}, T. Masubuchi¹⁵⁶, H. Matsunaga¹⁵⁶, T. Matsushita⁶⁶, P. Mättig¹⁷⁶, S. Mättig⁴²,
 J. Mattmann⁸², C. Mattravers^{119,e}, J. Maurer⁸⁴, S.J. Maxfield⁷³, D.A. Maximov^{108,h}, R. Mazini¹⁵²,
 L. Mazzaferro^{134a,134b}, M. Mazzanti^{90a}, G. Mc Goldrick¹⁵⁹, S.P. Mc Kee⁸⁸, A. McCarn¹⁶⁶, R.L. McCarthy¹⁴⁹,
 T.G. McCarthy²⁹, N.A. McCubbin¹³⁰, K.W. McFarlane^{56,*}, J.A. MCFayden¹⁴⁰, G. Mchedlidze^{51b}, T. McLaughlan¹⁸,
 S.J. McMahon¹³⁰, R.A. McPherson^{170,k}, A. Meade⁸⁵, J. Mechnich¹⁰⁶, M. Mechtel¹⁷⁶, M. Medinnis⁴², S. Meehan³¹,
 R. Meera-Lebbai¹¹², S. Mehlhase³⁶, A. Mehta⁷³, K. Meier^{58a}, C. Meineck⁹⁹, B. Meirose⁸⁰, C. Melachrinou³¹,
 B.R. Mellado Garcia^{146c}, F. Meloni^{90a,90b}, L. Mendoza Navas¹⁶³, A. Mengarelli^{20a,20b}, S. Menke¹⁰⁰, E. Meoni¹⁶²,
 K.M. Mercurio⁵⁷, S. Mergelmeyer²¹, N. Meric¹³⁷, P. Mermod⁴⁹, L. Merola^{103a,103b}, C. Meroni^{90a}, F.S. Merritt³¹,
 H. Merritt¹¹⁰, A. Messina^{30,ab}, J. Metcalfe²⁵, A.S. Mete¹⁶⁴, C. Meyer⁸², C. Meyer³¹, J-P. Meyer¹³⁷, J. Meyer³⁰,
 J. Meyer⁵⁴, S. Michal³⁰, R.P. Middleton¹³⁰, S. Migas⁷³, L. Mijović¹³⁷, G. Mikenberg¹⁷³, M. Mikestikova¹²⁶,
 M. Mikuz⁷⁴, D.W. Miller³¹, W.J. Mills¹⁶⁹, C. Mills⁵⁷, A. Milov¹⁷³, D.A. Milstead^{147a,147b}, D. Milstein¹⁷³,
 A.A. Minaenko¹²⁹, M. Miñano Moya¹⁶⁸, I.A. Minashvili⁶⁴, A.I. Mincer¹⁰⁹, B. Mindur^{38a}, M. Mineev⁶⁴, Y. Ming¹⁷⁴,
 L.M. Mir¹², G. Mirabelli^{133a}, T. Mitani¹⁷², J. Mitrevski¹³⁸, V.A. Mitsou¹⁶⁸, S. Mitsui⁶⁵, P.S. Miyagawa¹⁴⁰,
 J.U. Mjörnmark⁸⁰, T. Moa^{147a,147b}, V. Moeller²⁸, S. Mohapatra¹⁴⁹, W. Mohr⁴⁸, S. Molander^{147a,147b},
 R. Moles-Valls¹⁶⁸, A. Molfetas³⁰, K. Mönig⁴², C. Monini⁵⁵, J. Monk³⁶, E. Monnier⁸⁴, J. Montejo Berlingen¹²,
 F. Monticelli⁷⁰, S. Monzani^{20a,20b}, R.W. Moore³, C. Mora Herrera⁴⁹, A. Moraes⁵³, N. Morange⁶², J. Morel⁵⁴,
 D. Moreno⁸², M. Moreno Llácer¹⁶⁸, P. Morettini^{50a}, M. Morgenstern⁴⁴, M. Morii⁵⁷, S. Moritz⁸², A.K. Morley¹⁴⁸,
 G. Mornacchi³⁰, J.D. Morris⁷⁵, L. Morvaj¹⁰², H.G. Moser¹⁰⁰, M. Mosidze^{51b}, J. Moss¹¹⁰, R. Mount¹⁴⁴,
 E. Mountricha^{10,ac}, S.V. Mouraviev^{95,*}, E.J.W. Moyse⁸⁵, R.D. Mudd¹⁸, F. Mueller^{58a}, J. Mueller¹²⁴, K. Mueller²¹,
 T. Mueller²⁸, T. Mueller⁸², D. Muenstermann⁴⁹, Y. Munwes¹⁵⁴, J.A. Murillo Quijada¹⁸, W.J. Murray¹³⁰,
 I. Mussche¹⁰⁶, E. Musto¹⁵³, A.G. Myagkov^{129,ad}, M. Myska¹²⁶, O. Nackenhorst⁵⁴, J. Nadal¹², K. Nagai⁶¹,
 R. Nagai¹⁵⁸, Y. Nagai⁸⁴, K. Nagano⁶⁵, A. Nagarkar¹¹⁰, Y. Nagasaka⁵⁹, M. Nagel¹⁰⁰, A.M. Nairz³⁰, Y. Nakahama³⁰,
 K. Nakamura⁶⁵, T. Nakamura¹⁵⁶, I. Nakano¹¹¹, H. Namasivayam⁴¹, G. Nanava²¹, A. Napier¹⁶², R. Narayan^{58b},
 M. Nash^{77,e}, T. Nattermann²¹, T. Naumann⁴², G. Navarro¹⁶³, H.A. Neal⁸⁸, P.Yu. Nechaeva⁹⁵, T.J. Neep⁸³,
 A. Negri^{120a,120b}, G. Negri³⁰, M. Negrini^{20a}, S. Nektarijevic⁴⁹, A. Nelson¹⁶⁴, T.K. Nelson¹⁴⁴, S. Nemecek¹²⁶,
 P. Nemethy¹⁰⁹, A.A. Nepomuceno^{24a}, M. Nessi^{30,ae}, M.S. Neubauer¹⁶⁶, M. Neumann¹⁷⁶, A. Neusiedl⁸²,
 R.M. Neves¹⁰⁹, P. Nevski²⁵, F.M. Newcomer¹²¹, P.R. Newman¹⁸, D.H. Nguyen⁶, V. Nguyen Thi Hong¹³⁷,
 R.B. Nickerson¹¹⁹, R. Nicolaidou¹³⁷, B. Nicquevert³⁰, J. Nielsen¹³⁸, N. Nikiforou³⁵, A. Nikiforov¹⁶,
 V. Nikolaenko^{129,ad}, I. Nikolic-Audit⁷⁹, K. Nikolics⁴⁹, K. Nikolopoulos¹⁸, P. Nilsson⁸, Y. Ninomiya¹⁵⁶, A. Nisati^{133a},
 R. Nisius¹⁰⁰, T. Nobe¹⁵⁸, L. Nodulman⁶, M. Nomachi¹¹⁷, I. Nomidis¹⁵⁵, S. Norberg¹¹², M. Nordberg³⁰,
 J. Novakova¹²⁸, M. Nozaki⁶⁵, L. Nozka¹¹⁴, K. Ntekas¹⁰, A.-E. Nuncio-Quiroz²¹, G. Nunes Hanninger⁸⁷,
 T. Nunnemann⁹⁹, E. Nurse⁷⁷, B.J. O'Brien⁴⁶, F. O'grady⁷, D.C. O'Neil¹⁴³, V. O'Shea⁵³, L.B. Oakes⁹⁹,
 F.G. Oakham^{29,f}, H. Oberlack¹⁰⁰, J. Ocariz⁷⁹, A. Ochi⁶⁶, M.I. Ochoa⁷⁷, S. Oda⁶⁹, S. Odaka⁶⁵, J. Odier⁸⁴,
 H. Ogren⁶⁰, A. Oh⁸³, S.H. Oh⁴⁵, C.C. Ohm³⁰, T. Ohshima¹⁰², W. Okamura¹¹⁷, H. Okawa²⁵, Y. Okumura³¹,
 T. Okuyama¹⁵⁶, A. Olariu^{26a}, A.G. Olchevski⁶⁴, S.A. Olivares Pino⁴⁶, M. Oliveira^{125a,i}, D. Oliveira Damazio²⁵,
 E. Oliver Garcia¹⁶⁸, D. Olivito¹²¹, A. Olszewski³⁹, J. Olszowska³⁹, A. Onofre^{125a,af}, P.U.E. Onyisi^{31,ag},
 C.J. Oram^{160a}, M.J. Oreglia³¹, Y. Oren¹⁵⁴, D. Orestano^{135a,135b}, N. Orlando^{72a,72b}, C. Oropeza Barrera⁵³,
 R.S. Orr¹⁵⁹, B. Osculati^{50a,50b}, R. Ospanov¹²¹, G. Otero y Garzon²⁷, H. Otono⁶⁹, J.P. Ottersbach¹⁰⁶,
 M. Ouchrif^{136d}, E.A. Ouellette¹⁷⁰, F. Ould-Saada¹¹⁸, A. Ouraou¹³⁷, K.P. Oussoren¹⁰⁶, Q. Ouyang^{33a},
 A. Ovcharova¹⁵, M. Owen⁸³, S. Owen¹⁴⁰, V.E. Ozcan^{19a}, N. Ozturk⁸, K. Pachal¹¹⁹, A. Pacheco Pages¹²,
 C. Padilla Aranda¹², S. Pagan Griso¹⁵, E. Paganis¹⁴⁰, C. Pahl¹⁰⁰, F. Paige²⁵, P. Pais⁸⁵, K. Pajchel¹¹⁸,
 G. Palacino^{160b}, S. Palestini³⁰, D. Pallin³⁴, A. Palma^{125a}, J.D. Palmer¹⁸, Y.B. Pan¹⁷⁴, E. Panagiotopoulou¹⁰,
 J.G. Panduro Vazquez⁷⁶, P. Pani¹⁰⁶, N. Panikashvili⁸⁸, S. Panitkin²⁵, D. Pantea^{26a}, A. Papadelis^{147a},
 Th.D. Papadopoulou¹⁰, K. Papageorgiou^{155,q}, A. Paramonov⁶, D. Paredes Hernandez³⁴, M.A. Parker²⁸,
 F. Parodi^{50a,50b}, J.A. Parsons³⁵, U. Parzefall⁴⁸, S. Pashapour⁵⁴, E. Pasqualucci^{133a}, S. Passaggio^{50a}, A. Passeri^{135a},
 F. Pastore^{135a,135b,*}, Fr. Pastore⁷⁶, G. Pásztor^{49,ah}, S. Pataria¹⁷⁶, N.D. Patel¹⁵¹, J.R. Pater⁸³, S. Patricelli^{103a,103b},
 T. Pauly³⁰, J. Pearce¹⁷⁰, M. Pedersen¹¹⁸, S. Pedraza Lopez¹⁶⁸, M.I. Pedraza Morales¹⁷⁴, S.V. Peleganchuk¹⁰⁸,
 D. Pelikan¹⁶⁷, H. Peng^{33b}, B. Penning³¹, A. Penson³⁵, J. Penwell⁶⁰, D.V. Perepelitsa³⁵, T. Perez Cavalcanti⁴²,

E. Perez Codina^{160a}, M.T. Pérez García-Estañ¹⁶⁸, V. Perez Reale³⁵, L. Perini^{90a,90b}, H. Pernegger³⁰, R. Perrino^{72a}, V.D. Peshekhonov⁶⁴, K. Peters³⁰, R.F.Y. Peters^{54,ai}, B.A. Petersen³⁰, J. Petersen³⁰, T.C. Petersen³⁶, E. Petit⁵, A. Petridis^{147a,147b}, C. Petridou¹⁵⁵, E. Petrolo^{133a}, F. Petrucci^{135a,135b}, M. Petteni¹⁴³, R. Pezoa^{32b}, P.W. Phillips¹³⁰, G. Piacquadio¹⁴⁴, E. Pianori¹⁷¹, A. Picazio⁴⁹, E. Piccaro⁷⁵, M. Piccinini^{20a,20b}, S.M. Piec⁴², R. Piegai²⁷, D.T. Pignotti¹¹⁰, J.E. Pilcher³¹, A.D. Pilkington⁷⁷, J. Pina^{125a,d}, M. Pinamonti^{165a,165c,aj}, A. Pinder¹¹⁹, J.L. Pinfeld³, A. Pingel³⁶, B. Pinto^{125a}, C. Pizio^{90a,90b}, M.-A. Pleier²⁵, V. Pleskot¹²⁸, E. Plotnikova⁶⁴, P. Plucinski^{147a,147b}, S. Poddar^{58a}, F. Podlyski³⁴, R. Poettgen⁸², L. Poggioli¹¹⁶, D. Pohl²¹, M. Pohl⁴⁹, G. Polesello^{120a}, A. Policicchio^{37a,37b}, R. Polifka¹⁵⁹, A. Polini^{20a}, C.S. Pollard⁴⁵, V. Polychronakos²⁵, D. Pomeroy²³, K. Pommès³⁰, L. Pontecorvo^{133a}, B.G. Pope⁸⁹, G.A. Popeneciu^{26b}, D.S. Popovic^{13a}, A. Poppleton³⁰, X. Portell Bueso¹², G.E. Pospelov¹⁰⁰, S. Pospisil¹²⁷, K. Potamianos¹⁵, I.N. Potrap⁶⁴, C.J. Potter¹⁵⁰, C.T. Potter¹¹⁵, G. Poulard³⁰, J. Poveda⁶⁰, V. Pozdnyakov⁶⁴, R. Prabhu⁷⁷, P. Pralavorio⁸⁴, A. Pranko¹⁵, S. Prasad³⁰, R. Pravahan⁸, S. Prell⁶³, D. Price⁶⁰, J. Price⁷³, L.E. Price⁶, D. Prieur¹²⁴, M. Primavera^{72a}, M. Proissl⁴⁶, K. Prokofiev¹⁰⁹, F. Prokoshin^{32b}, E. Protopapadaki¹³⁷, S. Protopopescu²⁵, J. Proudfoot⁶, X. Prudent⁴⁴, M. Przybycien^{38a}, H. Przysieznia⁵, S. Psoroulas²¹, E. Ptacek¹¹⁵, E. Pueschel⁸⁵, D. Puldon¹⁴⁹, M. Purohit^{25,ak}, P. Puzo¹¹⁶, Y. Pylypchenko⁶², J. Qian⁸⁸, A. Quadt⁵⁴, D.R. Quarrie¹⁵, W.B. Quayle^{146c}, D. Quilty⁵³, V. Radeka²⁵, V. Radescu⁴², P. Radloff¹¹⁵, F. Ragusa^{90a,90b}, G. Rahal¹⁷⁹, S. Rajagopalan²⁵, M. Rammensee⁴⁸, M. Rammes¹⁴², A.S. Randle-Conde⁴⁰, C. Rangel-Smith⁷⁹, K. Rao¹⁶⁴, F. Rauscher⁹⁹, T.C. Rave⁴⁸, T. Ravenscroft⁵³, M. Raymond³⁰, A.L. Read¹¹⁸, D.M. Rebuffi^{120a,120b}, A. Redelbach¹⁷⁵, G. Redlinger²⁵, R. Reece¹²¹, K. Reeves⁴¹, A. Reinsch¹¹⁵, I. Reisinger⁴³, M. Relich¹⁶⁴, C. Rembser³⁰, Z.L. Ren¹⁵², A. Renaud¹¹⁶, M. Rescigno^{133a}, S. Resconi^{90a}, B. Resende¹³⁷, P. Reznicek⁹⁹, R. Rezvani⁹⁴, R. Richter¹⁰⁰, E. Richter-Was^{38b}, M. Ridel⁷⁹, P. Rieck¹⁶, M. Rijssenbeek¹⁴⁹, A. Rimoldi^{120a,120b}, L. Rinaldi^{20a}, R.R. Rios⁴⁰, E. Ritsch⁶¹, I. Riu¹², G. Rivoltella^{90a,90b}, F. Rizatdinova¹¹³, E. Rizvi⁷⁵, S.H. Robertson^{86,k}, A. Robichaud-Veronneau¹¹⁹, D. Robinson²⁸, J.E.M. Robinson⁸³, A. Robson⁵³, J.G. Rocha de Lima¹⁰⁷, C. Roda^{123a,123b}, D. Roda Dos Santos¹²⁶, L. Rodrigues³⁰, A. Roe⁵⁴, S. Roe³⁰, O. Röhne¹¹⁸, S. Rolli¹⁶², A. Romaniouk⁹⁷, M. Romano^{20a,20b}, G. Romeo²⁷, E. Romero Adam¹⁶⁸, N. Rompotis¹³⁹, L. Roos⁷⁹, E. Ros¹⁶⁸, S. Rosati^{133a}, K. Rosbach⁴⁹, A. Rose¹⁵⁰, M. Rose⁷⁶, P.L. Rosendahl¹⁴, O. Rosenthal¹⁴², V. Rossetti¹², E. Rossi^{103a,103b}, L.P. Rossi^{50a}, R. Rosten¹³⁹, M. Rotaru^{26a}, I. Roth¹⁷³, J. Rothberg¹³⁹, D. Rousseau¹¹⁶, C.R. Royon¹³⁷, A. Rozanov⁸⁴, Y. Rozen¹⁵³, X. Ruan^{146c}, F. Rubbo¹², I. Rubinskiy⁴², N. Ruckstuhl¹⁰⁶, V.I. Rud⁹⁸, C. Rudolph⁴⁴, M.S. Rudolph¹⁵⁹, F. Rühr⁷, A. Ruiz-Martinez⁶³, L. Rumyantsev⁶⁴, Z. Rurikova⁴⁸, N.A. Rusakovich⁶⁴, A. Ruschke⁹⁹, J.P. Rutherford⁷, N. Ruthmann⁴⁸, P. Ruzicka¹²⁶, Y.F. Ryabov¹²², M. Rybar¹²⁸, G. Rybkin¹¹⁶, N.C. Ryder¹¹⁹, A.F. Saavedra¹⁵¹, A. Saddique³, I. Sadeh¹⁵⁴, H.F.-W. Sadrozinski¹³⁸, R. Sadykov⁶⁴, F. Safai Tehrani^{133a}, H. Sakamoto¹⁵⁶, Y. Sakurai¹⁷², G. Salamanna⁷⁵, A. Salamon^{134a}, M. Saleem¹¹², D. Salek¹⁰⁶, D. Saliagic¹⁰⁰, A. Salnikov¹⁴⁴, J. Salt¹⁶⁸, B.M. Salvachua Ferrando⁶, D. Salvatore^{37a,37b}, F. Salvatore¹⁵⁰, A. Salvucci¹⁰⁵, A. Salzburger³⁰, D. Sampsonidis¹⁵⁵, A. Sanchez^{103a,103b}, J. Sánchez¹⁶⁸, V. Sanchez Martinez¹⁶⁸, H. Sandaker¹⁴, H.G. Sander⁸², M.P. Sanders⁹⁹, M. Sandhoff¹⁷⁶, T. Sandoval²⁸, C. Sandoval¹⁶³, R. Sandstroem¹⁰⁰, D.P.C. Sankey¹³⁰, A. Sansoni⁴⁷, C. Santoni³⁴, R. Santonico^{134a,134b}, H. Santos^{125a}, I. Santoyo Castillo¹⁵⁰, K. Sapp¹²⁴, A. Saponov⁶⁴, J.G. Saraiva^{125a}, E. Sarkisyan-Grinbaum⁸, B. Sarrazin²¹, F. Sarri^{123a,123b}, G. Sartisohn¹⁷⁶, O. Sasaki⁶⁵, Y. Sasaki¹⁵⁶, N. Sasao⁶⁷, I. Satsounkevitch⁹¹, G. Sauvage^{5,*}, E. Sauvan⁵, J.B. Sauvan¹¹⁶, P. Savard^{159,f}, V. Savinov¹²⁴, D.O. Savu³⁰, C. Sawyer¹¹⁹, L. Sawyer^{78,m}, D.H. Saxon⁵³, J. Saxon¹²¹, C. Sbarra^{20a}, A. Sbrizzi³, T. Scanlon³⁰, D.A. Scannicchio¹⁶⁴, M. Scarcella¹⁵¹, J. Schaarschmidt¹¹⁶, P. Schacht¹⁰⁰, D. Schaefer¹²¹, A. Schaelicke⁴⁶, S. Schaepe²¹, S. Schaezel^{58b}, U. Schäfer⁸², A.C. Schaffer¹¹⁶, D. Schaile⁹⁹, R.D. Schamberger¹⁴⁹, V. Scharf^{58a}, V.A. Schegelsky¹²², D. Scheirich⁸⁸, M. Schernau¹⁶⁴, M.I. Scherzer³⁵, C. Schiavi^{50a,50b}, J. Schieck⁹⁹, C. Schillo⁴⁸, M. Schioppa^{37a,37b}, S. Schlenker³⁰, E. Schmidt⁴⁸, K. Schmieden³⁰, C. Schmitt⁸², C. Schmitt⁹⁹, S. Schmitt^{58b}, B. Schneider¹⁷, Y.J. Schnellbach⁷³, U. Schnoor⁴⁴, L. Schoeffel¹³⁷, A. Schoening^{58b}, A.L.S. Schorlemmer⁵⁴, M. Schott⁸², D. Schouten^{160a}, J. Schovancova²⁵, M. Schram⁸⁶, S. Schramm¹⁵⁹, M. Schreyer¹⁷⁵, C. Schroeder⁸², N. Schroer^{58c}, N. Schuh⁸², M.J. Schultens²¹, H.-C. Schultz-Coulon^{58a}, H. Schulz¹⁶, M. Schumacher⁴⁸, B.A. Schumm¹³⁸, Ph. Schune¹³⁷, A. Schwartzman¹⁴⁴, Ph. Schwegler¹⁰⁰, Ph. Schwemling¹³⁷, R. Schwiendhorst⁸⁹, J. Schwindling¹³⁷, T. Schwindt²¹, M. Schwoerer⁵, F.G. Sciaccia¹⁷, E. Scifo¹¹⁶, G. Sciolla²³, W.G. Scott¹³⁰, F. Scutti²¹, J. Searcy⁸⁸, G. Sedov⁴², E. Sedykh¹²², S.C. Seidel¹⁰⁴, A. Seiden¹³⁸, F. Seifert⁴⁴, J.M. Seixas^{24a}, G. Sekhniaidze^{103a}, S.J. Sekula⁴⁰, K.E. Selbach⁴⁶, D.M. Seliverstov¹²², G. Sellers⁷³, M. Seman^{145b}, N. Semprini-Cesari^{20a,20b}, C. Serfon³⁰, L. Serin¹¹⁶, L. Serkin⁵⁴, T. Serre⁸⁴, R. Seuster^{160a}, H. Severini¹¹², F. Sforza¹⁰⁰, A. Sfyrly³⁰, E. Shabalina⁵⁴, M. Shamim¹¹⁵, L.Y. Shan^{33a}, J.T. Shank²², Q.T. Shao⁸⁷, M. Shapiro¹⁵, P.B. Shatalov⁹⁶, K. Shaw^{165a,165c}, P. Sherwood⁷⁷, S. Shimizu⁶⁶, M. Shimojima¹⁰¹, T. Shin⁵⁶, M. Shiyakova⁶⁴, A. Shmeleva⁹⁵, M.J. Shochet³¹, D. Short¹¹⁹, S. Shrestha⁶³, E. Shulga⁹⁷, M.A. Shupe⁷, S. Shushkevich⁴², P. Sicho¹²⁶, D. Sidorov¹¹³, A. Sidoti^{133a}, F. Siegert⁴⁸, Dj. Sijacki^{13a}, O. Silbert¹⁷³, J. Silva^{125a}, Y. Silver¹⁵⁴, D. Silverstein¹⁴⁴, S.B. Silverstein^{147a}, V. Simak¹²⁷, O. Simard⁵, Lj. Simic^{13a}, S. Simion¹¹⁶, E. Simioni⁸², B. Simmons⁷⁷, R. Simoniello^{90a,90b}, M. Simonyan³⁶, P. Sinervo¹⁵⁹, N.B. Sinev¹¹⁵, V. Sipica¹⁴², G. Siragusa¹⁷⁵, A. Sircar⁷⁸, A.N. Sisakyan^{64,*}, S.Yu. Sivoklov⁹⁸, J. Sjölin^{147a,147b}, T.B. Sjrursen¹⁴, L.A. Skinnari¹⁵, H.P. Skottowe⁵⁷, K.Yu. Skovpen¹⁰⁸, P. Skubic¹¹², M. Slater¹⁸,

T. Slavicek¹²⁷, K. Sliwa¹⁶², V. Smakhtin¹⁷³, B.H. Smart⁴⁶, L. Smestad¹¹⁸, S.Yu. Smirnov⁹⁷, Y. Smirnov⁹⁷, L.N. Smirnova^{98,al}, O. Smirnova⁸⁰, K.M. Smith⁵³, M. Smizanska⁷¹, K. Smolek¹²⁷, A.A. Snesarev⁹⁵, G. Snidero⁷⁵, J. Snow¹¹², S. Snyder²⁵, R. Sobie^{170,k}, J. Sodomka¹²⁷, A. Soffer¹⁵⁴, D.A. Soh^{152,x}, C.A. Solans³⁰, M. Solar¹²⁷, J. Solc¹²⁷, E.Yu. Soldatov⁹⁷, U. Soldevila¹⁶⁸, E. Solfaroli Camillocci^{133a,133b}, A.A. Solodkov¹²⁹, O.V. Solovyanov¹²⁹, V. Solovyev¹²², N. Soni¹, A. Sood¹⁵, V. Sopko¹²⁷, B. Sopko¹²⁷, M. Sosebee⁸, R. Soualah^{165a,165c}, P. Soueid⁹⁴, A.M. Soukharev¹⁰⁸, D. South⁴², S. Spagnolo^{72a,72b}, F. Spanò⁷⁶, W.R. Spearman⁵⁷, R. Spighi^{20a}, G. Spigo³⁰, M. Spousta^{128,am}, T. Spreitzer¹⁵⁹, B. Spurlock⁸, R.D. St. Denis⁵³, J. Stahlman¹²¹, R. Stamen^{58a}, E. Stanecka³⁹, R.W. Stanek⁶, C. Stanescu^{135a}, M. Stanescu-Bellu⁴², M.M. Stanitzki⁴², S. Stapnes¹¹⁸, E.A. Starchenko¹²⁹, J. Stark⁵⁵, P. Staroba¹²⁶, P. Starovoitov⁴², R. Staszewski³⁹, A. Stauder⁹⁹, P. Stavina^{145a,*}, G. Steele⁵³, P. Steinbach⁴⁴, P. Steinberg²⁵, I. Stekl¹²⁷, B. Stelzer¹⁴³, H.J. Stelzer⁸⁹, O. Stelzer-Chilton^{160a}, H. Stenzel⁵², S. Stern¹⁰⁰, G.A. Stewart³⁰, J.A. Stillings²¹, M.C. Stockton⁸⁶, M. Stoebe⁸⁶, K. Stoerig⁴⁸, G. Stoicica^{26a}, S. Stonjek¹⁰⁰, A.R. Stradling⁸, A. Straessner⁴⁴, J. Strandberg¹⁴⁸, S. Strandberg^{147a,147b}, A. Strandlie¹¹⁸, E. Strauss¹⁴⁴, M. Strauss¹¹², P. Strizenc^{145b}, R. Ströhmer¹⁷⁵, D.M. Strom¹¹⁵, R. Stroynowski⁴⁰, B. Stugu¹⁴, I. Stumer^{25,*}, J. Stupak¹⁴⁹, P. Sturm¹⁷⁶, N.A. Styles⁴², D. Su¹⁴⁴, H.S. Subramania³, R. Subramaniam⁷⁸, A. Succurro¹², Y. Sugaya¹¹⁷, C. Suhr¹⁰⁷, M. Suk¹²⁷, V.V. Sulin⁹⁵, S. Sultansoy^{4c}, T. Sumida⁶⁷, X. Sun⁵⁵, J.E. Sundermann⁴⁸, K. Suruliz¹⁴⁰, G. Susinno^{37a,37b}, M.R. Sutton¹⁵⁰, Y. Suzuki⁶⁵, M. Svatos¹²⁶, S. Swedish¹⁶⁹, M. Swiatlowski¹⁴⁴, I. Sykora^{145a}, T. Sykora¹²⁸, D. Ta⁸⁹, K. Tackmann⁴², J. Taenzer¹⁵⁹, A. Taffard¹⁶⁴, R. Tafirout^{160a}, N. Taiblum¹⁵⁴, Y. Takahashi¹⁰², H. Takai²⁵, R. Takashima⁶⁸, H. Takeda⁶⁶, T. Takeshita¹⁴¹, Y. Takubo⁶⁵, M. Talby⁸⁴, A.A. Talyshev^{108,h}, J.Y.C. Tam¹⁷⁵, M.C. Tamsett^{78,an}, K.G. Tan⁸⁷, J. Tanaka¹⁵⁶, R. Tanaka¹¹⁶, S. Tanaka¹³², S. Tanaka⁶⁵, A.J. Tanasijczuk¹⁴³, K. Tani⁶⁶, N. Tannoury⁸⁴, S. Tapprogge⁸², S. Tarem¹⁵³, F. Tarrade²⁹, G.F. Tartarelli^{90a}, P. Tas¹²⁸, M. Tasevsky¹²⁶, T. Tashiro⁶⁷, E. Tassi^{37a,37b}, A. Tavares Delgado^{125a}, Y. Tayalati^{136d}, C. Taylor⁷⁷, F.E. Taylor⁹³, G.N. Taylor⁸⁷, W. Taylor^{160b}, F.A. Teischinger³⁰, M. Teixeira Dias Castanheira⁷⁵, P. Teixeira-Dias⁷⁶, K.K. Temming⁴⁸, H. Ten Kate³⁰, P.K. Teng¹⁵², S. Terada⁶⁵, K. Terashi¹⁵⁶, J. Terron⁸¹, S. Terzo¹⁰⁰, M. Testa⁴⁷, R.J. Teuscher^{159,k}, J. Therhaag²¹, T. Theveneaux-Pelzer³⁴, S. Thoma⁴⁸, J.P. Thomas¹⁸, E.N. Thompson³⁵, P.D. Thompson¹⁸, P.D. Thompson¹⁵⁹, A.S. Thompson⁵³, L.A. Thomsen³⁶, E. Thomson¹²¹, M. Thomson²⁸, W.M. Thong⁸⁷, R.P. Thun^{88,*}, F. Tian³⁵, M.J. Tibbetts¹⁵, T. Tic¹²⁶, V.O. Tikhomirov^{95,ao}, Yu.A. Tikhonov^{108,h}, S. Timoshenko⁹⁷, E. Tiouchichine⁸⁴, P. Tipton¹⁷⁷, S. Tisserant⁸⁴, T. Todorov⁵, S. Todorova-Nova¹²⁸, B. Toggerson¹⁶⁴, J. Tojo⁶⁹, S. Tokár^{145a}, K. Tokushuku⁶⁵, K. Tollefson⁸⁹, L. Tomlinson⁸³, M. Tomoto¹⁰², L. Tompkins³¹, K. Toms¹⁰⁴, A. Tonoyan¹⁴, N.D. Topilin⁶⁴, E. Torrence¹¹⁵, H. Torres¹⁴³, E. Torrò Pastor¹⁶⁸, J. Toth^{84,ah}, F. Touchard⁸⁴, D.R. Tovey¹⁴⁰, H.L. Tran¹¹⁶, T. Trefzger¹⁷⁵, L. Tremblet³⁰, A. Tricoli³⁰, I.M. Trigger^{160a}, S. Trincaz-Duvoid⁷⁹, M.F. Tripiana⁷⁰, N. Triplett²⁵, W. Trischuk¹⁵⁹, B. Trocme⁵⁵, C. Troncon^{90a}, M. Trotter-McDonald¹⁴³, M. Trovatelli^{135a,135b}, P. True⁸⁹, M. Trzebinski³⁹, A. Trzupek³⁹, C. Tsarouchas³⁰, J.C-L. Tseng¹¹⁹, P.V. Tsiarehka⁹¹, D. Tsiou¹³⁷, G. Tsipolitis¹⁰, S. Tsiskaridze¹², V. Tsiskaridze⁴⁸, E.G. Tskhadadze^{51a}, I.I. Tsukerman⁹⁶, V. Tsulaia¹⁵, J.-W. Tsung²¹, S. Tsuno⁶⁵, D. Tsybychev¹⁴⁹, A. Tua¹⁴⁰, A. Tudorache^{26a}, V. Tudorache^{26a}, J.M. Tuggle³¹, A.N. Tuna¹²¹, S.A. Tupputi^{20a,20b}, S. Turchikhin^{98,al}, D. Turecek¹²⁷, I. Turk Cakir^{4d}, R. Turra^{90a,90b}, P.M. Tuts³⁵, A. Tykhonov⁷⁴, M. Tylmad^{147a,147b}, M. Tyndel¹³⁰, K. Uchida²¹, I. Ueda¹⁵⁶, R. Ueno²⁹, M. Ughetto⁸⁴, M. Uglund¹⁴, M. Uhlenbrock²¹, F. Ukegawa¹⁶¹, G. Unal³⁰, A. Undrus²⁵, G. Unel¹⁶⁴, F.C. Ungaro⁴⁸, Y. Unno⁶⁵, D. Urbaniec³⁵, P. Urquijo²¹, G. Usai⁸, A. Usanova⁶¹, L. Vacavant⁸⁴, V. Vacek¹²⁷, B. Vachon⁸⁶, S. Vahsen¹⁵, N. Valencic¹⁰⁶, S. Valentineti^{20a,20b}, A. Valero¹⁶⁸, L. Valery³⁴, S. Valkar¹²⁸, E. Valladolid Gallego¹⁶⁸, S. Vallecorsa⁴⁹, J.A. Valls Ferrer¹⁶⁸, R. Van Berg¹²¹, P.C. Van Der Deijl¹⁰⁶, R. van der Geer¹⁰⁶, H. van der Graaf¹⁰⁶, R. Van Der Leeuw¹⁰⁶, D. van der Ster³⁰, N. van Eldik³⁰, P. van Gemmeren⁶, J. Van Nieuwkoop¹⁴³, I. van Vulpen¹⁰⁶, M. Vanadia¹⁰⁰, W. Vandelli³⁰, A. Vaniachine⁶, P. Vankov⁴², F. Vannucci⁷⁹, R. Vari^{133a}, E.W. Varnes⁷, T. Varol⁸⁵, D. Varouchas¹⁵, A. Vartapetian⁸, K.E. Varvell¹⁵¹, V.I. Vassilikopoulos⁵⁶, F. Vazeille³⁴, T. Vazquez Schroeder⁵⁴, J. Veatch⁷, F. Veloso^{125a}, S. Veneziano^{133a}, A. Ventura^{72a,72b}, D. Ventura⁸⁵, M. Venturi⁴⁸, N. Venturi¹⁵⁹, V. Vercesi^{120a}, M. Verducci¹³⁹, W. Verkerke¹⁰⁶, J.C. Vermeulen¹⁰⁶, A. Vest⁴⁴, M.C. Vetterli^{143,f}, I. Vichou¹⁶⁶, T. Vickey^{146c,ap}, O.E. Vickey Boeriu^{146c}, G.H.A. Viehhauser¹¹⁹, S. Viel¹⁶⁹, R. Vigne³⁰, M. Villa^{20a,20b}, M. Villaplana Perez¹⁶⁸, E. Vilucchi⁴⁷, M.G. Vincker²⁹, V.B. Vinogradov⁶⁴, J. Virzi¹⁵, O. Vitells¹⁷³, M. Viti⁴², I. Vivarelli⁴⁸, F. Vives Vaque³, S. Vlachos¹⁰, D. Vladoiu⁹⁹, M. Vlasak¹²⁷, A. Vogel²¹, P. Vokac¹²⁷, G. Volpi⁴⁷, M. Volpi⁸⁷, G. Volpini^{90a}, H. von der Schmitt¹⁰⁰, H. von Radziewski⁴⁸, E. von Toerne²¹, V. Vorobel¹²⁸, M. Vos¹⁶⁸, R. Voss³⁰, J.H. Vosseveld⁷³, N. Vranjes¹³⁷, M. Vranjes Milosavljevic¹⁰⁶, V. Vrba¹²⁶, M. Vreeswijk¹⁰⁶, T. Vu Anh⁴⁸, R. Vuillermet³⁰, I. Vukotic³¹, Z. Vykydal¹²⁷, W. Wagner¹⁷⁶, P. Wagner²¹, S. Wahrenndorf⁴⁴, J. Wakabayashi¹⁰², S. Walch⁸⁸, J. Walder⁷¹, R. Walker⁹⁹, W. Walkowiak¹⁴², R. Wall¹⁷⁷, P. Waller⁷³, B. Walsh¹⁷⁷, C. Wang⁴⁵, H. Wang¹⁷⁴, H. Wang⁴⁰, J. Wang¹⁵², J. Wang^{33a}, K. Wang⁸⁶, R. Wang¹⁰⁴, S.M. Wang¹⁵², T. Wang²¹, X. Wang¹⁷⁷, A. Warburton⁸⁶, C.P. Ward²⁸, D.R. Wardrope⁷⁷, M. Warsinsky⁴⁸, A. Washbrook⁴⁶, C. Wasicki⁴², I. Watanabe⁶⁶, P.M. Watkins¹⁸, A.T. Watson¹⁸, I.J. Watson¹⁵¹, M.F. Watson¹⁸, G. Watts¹³⁹, S. Watts⁸³, A.T. Waugh¹⁵¹, B.M. Waugh⁷⁷, S. Webb⁸³, M.S. Weber¹⁷, S.W. Weber¹⁷⁵, J.S. Webster³¹, A.R. Weidberg¹¹⁹, P. Weigell¹⁰⁰, J. Weingarten⁵⁴, C. Weiser⁴⁸, H. Weits¹⁰⁶, P.S. Wells³⁰, T. Wenaus²⁵, D. Wendland¹⁶, Z. Weng^{152,x}, T. Wengler³⁰,

S. Wenig³⁰, N. Wermes²¹, M. Werner⁴⁸, P. Werner³⁰, M. Werth¹⁶⁴, M. Wessels^{58a}, J. Wetter¹⁶², K. Whalen²⁹, A. White⁸, M.J. White⁸⁷, R. White^{32b}, S. White^{123a,123b}, D. Whiteson¹⁶⁴, D. Whittington⁶⁰, D. Wicke¹⁷⁶, F.J. Wickens¹³⁰, W. Wiedenmann¹⁷⁴, M. Wielers^{80,e}, P. Wienemann²¹, C. Wiglesworth³⁶, L.A.M. Wiik-Fuchs²¹, P.A. Wijeratne⁷⁷, A. Wildauer¹⁰⁰, M.A. Wildt^{42,aq}, I. Wilhelm¹²⁸, H.G. Wilkens³⁰, J.Z. Will⁹⁹, E. Williams³⁵, H.H. Williams¹²¹, S. Williams²⁸, W. Willis^{35,*}, S. Willocq⁸⁵, J.A. Wilson¹⁸, A. Wilson⁸⁸, I. Wingerter-Seez⁵, S. Winkelmann⁴⁸, F. Winklmeier³⁰, M. Wittgen¹⁴⁴, T. Wittig⁴³, J. Wittkowski⁹⁹, S.J. Wollstadt⁸², M.W. Wolter³⁹, H. Wolters^{125a,i}, W.C. Wong⁴¹, G. Wooden⁸⁸, B.K. Wosiek³⁹, J. Wotschack³⁰, M.J. Woudstra⁸³, K.W. Wozniak³⁹, K. Wraight⁵³, M. Wright⁵³, B. Wrona⁷³, S.L. Wu¹⁷⁴, X. Wu⁴⁹, Y. Wu⁸⁸, E. Wulf³⁵, T.R. Wyatt⁸³, B.M. Wynne⁴⁶, S. Xella³⁶, M. Xiao¹³⁷, C. Xu^{33b,ac}, D. Xu^{33a}, L. Xu^{33b,ar}, B. Yabsley¹⁵¹, S. Yacoob^{146b,as}, M. Yamada⁶⁵, H. Yamaguchi¹⁵⁶, Y. Yamaguchi¹⁵⁶, A. Yamamoto⁶⁵, K. Yamamoto⁶³, S. Yamamoto¹⁵⁶, T. Yamamura¹⁵⁶, T. Yamanaka¹⁵⁶, K. Yamauchi¹⁰², Y. Yamazaki⁶⁶, Z. Yan²², H. Yang^{33e}, H. Yang¹⁷⁴, U.K. Yang⁸³, Y. Yang¹¹⁰, Z. Yang^{147a,147b}, S. Yanush⁹², L. Yao^{33a}, Y. Yasu⁶⁵, E. Yatsenko⁴², K.H. Yau Wong²¹, J. Ye⁴⁰, S. Ye²⁵, A.L. Yen⁵⁷, E. Yildirim⁴², M. Yilmaz^{4b}, R. Yoosoofmiya¹²⁴, K. Yorita¹⁷², R. Yoshida⁶, K. Yoshihara¹⁵⁶, C. Young¹⁴⁴, C.J.S. Young¹¹⁹, S. Youssef²², D.R. Yu¹⁵, J. Yu⁸, J. Yu¹¹³, L. Yuan⁶⁶, A. Yurkewicz¹⁰⁷, B. Zabinski³⁹, R. Zaidan⁶², A.M. Zaitsev^{129,ad}, S. Zambito²³, L. Zanello^{133a,133b}, D. Zanzi¹⁰⁰, A. Zaytsev²⁵, C. Zeitnitz¹⁷⁶, M. Zeman¹²⁷, A. Zemla³⁹, O. Zenin¹²⁹, T. Ženiš^{145a}, D. Zerwas¹¹⁶, G. Zevi della Porta⁵⁷, D. Zhang⁸⁸, H. Zhang⁸⁹, J. Zhang⁶, L. Zhang¹⁵², X. Zhang^{33d}, Z. Zhang¹¹⁶, Z. Zhao^{33b}, A. Zhemchugov⁶⁴, J. Zhong¹¹⁹, B. Zhou⁸⁸, L. Zhou³⁵, N. Zhou¹⁶⁴, C.G. Zhu^{33d}, H. Zhu⁴², J. Zhu⁸⁸, Y. Zhu^{33b}, X. Zhuang^{33a}, A. Zibell⁹⁹, D. Zieminska⁶⁰, N.I. Zimin⁶⁴, C. Zimmermann⁸², R. Zimmermann²¹, S. Zimmermann²¹, S. Zimmermann⁴⁸, Z. Zinonos^{123a,123b}, M. Ziolkowski¹⁴², R. Zitoun⁵, L. Živković³⁵, G. Zobernig¹⁷⁴, A. Zoccoli^{20a,20b}, M. zur Nedden¹⁶, G. Zurzolo^{103a,103b}, V. Zutshi¹⁰⁷, L. Zwalinski³⁰.

¹ School of Chemistry and Physics, University of Adelaide, Adelaide, Australia

² Physics Department, SUNY Albany, Albany NY, United States of America

³ Department of Physics, University of Alberta, Edmonton AB, Canada

⁴ (a) Department of Physics, Ankara University, Ankara; (b) Department of Physics, Gazi University, Ankara; (c) Division of Physics, TOBB University of Economics and Technology, Ankara; (d) Turkish Atomic Energy Authority, Ankara, Turkey

⁵ LAPP, CNRS/IN2P3 and Université de Savoie, Annecy-le-Vieux, France

⁶ High Energy Physics Division, Argonne National Laboratory, Argonne IL, United States of America

⁷ Department of Physics, University of Arizona, Tucson AZ, United States of America

⁸ Department of Physics, The University of Texas at Arlington, Arlington TX, United States of America

⁹ Physics Department, University of Athens, Athens, Greece

¹⁰ Physics Department, National Technical University of Athens, Zografou, Greece

¹¹ Institute of Physics, Azerbaijan Academy of Sciences, Baku, Azerbaijan

¹² Institut de Física d'Altes Energies and Departament de Física de la Universitat Autònoma de Barcelona, Barcelona, Spain

¹³ (a) Institute of Physics, University of Belgrade, Belgrade; (b) Vinca Institute of Nuclear Sciences, University of Belgrade, Belgrade, Serbia

¹⁴ Department for Physics and Technology, University of Bergen, Bergen, Norway

¹⁵ Physics Division, Lawrence Berkeley National Laboratory and University of California, Berkeley CA, United States of America

¹⁶ Department of Physics, Humboldt University, Berlin, Germany

¹⁷ Albert Einstein Center for Fundamental Physics and Laboratory for High Energy Physics, University of Bern, Bern, Switzerland

¹⁸ School of Physics and Astronomy, University of Birmingham, Birmingham, United Kingdom

¹⁹ (a) Department of Physics, Bogazici University, Istanbul; (b) Department of Physics, Dogus University, Istanbul;

(c) Department of Physics Engineering, Gaziantep University, Gaziantep, Turkey

²⁰ (a) INFN Sezione di Bologna; (b) Dipartimento di Fisica e Astronomia, Università di Bologna, Bologna, Italy

²¹ Physikalisches Institut, University of Bonn, Bonn, Germany

²² Department of Physics, Boston University, Boston MA, United States of America

²³ Department of Physics, Brandeis University, Waltham MA, United States of America

²⁴ (a) Universidade Federal do Rio De Janeiro COPPE/EE/IF, Rio de Janeiro; (b) Federal University of Juiz de Fora (UFJF), Juiz de Fora; (c) Federal University of Sao Joao del Rei (UFSJ), Sao Joao del Rei; (d) Instituto de Fisica, Universidade de Sao Paulo, Sao Paulo, Brazil

²⁵ Physics Department, Brookhaven National Laboratory, Upton NY, United States of America

²⁶ (a) National Institute of Physics and Nuclear Engineering, Bucharest; (b) National Institute for Research and Development of Isotopic and Molecular Technologies, Physics Department, Cluj Napoca; (c) University Politehnica

- Bucharest, Bucharest; ^(d) West University in Timisoara, Timisoara, Romania
- ²⁷ Departamento de Física, Universidad de Buenos Aires, Buenos Aires, Argentina
- ²⁸ Cavendish Laboratory, University of Cambridge, Cambridge, United Kingdom
- ²⁹ Department of Physics, Carleton University, Ottawa ON, Canada
- ³⁰ CERN, Geneva, Switzerland
- ³¹ Enrico Fermi Institute, University of Chicago, Chicago IL, United States of America
- ³² ^(a) Departamento de Física, Pontificia Universidad Católica de Chile, Santiago; ^(b) Departamento de Física, Universidad Técnica Federico Santa María, Valparaíso, Chile
- ³³ ^(a) Institute of High Energy Physics, Chinese Academy of Sciences, Beijing; ^(b) Department of Modern Physics, University of Science and Technology of China, Anhui; ^(c) Department of Physics, Nanjing University, Jiangsu; ^(d) School of Physics, Shandong University, Shandong; ^(e) Physics Department, Shanghai Jiao Tong University, Shanghai, China
- ³⁴ Laboratoire de Physique Corpusculaire, Clermont Université and Université Blaise Pascal and CNRS/IN2P3, Clermont-Ferrand, France
- ³⁵ Nevis Laboratory, Columbia University, Irvington NY, United States of America
- ³⁶ Niels Bohr Institute, University of Copenhagen, Kobenhavn, Denmark
- ³⁷ ^(a) INFN Gruppo Collegato di Cosenza; ^(b) Dipartimento di Fisica, Università della Calabria, Rende, Italy
- ³⁸ ^(a) AGH University of Science and Technology, Faculty of Physics and Applied Computer Science, Krakow; ^(b) Marian Smoluchowski Institute of Physics, Jagiellonian University, Krakow, Poland
- ³⁹ The Henryk Niewodniczanski Institute of Nuclear Physics, Polish Academy of Sciences, Krakow, Poland
- ⁴⁰ Physics Department, Southern Methodist University, Dallas TX, United States of America
- ⁴¹ Physics Department, University of Texas at Dallas, Richardson TX, United States of America
- ⁴² DESY, Hamburg and Zeuthen, Germany
- ⁴³ Institut für Experimentelle Physik IV, Technische Universität Dortmund, Dortmund, Germany
- ⁴⁴ Institut für Kern- und Teilchenphysik, Technische Universität Dresden, Dresden, Germany
- ⁴⁵ Department of Physics, Duke University, Durham NC, United States of America
- ⁴⁶ SUPA - School of Physics and Astronomy, University of Edinburgh, Edinburgh, United Kingdom
- ⁴⁷ INFN Laboratori Nazionali di Frascati, Frascati, Italy
- ⁴⁸ Fakultät für Mathematik und Physik, Albert-Ludwigs-Universität, Freiburg, Germany
- ⁴⁹ Section de Physique, Université de Genève, Geneva, Switzerland
- ⁵⁰ ^(a) INFN Sezione di Genova; ^(b) Dipartimento di Fisica, Università di Genova, Genova, Italy
- ⁵¹ ^(a) E. Andronikashvili Institute of Physics, Iv. Javakishvili Tbilisi State University, Tbilisi; ^(b) High Energy Physics Institute, Tbilisi State University, Tbilisi, Georgia
- ⁵² II Physikalisches Institut, Justus-Liebig-Universität Giessen, Giessen, Germany
- ⁵³ SUPA - School of Physics and Astronomy, University of Glasgow, Glasgow, United Kingdom
- ⁵⁴ II Physikalisches Institut, Georg-August-Universität, Göttingen, Germany
- ⁵⁵ Laboratoire de Physique Subatomique et de Cosmologie, Université Joseph Fourier and CNRS/IN2P3 and Institut National Polytechnique de Grenoble, Grenoble, France
- ⁵⁶ Department of Physics, Hampton University, Hampton VA, United States of America
- ⁵⁷ Laboratory for Particle Physics and Cosmology, Harvard University, Cambridge MA, United States of America
- ⁵⁸ ^(a) Kirchhoff-Institut für Physik, Ruprecht-Karls-Universität Heidelberg, Heidelberg; ^(b) Physikalisches Institut, Ruprecht-Karls-Universität Heidelberg, Heidelberg; ^(c) ZITI Institut für technische Informatik, Ruprecht-Karls-Universität Heidelberg, Mannheim, Germany
- ⁵⁹ Faculty of Applied Information Science, Hiroshima Institute of Technology, Hiroshima, Japan
- ⁶⁰ Department of Physics, Indiana University, Bloomington IN, United States of America
- ⁶¹ Institut für Astro- und Teilchenphysik, Leopold-Franzens-Universität, Innsbruck, Austria
- ⁶² University of Iowa, Iowa City IA, United States of America
- ⁶³ Department of Physics and Astronomy, Iowa State University, Ames IA, United States of America
- ⁶⁴ Joint Institute for Nuclear Research, JINR Dubna, Dubna, Russia
- ⁶⁵ KEK, High Energy Accelerator Research Organization, Tsukuba, Japan
- ⁶⁶ Graduate School of Science, Kobe University, Kobe, Japan
- ⁶⁷ Faculty of Science, Kyoto University, Kyoto, Japan
- ⁶⁸ Kyoto University of Education, Kyoto, Japan
- ⁶⁹ Department of Physics, Kyushu University, Fukuoka, Japan
- ⁷⁰ Instituto de Física La Plata, Universidad Nacional de La Plata and CONICET, La Plata, Argentina
- ⁷¹ Physics Department, Lancaster University, Lancaster, United Kingdom
- ⁷² ^(a) INFN Sezione di Lecce; ^(b) Dipartimento di Matematica e Fisica, Università del Salento, Lecce, Italy
- ⁷³ Oliver Lodge Laboratory, University of Liverpool, Liverpool, United Kingdom

- ⁷⁴ Department of Physics, Jožef Stefan Institute and University of Ljubljana, Ljubljana, Slovenia
- ⁷⁵ School of Physics and Astronomy, Queen Mary University of London, London, United Kingdom
- ⁷⁶ Department of Physics, Royal Holloway University of London, Surrey, United Kingdom
- ⁷⁷ Department of Physics and Astronomy, University College London, London, United Kingdom
- ⁷⁸ Louisiana Tech University, Ruston LA, United States of America
- ⁷⁹ Laboratoire de Physique Nucléaire et de Hautes Energies, UPMC and Université Paris-Diderot and CNRS/IN2P3, Paris, France
- ⁸⁰ Fysiska institutionen, Lunds universitet, Lund, Sweden
- ⁸¹ Departamento de Física Teórica C-15, Universidad Autónoma de Madrid, Madrid, Spain
- ⁸² Institut für Physik, Universität Mainz, Mainz, Germany
- ⁸³ School of Physics and Astronomy, University of Manchester, Manchester, United Kingdom
- ⁸⁴ CPPM, Aix-Marseille Université and CNRS/IN2P3, Marseille, France
- ⁸⁵ Department of Physics, University of Massachusetts, Amherst MA, United States of America
- ⁸⁶ Department of Physics, McGill University, Montreal QC, Canada
- ⁸⁷ School of Physics, University of Melbourne, Victoria, Australia
- ⁸⁸ Department of Physics, The University of Michigan, Ann Arbor MI, United States of America
- ⁸⁹ Department of Physics and Astronomy, Michigan State University, East Lansing MI, United States of America
- ⁹⁰ ^(a) INFN Sezione di Milano; ^(b) Dipartimento di Fisica, Università di Milano, Milano, Italy
- ⁹¹ B.I. Stepanov Institute of Physics, National Academy of Sciences of Belarus, Minsk, Republic of Belarus
- ⁹² National Scientific and Educational Centre for Particle and High Energy Physics, Minsk, Republic of Belarus
- ⁹³ Department of Physics, Massachusetts Institute of Technology, Cambridge MA, United States of America
- ⁹⁴ Group of Particle Physics, University of Montreal, Montreal QC, Canada
- ⁹⁵ P.N. Lebedev Institute of Physics, Academy of Sciences, Moscow, Russia
- ⁹⁶ Institute for Theoretical and Experimental Physics (ITEP), Moscow, Russia
- ⁹⁷ Moscow Engineering and Physics Institute (MEPhI), Moscow, Russia
- ⁹⁸ D.V.Skobeltzyn Institute of Nuclear Physics, M.V.Lomonosov Moscow State University, Moscow, Russia
- ⁹⁹ Fakultät für Physik, Ludwig-Maximilians-Universität München, München, Germany
- ¹⁰⁰ Max-Planck-Institut für Physik (Werner-Heisenberg-Institut), München, Germany
- ¹⁰¹ Nagasaki Institute of Applied Science, Nagasaki, Japan
- ¹⁰² Graduate School of Science and Kobayashi-Maskawa Institute, Nagoya University, Nagoya, Japan
- ¹⁰³ ^(a) INFN Sezione di Napoli; ^(b) Dipartimento di Scienze Fisiche, Università di Napoli, Napoli, Italy
- ¹⁰⁴ Department of Physics and Astronomy, University of New Mexico, Albuquerque NM, United States of America
- ¹⁰⁵ Institute for Mathematics, Astrophysics and Particle Physics, Radboud University Nijmegen/Nikhef, Nijmegen, Netherlands
- ¹⁰⁶ Nikhef National Institute for Subatomic Physics and University of Amsterdam, Amsterdam, Netherlands
- ¹⁰⁷ Department of Physics, Northern Illinois University, DeKalb IL, United States of America
- ¹⁰⁸ Budker Institute of Nuclear Physics, SB RAS, Novosibirsk, Russia
- ¹⁰⁹ Department of Physics, New York University, New York NY, United States of America
- ¹¹⁰ Ohio State University, Columbus OH, United States of America
- ¹¹¹ Faculty of Science, Okayama University, Okayama, Japan
- ¹¹² Homer L. Dodge Department of Physics and Astronomy, University of Oklahoma, Norman OK, United States of America
- ¹¹³ Department of Physics, Oklahoma State University, Stillwater OK, United States of America
- ¹¹⁴ Palacký University, RCPTM, Olomouc, Czech Republic
- ¹¹⁵ Center for High Energy Physics, University of Oregon, Eugene OR, United States of America
- ¹¹⁶ LAL, Université Paris-Sud and CNRS/IN2P3, Orsay, France
- ¹¹⁷ Graduate School of Science, Osaka University, Osaka, Japan
- ¹¹⁸ Department of Physics, University of Oslo, Oslo, Norway
- ¹¹⁹ Department of Physics, Oxford University, Oxford, United Kingdom
- ¹²⁰ ^(a) INFN Sezione di Pavia; ^(b) Dipartimento di Fisica, Università di Pavia, Pavia, Italy
- ¹²¹ Department of Physics, University of Pennsylvania, Philadelphia PA, United States of America
- ¹²² Petersburg Nuclear Physics Institute, Gatchina, Russia
- ¹²³ ^(a) INFN Sezione di Pisa; ^(b) Dipartimento di Fisica E. Fermi, Università di Pisa, Pisa, Italy
- ¹²⁴ Department of Physics and Astronomy, University of Pittsburgh, Pittsburgh PA, United States of America
- ¹²⁵ ^(a) Laboratório de Instrumentação e Física Experimental de Partículas - LIP, Lisboa, Portugal; ^(b) Departamento de Física Teórica y del Cosmos and CAFPE, Universidad de Granada, Granada, Spain
- ¹²⁶ Institute of Physics, Academy of Sciences of the Czech Republic, Praha, Czech Republic
- ¹²⁷ Czech Technical University in Prague, Praha, Czech Republic

- 128 Faculty of Mathematics and Physics, Charles University in Prague, Praha, Czech Republic
- 129 State Research Center Institute for High Energy Physics, Protvino, Russia
- 130 Particle Physics Department, Rutherford Appleton Laboratory, Didcot, United Kingdom
- 131 Physics Department, University of Regina, Regina SK, Canada
- 132 Ritsumeikan University, Kusatsu, Shiga, Japan
- 133 (a) INFN Sezione di Roma I; (b) Dipartimento di Fisica, Università La Sapienza, Roma, Italy
- 134 (a) INFN Sezione di Roma Tor Vergata; (b) Dipartimento di Fisica, Università di Roma Tor Vergata, Roma, Italy
- 135 (a) INFN Sezione di Roma Tre; (b) Dipartimento di Matematica e Fisica, Università Roma Tre, Roma, Italy
- 136 (a) Faculté des Sciences Ain Chock, Réseau Universitaire de Physique des Hautes Energies - Université Hassan II, Casablanca; (b) Centre National de l'Énergie des Sciences Techniques Nucleaires, Rabat; (c) Faculté des Sciences Semlalia, Université Cadi Ayyad, LPHEA-Marrakech; (d) Faculté des Sciences, Université Mohamed Premier and LPTPM, Oujda; (e) Faculté des sciences, Université Mohammed V-Agdal, Rabat, Morocco
- 137 DSM/IRFU (Institut de Recherches sur les Lois Fondamentales de l'Univers), CEA Saclay (Commissariat à l'Énergie Atomique et aux Énergies Alternatives), Gif-sur-Yvette, France
- 138 Santa Cruz Institute for Particle Physics, University of California Santa Cruz, Santa Cruz CA, United States of America
- 139 Department of Physics, University of Washington, Seattle WA, United States of America
- 140 Department of Physics and Astronomy, University of Sheffield, Sheffield, United Kingdom
- 141 Department of Physics, Shinshu University, Nagano, Japan
- 142 Fachbereich Physik, Universität Siegen, Siegen, Germany
- 143 Department of Physics, Simon Fraser University, Burnaby BC, Canada
- 144 SLAC National Accelerator Laboratory, Stanford CA, United States of America
- 145 (a) Faculty of Mathematics, Physics & Informatics, Comenius University, Bratislava; (b) Department of Subnuclear Physics, Institute of Experimental Physics of the Slovak Academy of Sciences, Kosice, Slovak Republic
- 146 (a) Department of Physics, University of Cape Town, Cape Town; (b) Department of Physics, University of Johannesburg, Johannesburg; (c) School of Physics, University of the Witwatersrand, Johannesburg, South Africa
- 147 (a) Department of Physics, Stockholm University; (b) The Oskar Klein Centre, Stockholm, Sweden
- 148 Physics Department, Royal Institute of Technology, Stockholm, Sweden
- 149 Departments of Physics & Astronomy and Chemistry, Stony Brook University, Stony Brook NY, United States of America
- 150 Department of Physics and Astronomy, University of Sussex, Brighton, United Kingdom
- 151 School of Physics, University of Sydney, Sydney, Australia
- 152 Institute of Physics, Academia Sinica, Taipei, Taiwan
- 153 Department of Physics, Technion: Israel Institute of Technology, Haifa, Israel
- 154 Raymond and Beverly Sackler School of Physics and Astronomy, Tel Aviv University, Tel Aviv, Israel
- 155 Department of Physics, Aristotle University of Thessaloniki, Thessaloniki, Greece
- 156 International Center for Elementary Particle Physics and Department of Physics, The University of Tokyo, Tokyo, Japan
- 157 Graduate School of Science and Technology, Tokyo Metropolitan University, Tokyo, Japan
- 158 Department of Physics, Tokyo Institute of Technology, Tokyo, Japan
- 159 Department of Physics, University of Toronto, Toronto ON, Canada
- 160 (a) TRIUMF, Vancouver BC; (b) Department of Physics and Astronomy, York University, Toronto ON, Canada
- 161 Faculty of Pure and Applied Sciences, University of Tsukuba, Tsukuba, Japan
- 162 Department of Physics and Astronomy, Tufts University, Medford MA, United States of America
- 163 Centro de Investigaciones, Universidad Antonio Narino, Bogota, Colombia
- 164 Department of Physics and Astronomy, University of California Irvine, Irvine CA, United States of America
- 165 (a) INFN Gruppo Collegato di Udine; (b) ICTP, Trieste; (c) Dipartimento di Chimica, Fisica e Ambiente, Università di Udine, Udine, Italy
- 166 Department of Physics, University of Illinois, Urbana IL, United States of America
- 167 Department of Physics and Astronomy, University of Uppsala, Uppsala, Sweden
- 168 Instituto de Física Corpuscular (IFIC) and Departamento de Física Atómica, Molecular y Nuclear and Departamento de Ingeniería Electrónica and Instituto de Microelectrónica de Barcelona (IMB-CNM), University of Valencia and CSIC, Valencia, Spain
- 169 Department of Physics, University of British Columbia, Vancouver BC, Canada
- 170 Department of Physics and Astronomy, University of Victoria, Victoria BC, Canada
- 171 Department of Physics, University of Warwick, Coventry, United Kingdom
- 172 Waseda University, Tokyo, Japan
- 173 Department of Particle Physics, The Weizmann Institute of Science, Rehovot, Israel

- ¹⁷⁴ Department of Physics, University of Wisconsin, Madison WI, United States of America
- ¹⁷⁵ Fakultät für Physik und Astronomie, Julius-Maximilians-Universität, Würzburg, Germany
- ¹⁷⁶ Fachbereich C Physik, Bergische Universität Wuppertal, Wuppertal, Germany
- ¹⁷⁷ Department of Physics, Yale University, New Haven CT, United States of America
- ¹⁷⁸ Yerevan Physics Institute, Yerevan, Armenia
- ¹⁷⁹ Centre de Calcul de l'Institut National de Physique Nucléaire et de Physique des Particules (IN2P3), Villeurbanne, France
- ^a Also at Department of Physics, King's College London, London, United Kingdom
- ^b Also at Laboratório de Instrumentação e Física Experimental de Partículas - LIP, Lisboa, Portugal
- ^c Also at Institute of Physics, Azerbaijan Academy of Sciences, Baku, Azerbaijan
- ^d Also at Faculdade de Ciências and CFNUL, Universidade de Lisboa, Lisboa, Portugal
- ^e Also at Particle Physics Department, Rutherford Appleton Laboratory, Didcot, United Kingdom
- ^f Also at TRIUMF, Vancouver BC, Canada
- ^g Also at Department of Physics, California State University, Fresno CA, United States of America
- ^h Also at Novosibirsk State University, Novosibirsk, Russia
- ⁱ Also at Department of Physics, University of Coimbra, Coimbra, Portugal
- ^j Also at Università di Napoli Parthenope, Napoli, Italy
- ^k Also at Institute of Particle Physics (IPP), Canada
- ^l Also at Department of Physics, Middle East Technical University, Ankara, Turkey
- ^m Also at Louisiana Tech University, Ruston LA, United States of America
- ⁿ Also at Dep Física and CEFITEC of Faculdade de Ciências e Tecnologia, Universidade Nova de Lisboa, Caparica, Portugal
- ^o Also at CPPM, Aix-Marseille Université and CNRS/IN2P3, Marseille, France
- ^p Also at Department of Physics and Astronomy, Michigan State University, East Lansing MI, United States of America
- ^q Also at Department of Financial and Management Engineering, University of the Aegean, Chios, Greece
- ^r Also at Institutio Catalana de Recerca i Estudis Avancats, ICREA, Barcelona, Spain
- ^s Also at Department of Physics, University of Cape Town, Cape Town, South Africa
- ^t Also at CERN, Geneva, Switzerland
- ^u Also at Ochadai Academic Production, Ochanomizu University, Tokyo, Japan
- ^v Also at Manhattan College, New York NY, United States of America
- ^w Also at Institute of Physics, Academia Sinica, Taipei, Taiwan
- ^x Also at School of Physics and Engineering, Sun Yat-sen University, Guanzhou, China
- ^y Also at Academia Sinica Grid Computing, Institute of Physics, Academia Sinica, Taipei, Taiwan
- ^z Also at Laboratoire de Physique Nucléaire et de Hautes Energies, UPMC and Université Paris-Diderot and CNRS/IN2P3, Paris, France
- ^{aa} Also at School of Physical Sciences, National Institute of Science Education and Research, Bhubaneswar, India
- ^{ab} Also at Dipartimento di Fisica, Università La Sapienza, Roma, Italy
- ^{ac} Also at DSM/IRFU (Institut de Recherches sur les Lois Fondamentales de l'Univers), CEA Saclay (Commissariat à l'Energie Atomique et aux Energies Alternatives), Gif-sur-Yvette, France
- ^{ad} Also at Moscow Institute of Physics and Technology State University, Dolgoprudny, Russia
- ^{ae} Also at Section de Physique, Université de Genève, Geneva, Switzerland
- ^{af} Also at Departamento de Física, Universidade de Minho, Braga, Portugal
- ^{ag} Also at Department of Physics, The University of Texas at Austin, Austin TX, United States of America
- ^{ah} Also at Institute for Particle and Nuclear Physics, Wigner Research Centre for Physics, Budapest, Hungary
- ^{ai} Also at DESY, Hamburg and Zeuthen, Germany
- ^{aj} Also at International School for Advanced Studies (SISSA), Trieste, Italy
- ^{ak} Also at Department of Physics and Astronomy, University of South Carolina, Columbia SC, United States of America
- ^{al} Also at Faculty of Physics, M.V.Lomonosov Moscow State University, Moscow, Russia
- ^{am} Also at Nevis Laboratory, Columbia University, Irvington NY, United States of America
- ^{an} Also at Physics Department, Brookhaven National Laboratory, Upton NY, United States of America
- ^{ao} Also at Moscow Engineering and Physics Institute (MEPhI), Moscow, Russia
- ^{ap} Also at Department of Physics, Oxford University, Oxford, United Kingdom
- ^{aq} Also at Institut für Experimentalphysik, Universität Hamburg, Hamburg, Germany
- ^{ar} Also at Department of Physics, The University of Michigan, Ann Arbor MI, United States of America
- ^{as} Also at Discipline of Physics, University of KwaZulu-Natal, Durban, South Africa
- * Deceased